Palaeomagnetism and Palaeogeography of the Variscan Formations of the Bohemian Massif, Comparison with other European Regions

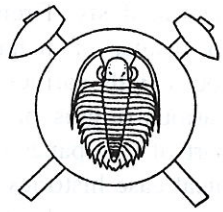

Paleomagnetismus a paleogeografie variských formací Českého masívu, srovnání s ostatními regiony v Evropě (Czech summary)

(45 text-figs.)

MIROSLAV KRS – PETR PRUNER

Geological Institute, Academy of Sciences of the Czech Republic, Rozvojová 135, 165 00 Praha 6, Czech Republic

Palaeomagnetic data published during approximately the last 30 years and derived from rocks from the Triassic to the Devonian periods have been statistically evaluated. The data cover the territories to the north of the Alpine tectonic belt, west of the Ural Mts. and reach up to Great Britain. The aim was to define the palaeotectonic deformations and the palaeogeography of rock complexes of the Hercynian orogene. The data document the consolidation of the European lithospheric plate in the Early Permian as a part of the formation of the Pangea supercontinent. They confirm that, due to continental drift, the European plate moved from the palaeo-equatorial Early Permian position to its present one. Rocks from the Middle to Late Carboniferous age from the western part of the Bohemian Massif, from the Middle to the Late Devonian from the Moravian Zone and rocks from the West-European Hercynides show clear clockwise palaeotectonic rotation deformations. For the West-European Hercynides, these rotation deformations reach very high values (Edel 1987). For the Middle Carboniferous rocks, they represent about 50° and, for the Early Carboniferous, they go up to 120° in a clockwise direction. Such large deformations are related to palaeomeridians of the Early Permian palaeogeographic net of the consolidated European plate. Deformations of comparable magnitude have been found in the Moravian Zone and on the Polish side, in the Holy Cross Mts. Palaeotectonic rotations of similar magnitude were demonstrated in a number of cases in the Alpine tectonic belt. In this paper, we discuss the similarities and differences between the palaeotectonic deformations recognized on rocks affected by the Variscan orogeny to the north of the Alpine belt and with those derived from rocks affected by the Alpine orogeny. Experimental palaeomagnetic data are tested on a model simulating palaeotectonic rotations. Such rotations are regarded as the characteristic sign of tectonic collision zones. A major part of the paper is devoted to the problem of overprint of several Early Variscan and pre-Variscan rock formations in the Bohemian Massif during the Variscan orogeny, which occurred during the Late Carboniferous epoch with possible extension to the Early Permian. The overprint effects were found by magnetomineralogical analyses and by means of the multi-component analysis of remanence applied to Devonian limestones from the Moravian Zone and the Barrandian, to Late Cambrian volcanics and Early Cambrian shales with micro-organic matter of the Barrandian.

Key words: Palaeomagnetism, palaeogeography, Variscan formations in Europe, Bohemian Massif, palaeotectonic rotations, model interpretations

1. Introduction

The goal of the present study consists of evaluating the Variscan palaeomagnetic data derived from the region of the Bohemian Massif and in comparing these findings with the coeval data from other European regions to the north of the Alpine tectonic belt in order to carry out palaeogeographic reconstructions and to determine some development features of the Hercynian fold belt from Early Devonian to Triassic times. To meet such a goal, it was necessary to survey all the major palaeotectonic deformations and palaeogeographic reconstructions regarding the development of corresponding formations during the Variscan orogeny. The analysis is based on previously published results and data compilations, the basic reference to these data may be obtained from the Appendix attached at the end of this paper. Results of statistical evaluation of pole positions for respective regions in Europe, such as Russian Platform, Fennoscandia, England, Scotland, West European Hercynides and Bohemian Massif, from the Triassic to the Early Devonian are summarized in Tables 1 to 4. For the Bohemian Massif, three tables were set up summarizing primary palaeomagnetic data either previously published or recently derived, for the Early Permian, Carboniferous and Devonian (Tables 5-7).

The Variscan overprint of many rock formations might have a serious impact on palaeogeographic reconstructions so that this problem requires a critical discussion. Consequently, special attention is paid to this problem not only from the point of view of results of multi-compo-

nent analysis of remanence, but also with respect to results of magnetomineralogical analysis of rocks with various unblocking temperatures and various origins of palaeomagnetization. A major part of this paper is devoted to discussion of typical case histories of Variscan overprint. Table 8 summarizes pole positions derived on statistically evaluated Variscan components overprinted on various rocks in the territory of the Bohemian Massif.

The palaeogeographic latitudes and orientations of palaeomeridians have been derived and comparison of these data according to their geographic origin and age, starting from the Middle Triassic to the Early Devonian, provide constraints for the palaeogeographic reconstructions. They also can be used for quantitative evaluation of palaeotectonic movements of respective rock formations or blocks during the Variscan orogeny. The palaeomagnetic data make it possible to reconstruct the gradual welding of blocks (microblocks, nappe systems) during the formation of the Pangea supercontinent. This study also highlights the regions in which further palaeomagnetic studies are required.

2. Palaeomagnetism and palaeogeography of the European Variscides

European geological formations affected by the Variscan orogeny have been studied by means of the palaeomagnetic method during approximately the last thirty years. Permo-Carboniferous formations are often represented by palaeovolcanics or „red beds", which were easily measured by laboratory equipment already available two to three decades ago. As more advanced laboratory techniques and interpretation procedures were introduced, an increasing number of rock types were covered by research, e.g. limestones, rocks with micro-organic matter on different levels of carbonification (oil-shales, coal-bearing shales, black shales, etc.). Progress in laboratory techniques was enhanced by the development of magnetometers, and with the progressive thermal demagnetization which led to further development of the equipment creating a high magnetic vacuum (MAVACS, Magnetic Vacuum Control System, cf. Příhoda et al. 1989). Consequently, multi-component analysis methods were developed (e.g. Kirschvink 1980, Kent – Briden – Mardia 1983).

This report contains an analysis of palaeomagnetic data covering the Triassic, Permian, Carboniferous and Devonian periods. The main reason for such a survey has been to elaborate synoptical maps depicting the orientation of palaeomeridians and palaeogeographic latitudes calculated from statistically determined mean pole positions for the respective blocks (regions). Tables of mean pole positions including the scatter of palaeomagnetic data have been set up as well. The methodology implemented is described by Krs (1982). Such a method of analysis makes it possible to derive palaeogeographic reference coordinates, to assess the palaeogeographic affinity of partial blocks (regions) and to quantitatively evaluate palaeotectonic deformations due to the Variscan orogeny. The reference coordinate net derived will be used in the next chapter to discuss similar palaeomagnetic and palaeogeographic data derived from the Bohemian Massif.

The analysis is based on previously published results and data compilation (Krs 1968; Edel 1987; Irving et al. 1976a,b; Krs et al. 1992a, 1993a; Pesonen et al. 1991; Khramov 1984; Torsvik et al. 1990, 1992; Van der Voo 1990; Westphal 1990). These catalogues and publications ensure that only a minor part of the data published on palaeomagnetism of the Variscides was not incorporated into our evaluation. In contrast to the paper by Krs (1982), this analysis does not include palaeomagnetic data from regions of the Alpine tectonic belt.

The Triassic, Permian, Carboniferous and Devonian palaeomagnetic pole positions used for statistical evaluation and construction of Figs 1 to 15 were obtained from cataloques and publications whose references are mentioned in Appendix. Geographical coordinates (latitude and longitude) are provided for each of the geological formations, and the name of the region is mentioned as well. This is followed by brief notes on the type of rocks examined, and notes on the experimental techniques used for demagnetization (thermal demagnetization – TC, alternating field demagnetization – AC, combined demagnetization – TC + AC). The palaeomagnetization is mentioned as being of either normal (N), reverse (R) or combined (N+R) polarization, and the reference number of the catalogue or publication in question comes last. Palaeomagnetic data that do not meet one of the following criteria, i.e. whose $\alpha_{95} > 15^{o}$ (Fisher 1953), whose reliability criterion is B (Irving et al. 1976a,b) or quality Q < 3 (Van der Voo 1990) were not taken into account.

Table 1. Triassic mean pole positions

	Russian Platform, Ural Mts.				
	$\varphi_p(^\circ)N$	$\lambda_p(^\circ)E$	$\alpha'_{95}(^\circ)$	k	N_p
T_3					
T_2	51.8	142.7	6.7	132.6	5
T_1	45.9	160.8	5.2	71.8	12

England, Ireland, France, Germany					Fennoscandia				
$\varphi_p(^\circ)N$	$\lambda_p(^\circ)E$	$\alpha_{95}(^\circ)$	k	N_p	$\varphi_p(^\circ)N$	$\lambda_p(^\circ)E$	$\alpha_{95}(^\circ)$	k	N_p
48.8	143.3	5.7	82.9	9	58.5	138.1	10.9	50.6	5

N_p - number of pole positions

Table 2. Permian mean pole positions

	Russian Platform, Ural Mts.					Bohemian Massif				
	$\varphi_p(^\circ)N$	$\lambda_p(^\circ)E$	$\alpha_{95}(^\circ)$	k	N_p	$\varphi_p(^\circ)N$	$\lambda_p(^\circ)E$	$\alpha_{95}(^\circ)$	k	N_p
P_3										
P_2	46.2	166.3	2.3	117.0	33					
P_1						38.2	162.2	4.1	114.1	12

England, Scotland					Fennoscandia				
$\varphi_p(^\circ)N$	$\lambda_p(^\circ)E$	$\alpha_{95}(^\circ)$	k	N_p	$\varphi_p(^\circ)N$	$\lambda_p(^\circ)E$	$\alpha_{95}(^\circ)$	k	N_p
43.5	164.3	7.0	93.7	6	45.4	157.6	3.7	71.2	22

West-European Hercynides				
$\varphi_p(^\circ)N$	$\lambda_p(^\circ)E$	$\alpha_{95}(^\circ)$	k	N_p
40.9	165.6	9.3	25.1	11

N_p - number of pole positions

In Figs. 1 to 7, full short lines represent the orientations of palaeomeridians correlated to recent meridians for corresponding collecting sites (localities, areas). In Figs 8 to 15 Fisher's (1953) statistics were used to calculate the mean pole positions; α_{95} – the semi-vertical angle of the confidence cone at the 95% probability level, k – the precision parameter, N_p – the corresponding number of poles. The mean pole positions were calculated for each region (lithospheric plate or its parts): the Russian Platform, Fennoscandia, Bohemian Massif, West-European Hercynides, the area covering England and Scotland or the area comprising England, France and western part of Germany. The data derived by means of statistical analysis (making use of

Table 3. Carboniferous mean pole positions

	Russian Platform,					Russian Platform, Ural Mts.				
	$\varphi_p(^o)N$	$\lambda_p(^o)E$	$\alpha_{95}(^o)$	k	N_p	$\varphi_p(^o)N$	$\lambda_p(^o)E$	$\alpha_{95}(^o)$	k	N_p
C_3						40.4	169.1	5.0	95.0	10
C_2	31.9	163.3	6.0	85.5	8					
C_1						33.5	151.2	12.0	9.9	17

	West-European Hercynides					Bohemia, Poland				
	$\varphi_p(^o)N$	$\lambda_p(^o)E$	$\alpha_{95}(^o)$	k	N_p	$\varphi_p(^o)N$	$\lambda_p(^o)E$	$\alpha_{95}(^o)$	k	N_p
C_3	41.0	158.1	8.9	39.7	8	39.1	164.5	6.3	78.6	8
C_2	12.6	118.2	5.9	45.8	14					
C_1	-21.6	56.5	16.2	8.9	11					

England, Scotland					Fennoscandia				
$\varphi_p(^o)N$	$\lambda_p(^o)E$	$\alpha_{95}(^o)$	k	N_p	$\varphi_p(^o)N$	$\lambda_p(^o)E$	$\alpha_{95}(^o)$	k	N_p
38.5	151.1	6.5	24.6	21	36.9	166.0	4.1	70.9	18

N_p - number of pole positions

„trial and error" procedure) are displayed in the Tables 1, 2, 3 and 4. From the mean pole positions calculated for each region (with scatters stated in the above tables), palaeogeographic latitudes were calculated. They are shown in Figs 1 to 7, cf. also Soffel (1991), Butler (1992) and Van der Voo (1993).

Triassic

For the Middle Triassic and Triassic periods, the orientation of palaeomeridians (the Russian Platform, Fennoscandia, Western Europe) is in mutual agreement within the geocentric dipole field. Within the limits of scatter of the palaeomagnetic data, the palaeolatitudes are also in agreement for all territories to the north of the Alpine tectonic belt, (see Fig. 1). Furthermore, for the region west of the Ural Mts. and north of the Alpine tectonic belt up to Scandinavia, the lithospheric plate can be considered as being tectonically nearly stable and without any pronounced horizontal palaeotectonic deformations, incl. fault-bound traslations. There is a gap, however, between the palaeolatitudes for Western Europe and Fennoscandia.

Early Triassic rocks have been studied only in the area of the Russian Platform. Absolute palaeogeographic latitudes are about 10° lower when compared to the Middle Triassic ones, see Fig. 2. If $\alpha_{95} = 6.7^o$ for the Middle Triassic and $\alpha_{95} = 5.2^o$ for the Early Triassic, the resulting difference of 10° is statistically provable, (see Table 1). Comparing the Middle Triassic with the Early Triassic, the orientation of palaeolatitudes and palaeomeridians shows a small clockwise rotation. These movements affect the whole territory of the Russian Platform and reflect continental drift of the whole lithospheric plate. It is worth mentioning that the palaeomagnetic results from

Table 4. Devonian mean pole positions

	Russian Platform - NW of Moscow					Ural Mts.				
	$\varphi_p(^o)N$	$\lambda_p(^o)E$	$\alpha_{95}(^o)$	k	N_p	$\varphi_p(^o)N$	$\lambda_p(^o)E$	$\alpha_{95}(^o)$	k	N_p
D_3	32.2	161.3	4.9	245.0	5	35.2	166.4	8.9	27.1	11
D_2										
D_1										

	Russian Platform, northern region					Russian Platform - Dniester area				
	$\varphi_p(^o)N$	$\lambda_p(^o)E$	$\alpha_{95}(^o)$	k	N_p	$\varphi_p(^o)N$	$\lambda_p(^o)E$	$\alpha_{95}(^o)$	k	N_p
D_3	6.2	165.1	17.8	27.2	4					
D_2										
D_1						38.8	163.0	3.8	246.9	7

Fennoscandia					Britain, north of the Great Glen Fault				
$\varphi_p(^o)N$	$\lambda_p(^o)E$	$\alpha_{95}(^o)$	k	N_p	$\varphi_p(^o)N$	$\lambda_p(^o)E$	$\alpha_{95}(^o)$	k	N_p
16.3	156.5	7.5	42.5	10	10.0	146.5	8.1	29.9	12

Britain, south of the Great Glen Fault, north of the Iapetus Sut.					Britain, south of the Iapetus Suture				
$\varphi_p(^o)N$	$\lambda_p(^o)E$	$\alpha_{95}(^o)$	k	N_p	$\varphi_p(^o)N$	$\lambda_p(^o)E$	$\alpha_{95}(^o)$	k	N_p
6.4	140.5	9.0	19.1	15	15.6	140.4	38.6	6.6	4

	West-European Hercynides, incl. Armorican Massif, Poland, Moravian Zone				
	$\varphi_p(^o)N$	$\lambda_p(^o)E$	$\alpha_{95}(^o)$	k	N_p
D_3	30.1	159.0	11.2	19.4	10
D_2					

N_p - number of mean pole positions

the Russian Platform (red beds) and from the Ural Mts. (sandstones, basalts and tuffs) are mutally consistent.

Permian

The original Permian palaeomagnetic pole positions for each region are in good mutual agreement (Table 2). They demonstrate that in the Early Permian the palaeoequator was situated just to the South of Paris (Fig. 3).

Carboniferous

The Late Carboniferous formations (Fig. 4) provide data that document a position close to the eguator, (pronounced drift for the Russian Platform and Fennoscandia). This displacement

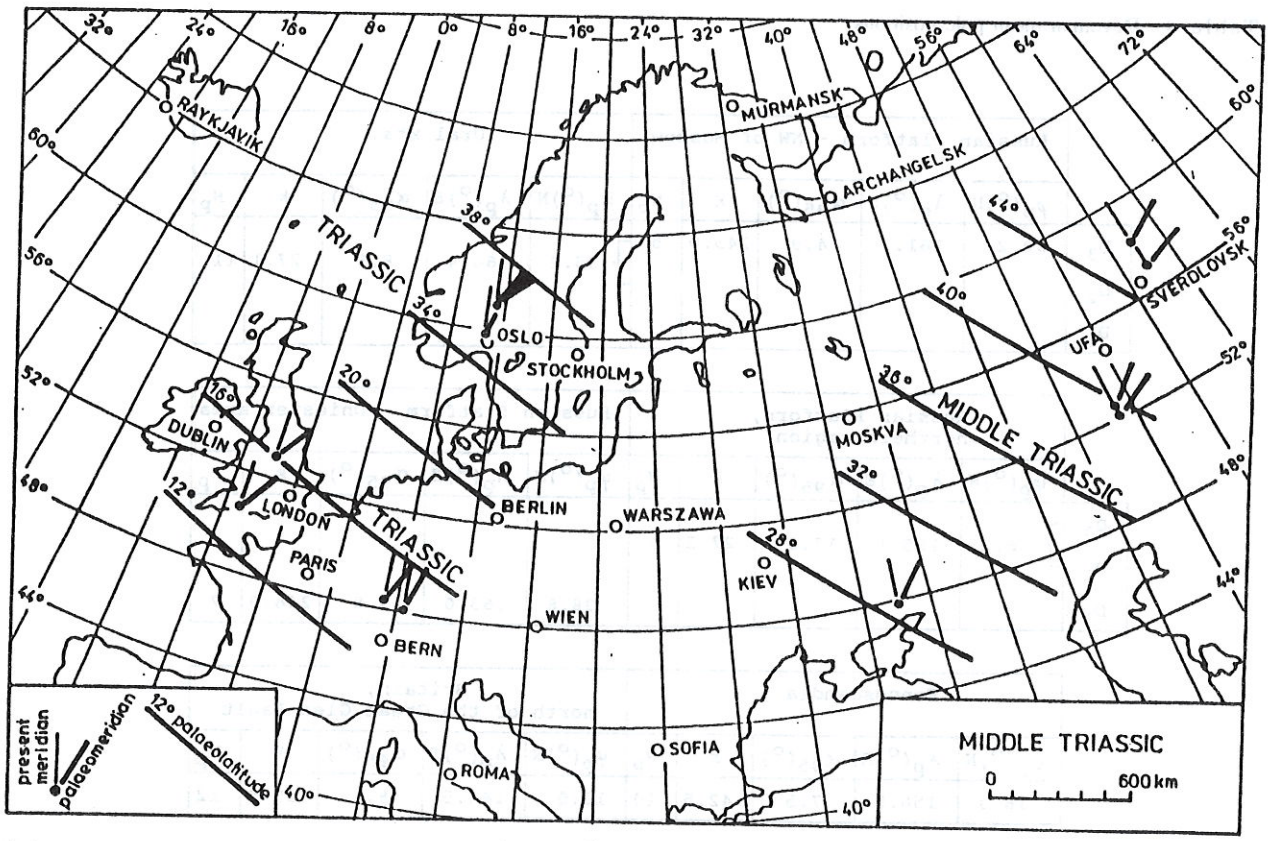

Fig. 1. Triassic and Middle Triassic palaeolatitudes derived from statistically evaluated palaeomagnetic data. Russian Platform, Ural Mts. – Middle Triassic, prevailingly red sediments; Fennoscandia – Triassic, lavas; Western Europe – Triassic, prevailingly red beds

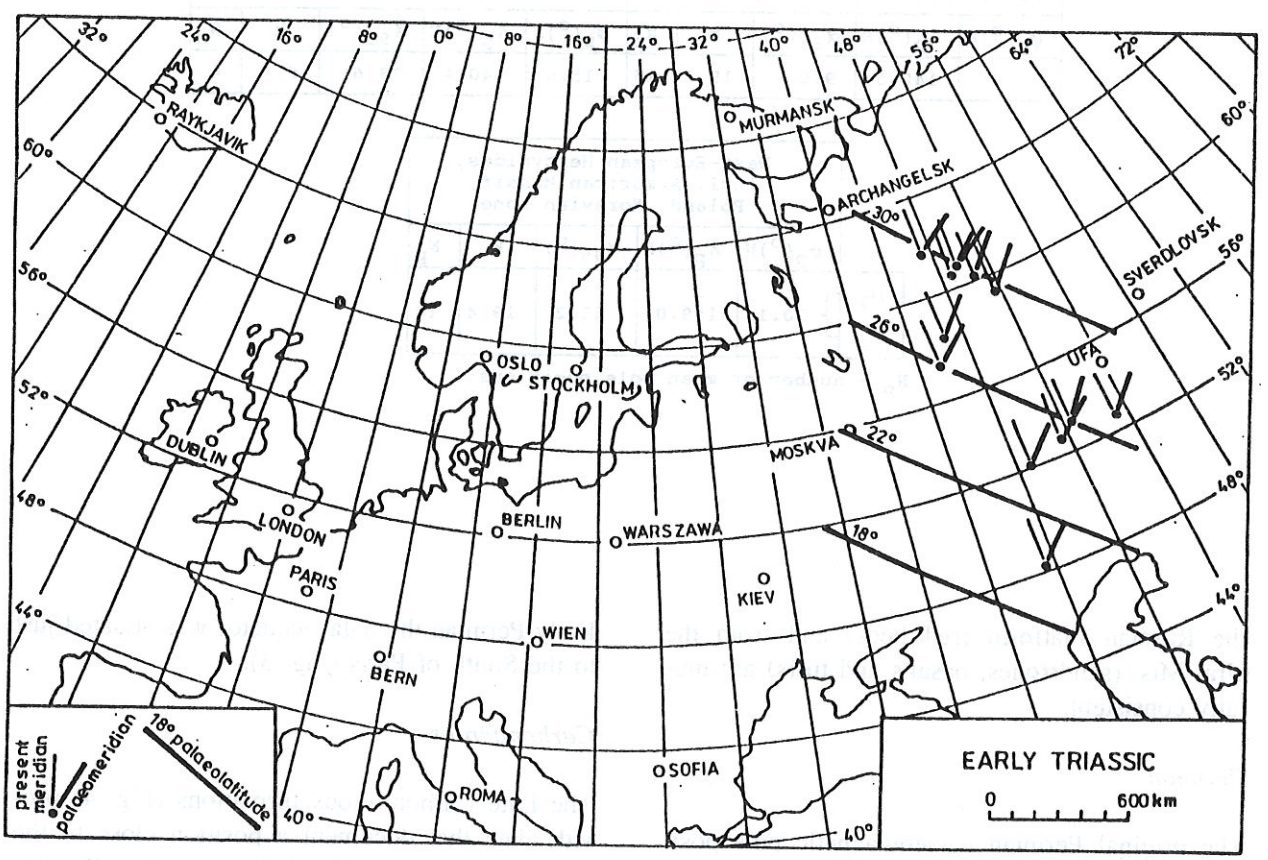

Fig. 2. Early Triassic palaeolatitudes derived from statistically evaluated palaeomagnetic data. Russian Platform, Ural Mts. – prevailingly red beds, sandstones, basalts, tuffs

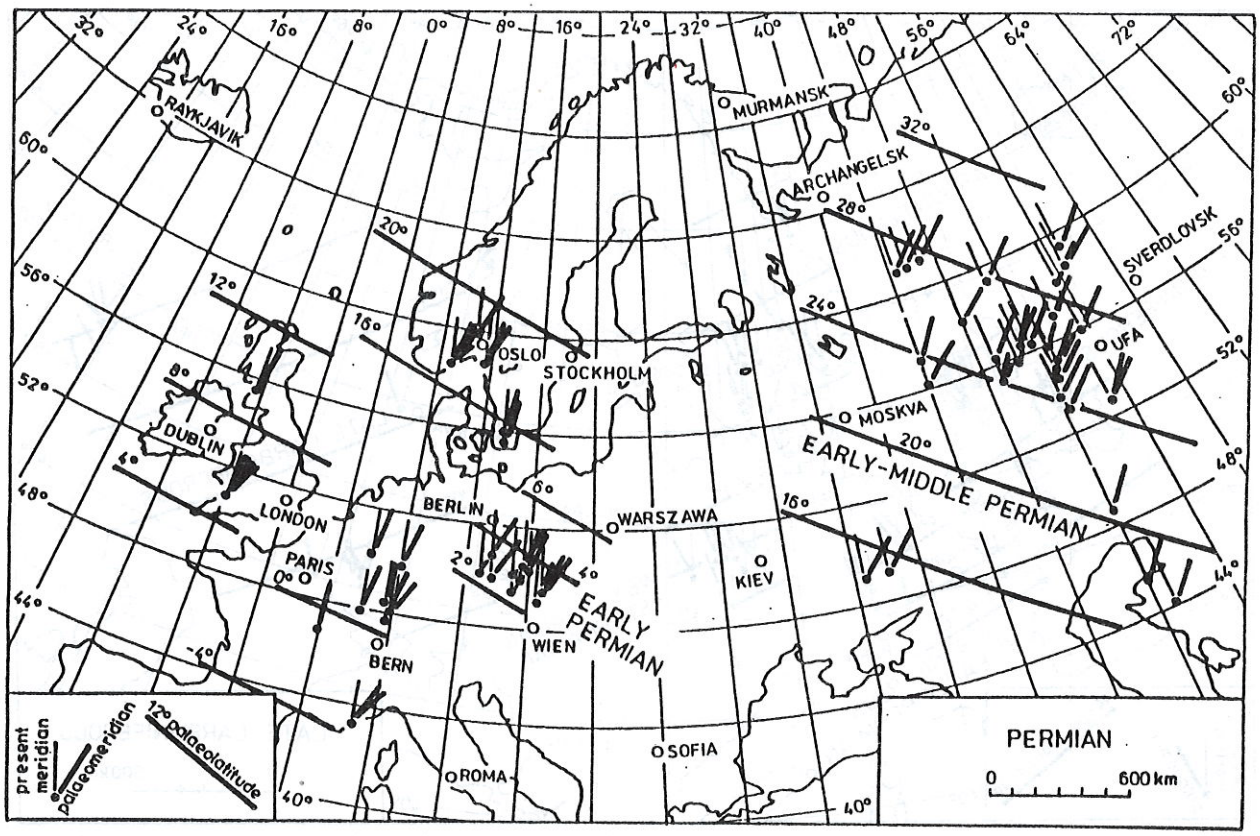

Fig. 3. Permian, Early and Middle Permian palaeolatitudes derived from statistically evaluated palaeomagnetic data. Russian Platform, Ural Mts. – Early to Middle Permian, prevailingly red beds; Fennoscandia – Permian, igneous rocks of different genesis; England, Scotland – Permian, Exeter traps, lavas, some red sandstones; West-European Hercynides – Permian, volcanics and red beds; Bohemian Massif – Early Permian, prevailingly red beds, some ignimbrite, oil-shale, (microgranodiorite and haematite mineralization of presumably Early Permian age)

falls, once again, in the movements generated by the continental drift. In the south-western part of the Bohemian Massif, the declination of palaeomeridians is close to values observable in the West-European Hercynides. This deviation has been pointed out already during the early stages of palaeomagnetic investigations of the Bohemian Massif (Birkenmajer – Krs – Nairn 1968).

Middle Carboniferous rocks show further displacement towards the south; data from the Russian Platform document a slight clockwise rotation in comparison with data from the Late Carboniferous. However, the Middle Carboniferous rocks from the West-European Hercynides show a strong palaeotectonic clockwise rotation as pointed out by Edel (1987), see Fig. 5. This can be demonstrated by the marked dislocation of palaeomagnetic pole positions, see Tab. 3. Rocks of the West-European Hercynides are found in equatorial palaeogeographic latitudes, mostly in the southern hemisphere.

The Early Carboniferous palaeopoles obtaind from the Russian Platform and the West-European Hercynides indicate palaeogeographic latitudes in the northern hemisphere. However, relatively scarce and rather unhomogeneous data are statistically less significant, see Table 3. In spite of this, there is a clear deviation of the palaeomagnetic declinations from those for Early to Late Carboniferous rocks which *a priori* indicates a clockwise palaeotectonic rotation of formations in the West-European Hercynides, see Fig. 6.

Devonian

The Devonian rocks palaeomagnetically investigated are from the Russian Platform (its northern territories, NW of Moscow and Dniester area), from the West-European Hercynides incl. Armorican Massif, from Poland (Holy Cross Mts.) and the Moravian Zone of the Bohemian Massif. The palaeomagnetic directions from the Dniester area and region NW of Moscow evidently do not represent the Devonian directions but the remagnetization directions during the (Early) Permian period, e.g. the mean pole positions for

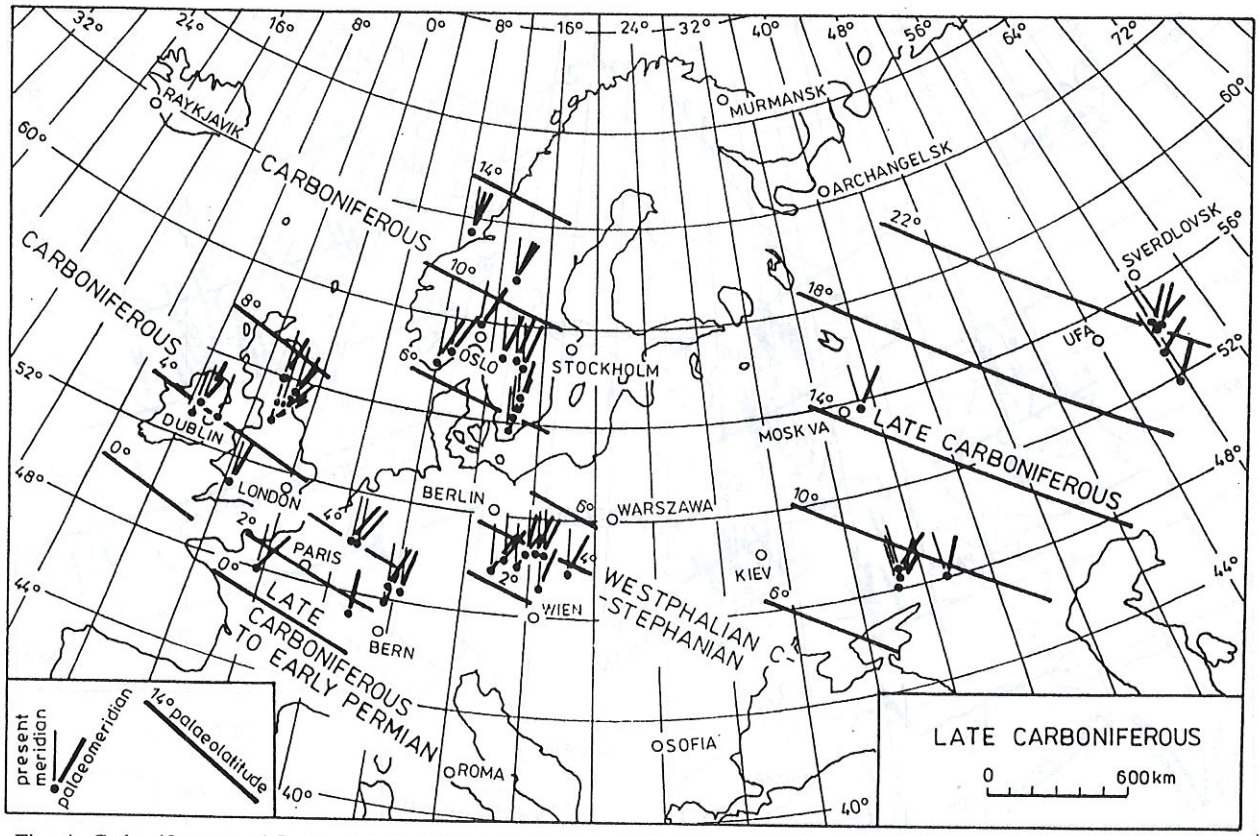

Fig. 4. Carboniferous and Late Carboniferous palaeolatitudes derived from statistically evaluated palaeomagnetic data. Russian Platform, Ural Mts. – Late Carboniferous, red beds, igneous rocks; Fennoscandia – Carboniferous, igneous rocks of different origin; England, Scotland – Carboniferous, limestones, red beds, volcanics; West-European Hercynides – Late Carboniferous, prevailingly volcanics, some sediments; Bohemia, Poland – Late Carboniferous, prevailingly red beds, some tuffs

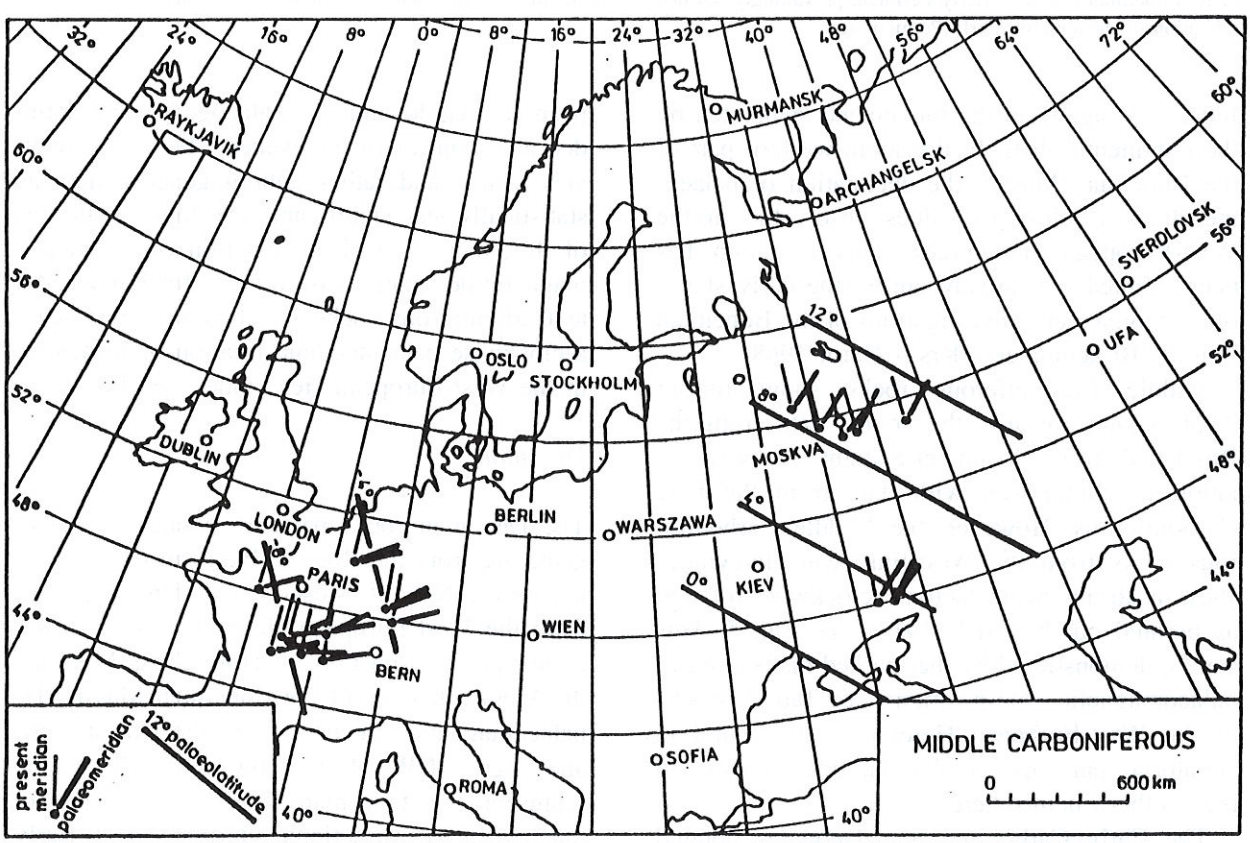

Fig. 5. Middle Carboniferous palaeolatitudes derived from statistically evaluated palaeomagnetic data. Russian Platform – red beds; West-European Hercynides – rocks of different genesis: volcanics, granitoids, ignimbrites, tuffs, sediments

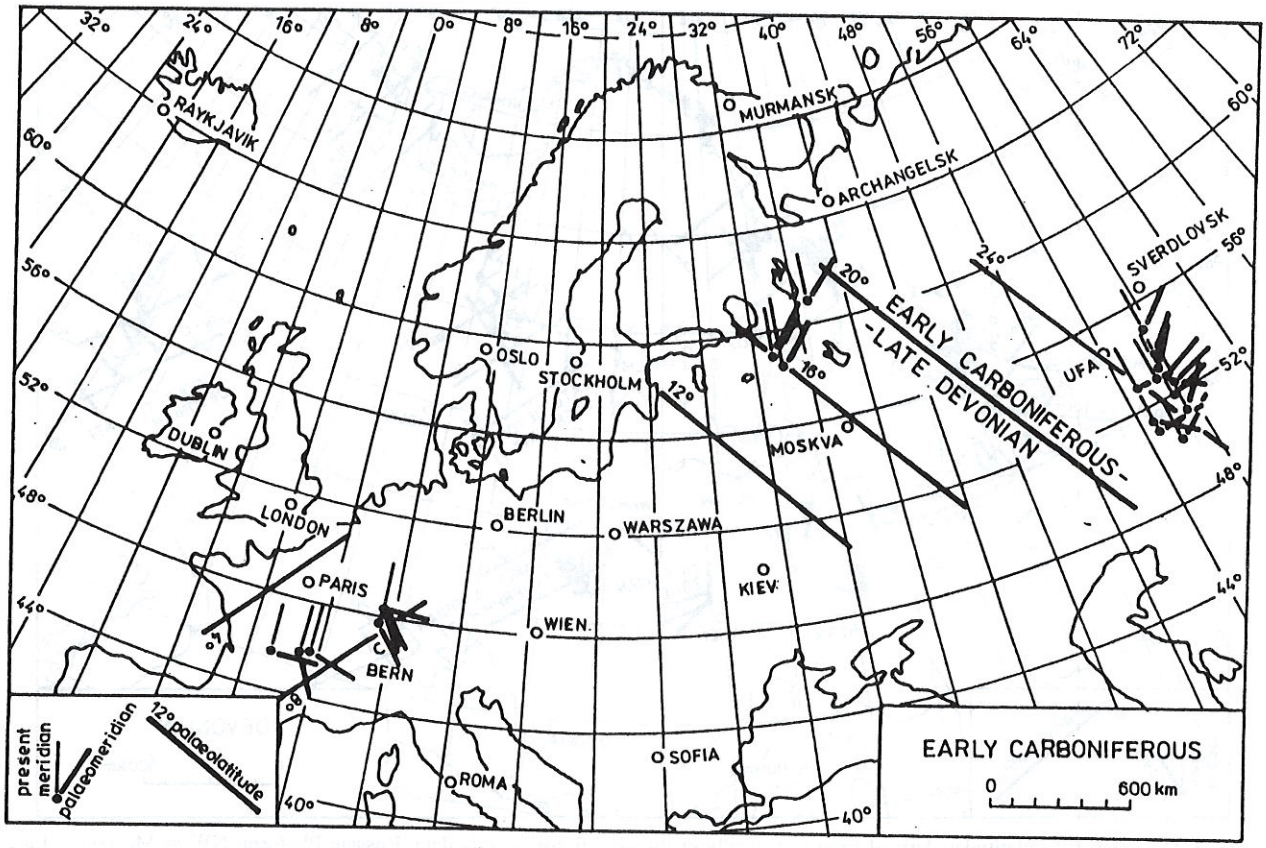

Fig. 6. Early Carboniferous palaeolatitudes derived from statistically evaluated palaeomagnetic data. Russian Platform, Ural Mts. – Early Carboniferous to Late Devonian, red beds, tuffs, granitoids, limestones; West-European Hercynides – diorites, volcanics, ignimbrites, tuffs

the Devonian rocks from the Dniester area are practically identical with the mean pole positions for the (Early) Permian rocks of the Bohemian Massif, cf. Tables 2 and 4. Palaeomagnetic directions for the Devonian rocks from Great Britain, West-European Hercynides, Poland (Holy Cross Mts.), the Moravian Zone and the Ural Mts. show predominantly clockwise rotations, see Fig. 7 and Table 4.

Thus it becomes evident that the Trans-European Suture Zone forms a boundary SW of which the Carboniferous rocks show, as a consequence of palaeotectonic rotations, deviations in palaeomagnetic declinations. To the NE of the boundary, i.e. on the East-European Platform, palaeomagnetic data are homogeneous.

From the Early Permian to younger formations, palaeomagnetic data are homogeneous for the whole plate – from the Ural Mts. up to Great Britain and north of the Alpine tectonic belt up to Scandinavia.

Figs. 8 to 15 depict pole positions and mean pole positions calculated by means of Fisher's (1953) statistics for each of the regions (parts of the lithospheric plate) from the Triassic to the Early Devonian periods, see Tables 1 to 4.

3. Palaeomagnetism and palaeogeography of Variscan Formations of the Bohemian Massif

Since the Early Permian, the Bohemian Massif represents a tectonically stable block. Palaeomagnetic investigations on Early Permian and Carboniferous rocks have pointed to the continuous drift from the equatorial zone, to partial horizontal rotation of blocks from the Westphalian B to Stephanian (Krs 1968, 1978; Krs et al. 1992a), and, finally, to the palaeogeographic affinity of the Bohemian Massif to the North-European Platform since the Early Permian.

Palaeomagnetic findings on the Early Permian and Carboniferous rocks compiled by Krs (1968) were predominantly derived from „red beds", to a lesser extent from tuffs, usually on rocks filling shallow basins or furrows. The data presented in the paper mentioned above were obtained through a statistical evaluation of palaeomagnetic directions of strata (strata means) using Fisher's (1953) statistics; see palaeomagnetic data for the Early Permian 1-6 and the Carboniferous 8-14 on Fig. 16. The development of a new type of thermal demagnetizer MAVACS – Magnetic Va-

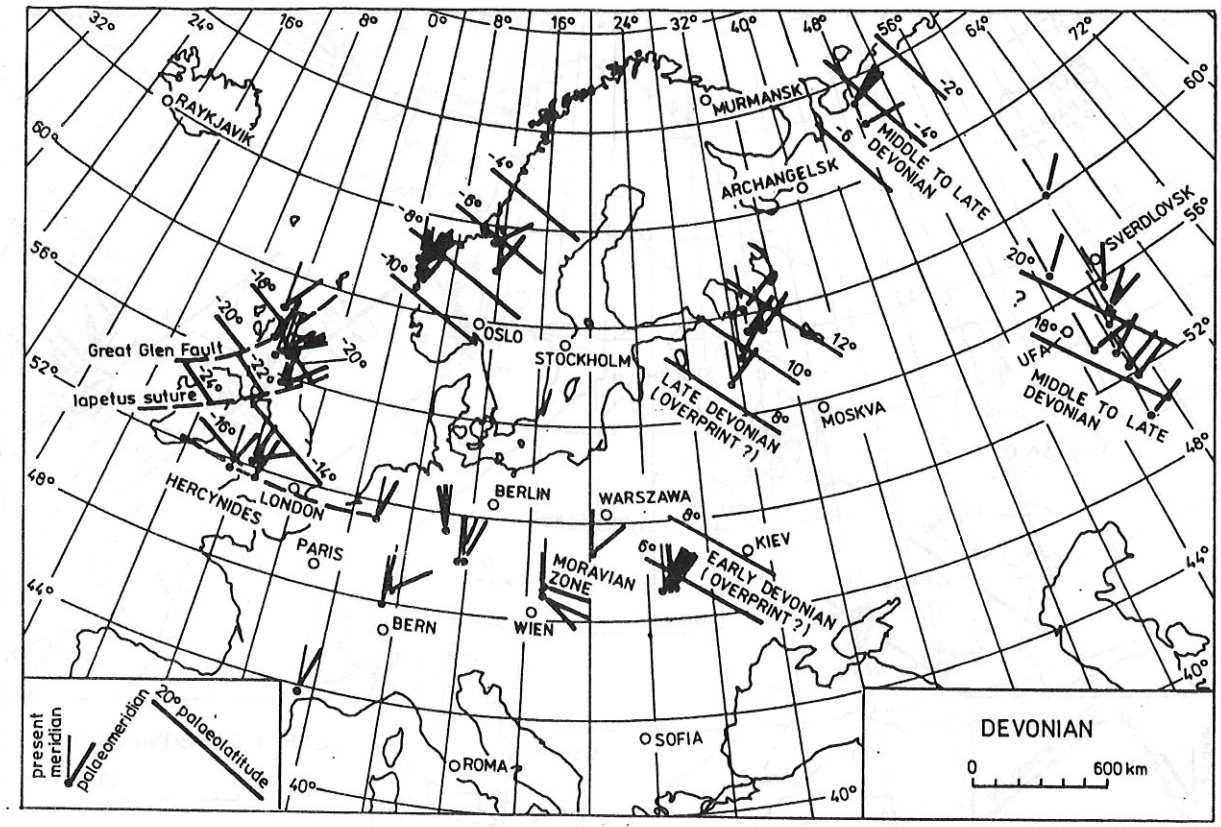

Fig. 7. Devonian palaeolatitudes derived from statistically evaluated palaeomagnetic data. Russian Platform, NW of Moscow – Late Devonian, sediments; larger region of the Ural Mts. – Middle to Late Devonian, variable sediments (limestone, tuffite, sandstone, bauxite) and igneous rocks (tuff and tuff-breccia, granite, diabase); Russian Platform, northern region – Middle to Late Devonian, sediments; Russian Platform, Dniester area – Early Devonian, sediments; Fennoscandia – Devonian, sediments, igneous rocks; West-European Hercynides, incl. Armorican Massif, Poland – Middle to Late Devonian, sediments, igneous rocks; Great Britain, north of the Great Glen Fault – Devonian, sediments, igneous rocks; Great Britain, south of the Great Glen Fault – Devonian, sandstones and lavas prevail; Great Britain – south of the Iapetus Suture – Devonian, sandstones, intrusives; Bohemian Massif, Moravian Zone – limestones of the Late Eifelian to the Late Famennian

cuum Control System (Příhoda et al. 1989), and the improvement of interpretation methods, e.g. introduction of multi-component analysis of remanence, have helped both to verify some of the earlier findings with more sophisticated equipment (Krs – Chvojka – Valín 1988) and to study other rock types of very different origins. There have been studies for instance, on oil-shales (Krs et al. 1992a), coal-bearing and roof shales (Krs et al. 1993a), and microgranodiorite (Krs – Vrána 1993). Tables 5 to 7 summarize the fundamental palaeomagnetic data derived so far from rocks located on the Czech part of the Bohemian Massif and dating from the Early Permian to the Devonian period. In the early years of palaeomagnetic investigations, mean palaeomagnetic directions were calculated from palaeomagnetic directions of strata (so-called strata means). Later on, other statistical procedures were introduced respecting newly employed laboratory techniques for the derivation of primary palaeomagnetic data. Mean palaeomagnetic directions of any geological formation are calculated either from the palaeomagnetic directions of sites (site means) or of localities (locality means). In other words, the first step is to calculate the virtual pole position of a particular site or locality; then, from virtual pole positions, mean palaeomagnetic pole positions for respective formation are calculated utilizing the statistical method (Fisher 1953). There are, in fact, three different statistical ways of deriving the mean palaeomagnetic pole positions. All three approaches have been tested and the results show that the mean pole positions are, within the limits of statistical errors, mutually identical. For that reason, even earlier palaeomagnetic data can be well utilized for the interpretation; for experimental data on this topic see, for instance, (Krs et al. 1987; Pruner 1987, 1992; Krs et al. 1993a,b).

The impact of palaeotectonics on the scatter of the Late Carboniferous palaeomagnetic data was already seen in the early years of palaeomagnetic investigations (Birkenmajer – Krs – Nairn 1968).

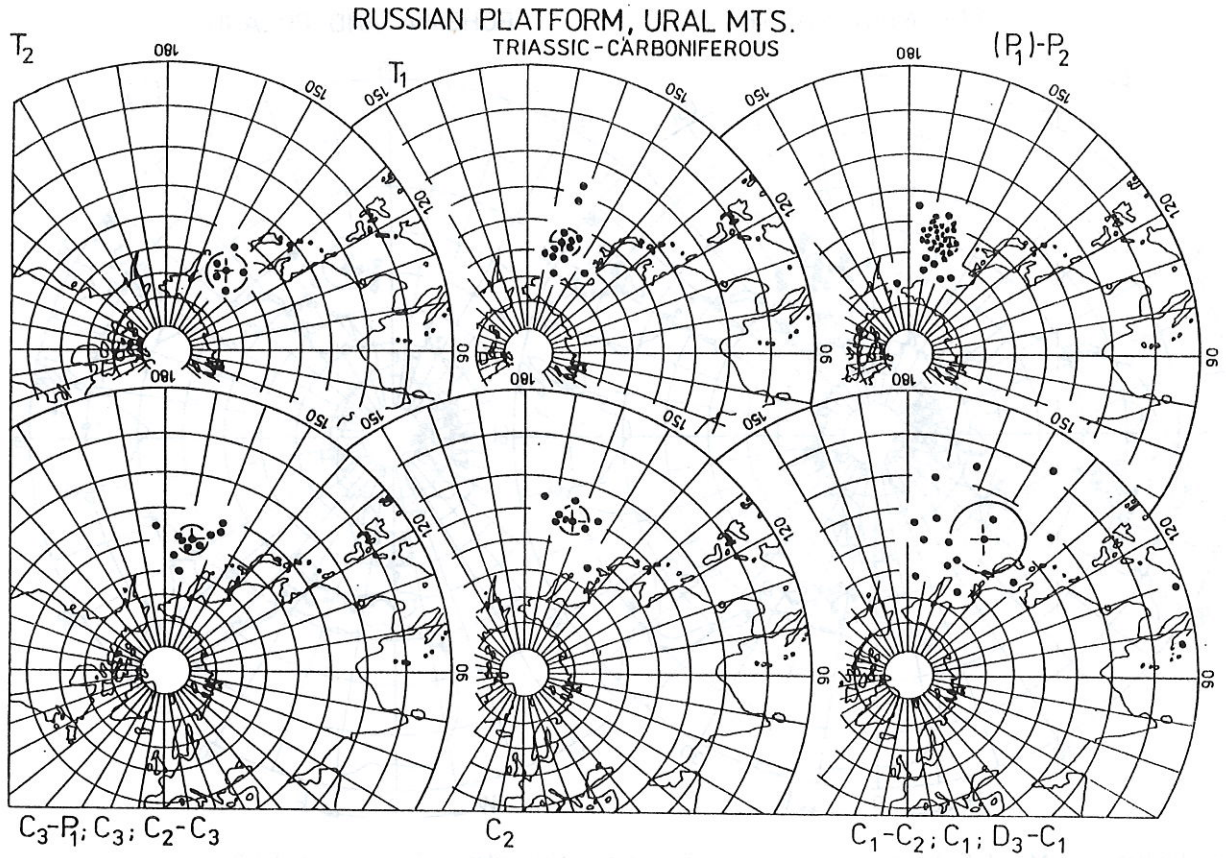

Fig. 8. Russian Platform, Ural Mts; Triassic-Carboniferous. Palaeomagnetic pole positions (*full circles*), mean pole positions (*crossed circles*), confidence circles at the 95% probability level according to Fisher (1953)

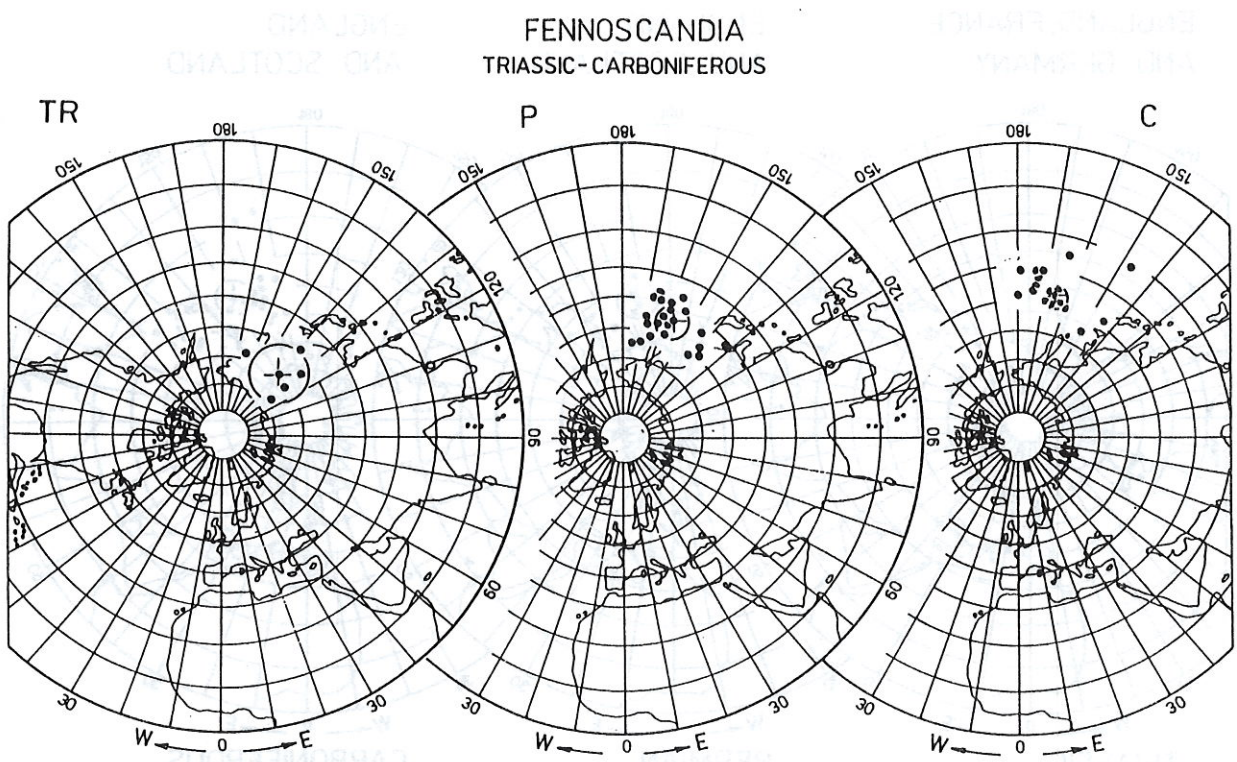

Fig. 9. Fennoscandia; Triassic-Carboniferous. See caption to Fig. 8

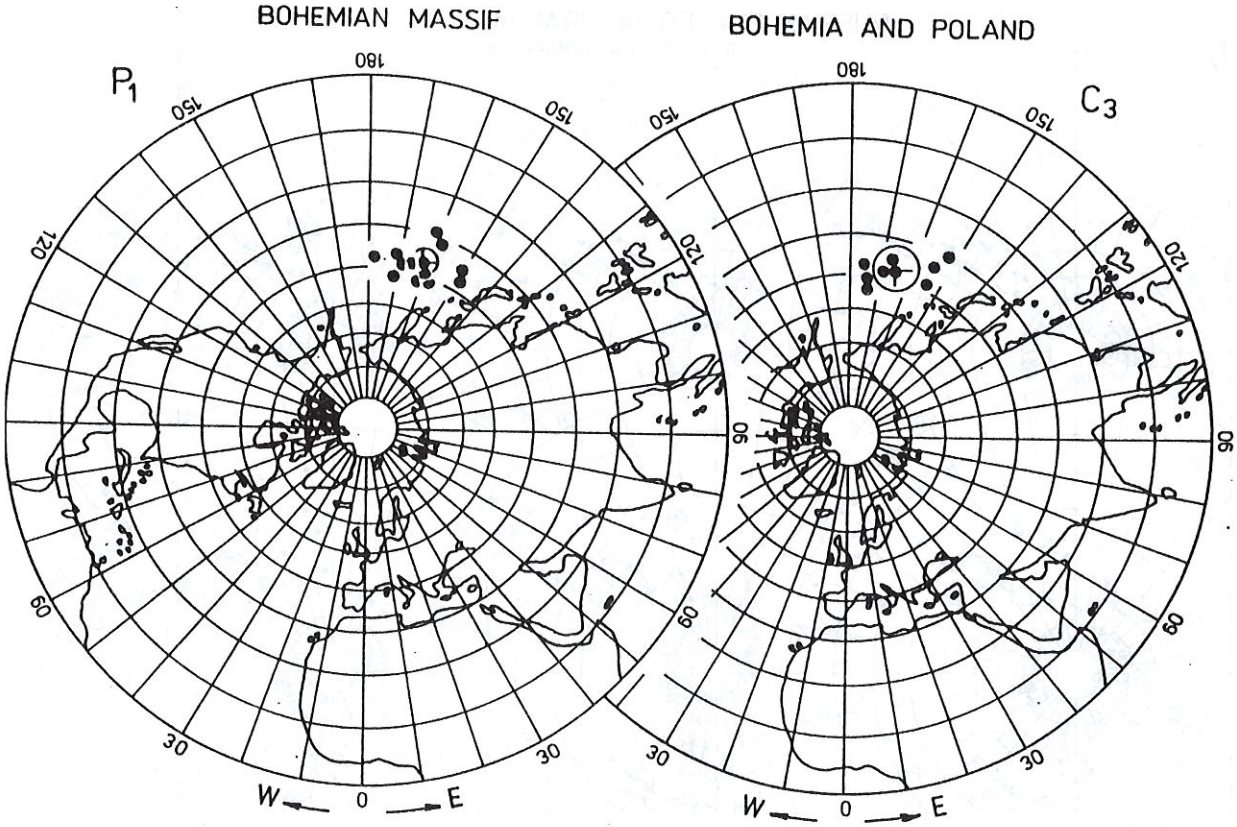

Fig. 10. Bohemian Massif, Early Permian; Bohemia and Poland, Late Carboniferous. See caption to Fig.8

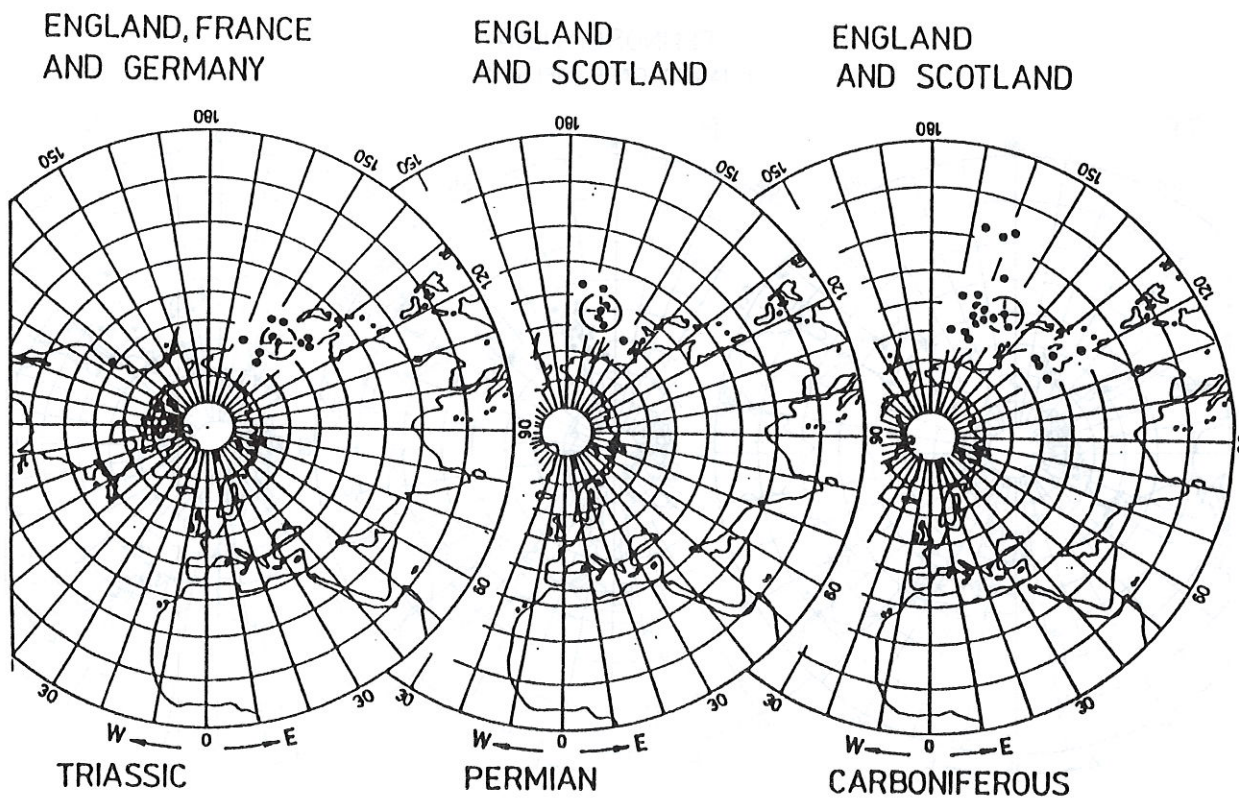

Fig. 11. England and Scotland, France, Germany; Triassic to Carboniferous. See caption to Fig.8

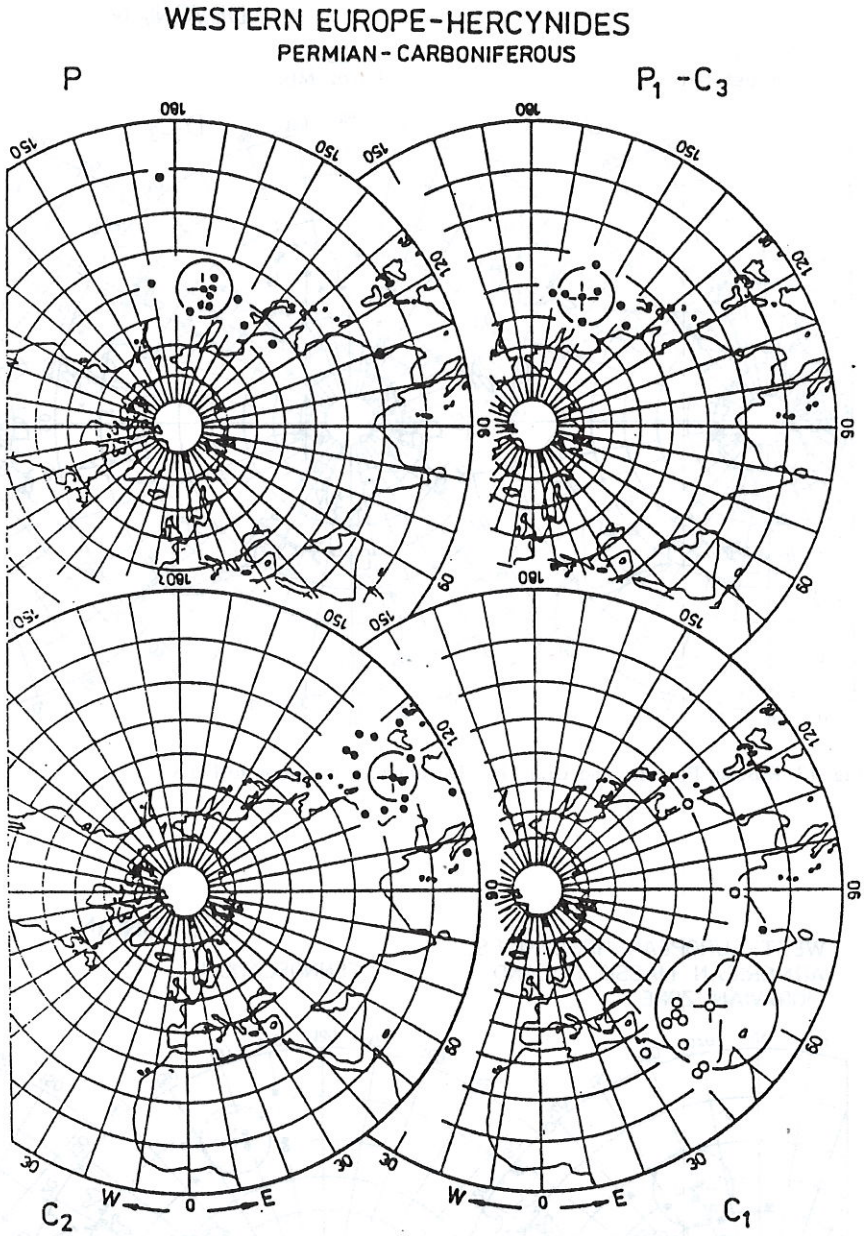

Fig. 12. West-European Hercynides; Permian – Carboniferous. See caption to Fig.8

The largest difference between palaeomeridians was found between the Inner-Sudetic and Krkonoše-Piedmont Basins on one hand, and the Plzeň and Kladno-Rakovník Basins on the other. The azimuthal difference amounts to $17^{o} \pm 4^{o}$ (Krs 1978).

The Moravian-Silesian region incl. the Upper-Silesian Black-coal Basin are located near the lithospheric boundary that divides the North-European Platform from the Alpine-Carpathian collision zone. The vicinity of such a boundary originated by Alpine tectonics did not significantly affect palaeomagnetic data from the Upper-Silesian Basin; e.g. palaeodeclinations do not show any anomalous deviations.

Heterogeneity of the Late Carboniferous palaeomeridians from the Bohemian Massif region contrasts with the uniformity of the Early Permian palaeomeridians. This documents block consolidation of the Bohemian Massif during the Early Permian. That result is corroborated by the scatter of pole positions calculated by Fisher's (1953) statistics: for seven pole positions derived for the Early Permian biostratigraphically dated rocks $\alpha_{95} = 2.9^{o}$, and for the seven pole positions for the Carboniferous biostratigraphically dated rocks $\alpha_{95} = 6.8^{o}$, where α_{95} stands for the semi-vertical angle of the confidence cone calculated at the 95 % probability level.

Palaeomagnetic data make it possible to calculate palaeolatitudes of a particular block. Fig. 17 shows the Autunian palaeogeographic latitudes

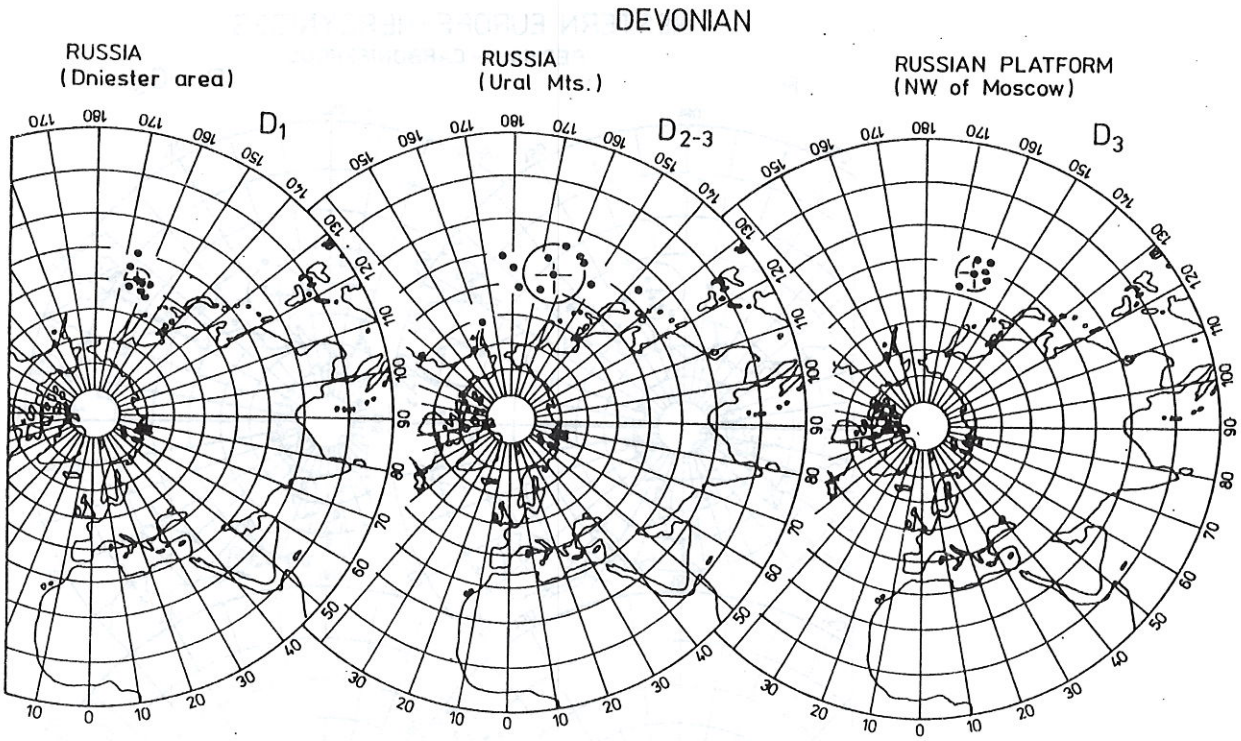

Fig. 13. Russian Platform and Ural Mts.; Devonian. See caption to Fig.8

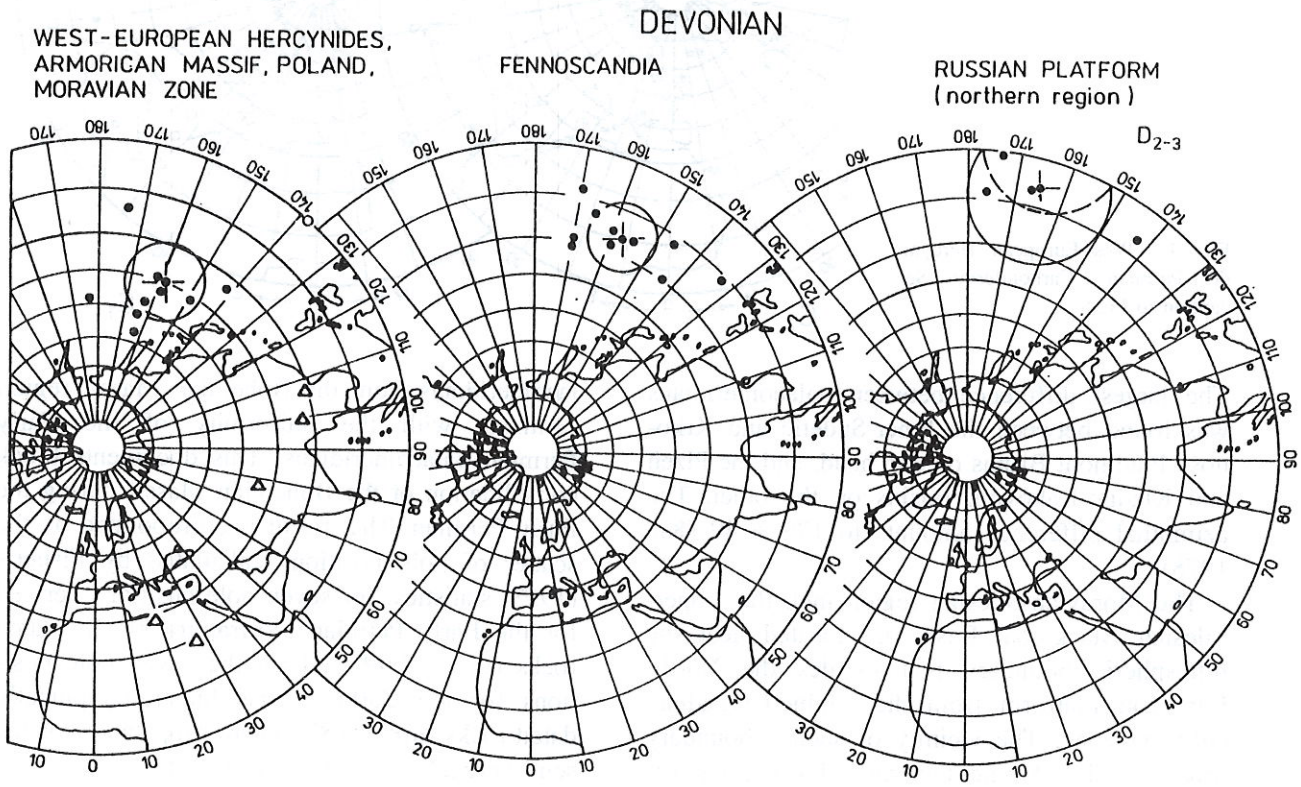

Fig. 14. West-European Hercynides, Armorican Massif, Poland, Moravian Zone, Devonian; Fennoscandia, Devonian; Russian Platform, northern part, Middle to Late Devonian. See caption to Fig.8

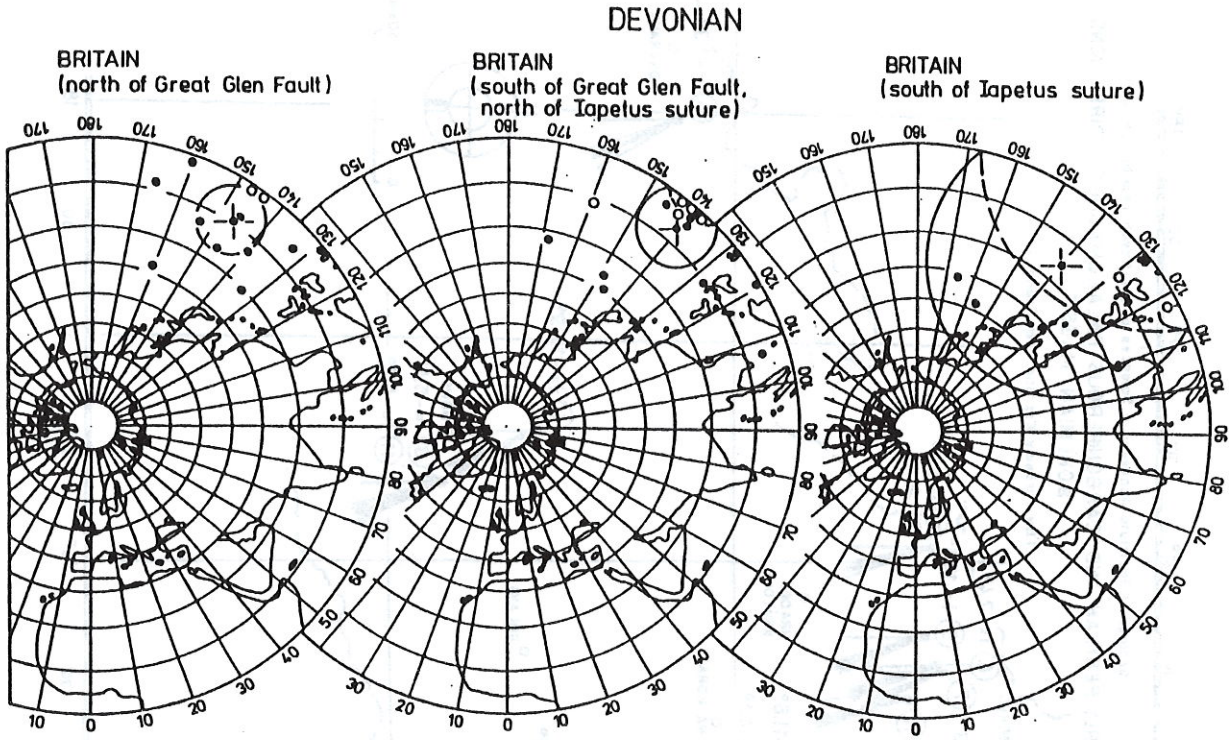

Fig. 15. Britain, Devonian. See caption to Fig.8

derived from the palaeomagnetism of rocks from the Blanice and Boskovice Furrows and palaeolatitudes derived from the Autunian and „Rotliegendes" rocks from the Krkonoše-Piedmont and Inner-Sudetic Basins (Table 5). Fig. 18 shows palaeolatitudes for the Westphalian C to Stephanian rocks from the Plzeň and Kladno-Rakovník Basins, for Stephanian rocks from the Blanice and Boskovice Furrows, and, finally, for the Westphalian B to Stephanian rocks from the Krkonoše-Piedmont and Inner-Sudetic Basins (Table 6). Inaccuracy of calculated palaeolatitudes varies within ±3°. The equatorial position of the Carboniferous formations and close sub-equatorial position of the Early Permian formations from the corresponding blocks in the Bohemian Massif correlate with palaeomagnetic findings obtained from the North-European Platform (Krs 1982), see also Figs. 3 and 4 of this paper. Partial blocks from the Bohemian Massif consolidated, evidently as a consequence of the consolidation of lithospheric plates during the formation of the Pangea supercontinent.

4. Overprint of rocks during the Variscan orogeny

The first study into the problem of remagnetization of the Barrandian rocks during the Variscan orogeny was focused on the remagnetization of the Devonian rocks (Chlupáč – Krs 1967). The results obtained were similar to those found in other regions by Chamalaun – Creer (1963, 1964). Rocks of the „red beds" type are, in cases where they are represented by porous sandstones, especially susceptible to remagnetization. Exogenous factors like various types of atmospheric influence or water circulation with dissociated oxygen lead to the generation of chemoremanent magnetization, usually with hard magnetic properties and with high unblocking temperatures (as in the case of haematite, Krs 1967).

However, all the earlier palaeomagnetic data (*1-6* in Table 5, and *8-13* in Table 6) were derived from rocks which had been subjected to thorough tests of palaeomagnetic stability using alternating and above all, thermal fields. Some of the earlier findings have recently been verified by new methods which make use of the recently developed MAVACS demagnetizer (Příhoda et al. 1989). Multi-component analysis methods were introduced utilizing PCA (principal componennt analysis) and LINEFIND algorithms by Kirschvink (1980); Kent – Briden – Mardia (1983), respectively. For the test, rocks were chosen with exceptionally high portions of secondary magnetization components; the MAVACS apparatus ma-

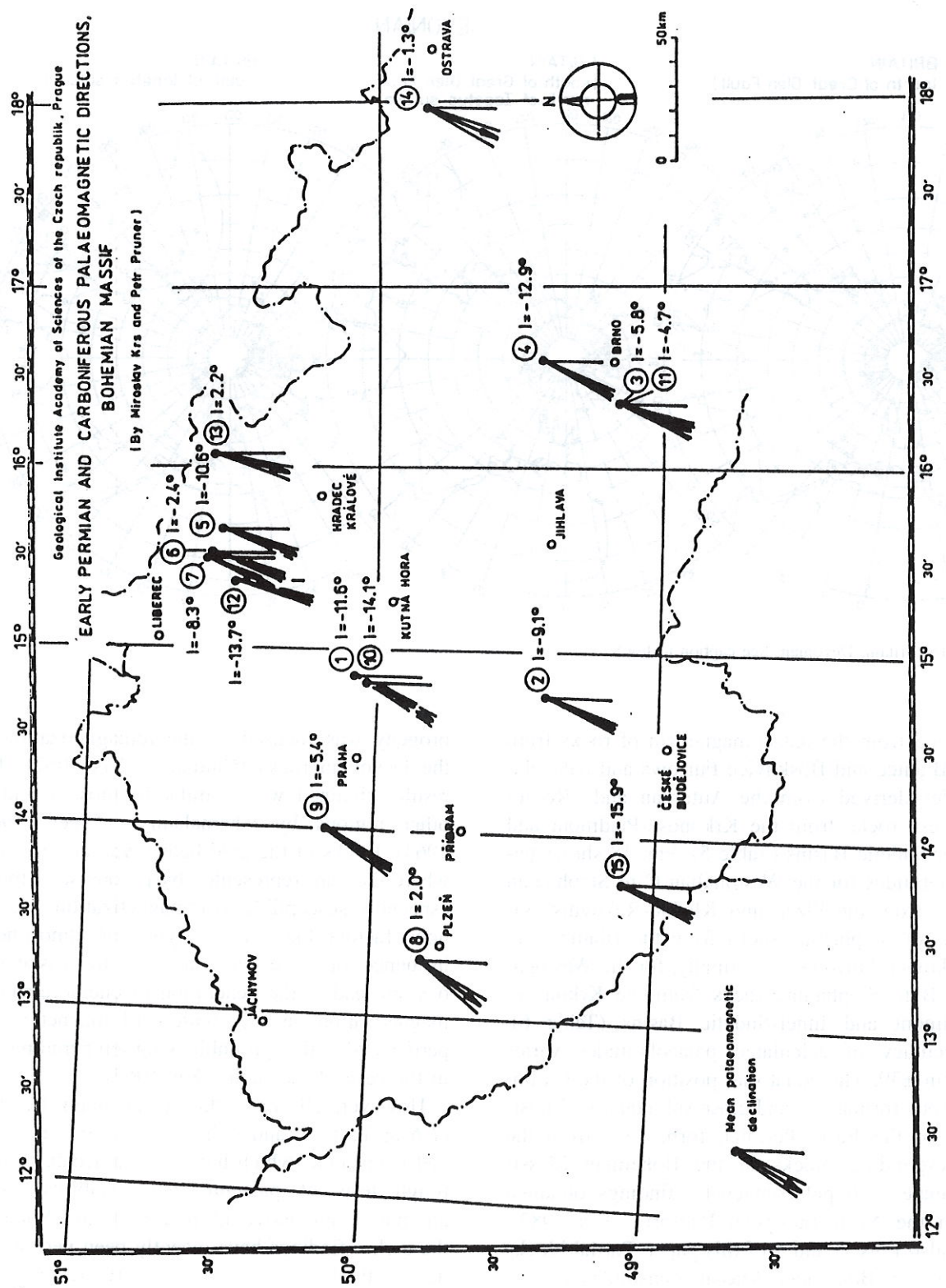

Fig. 16. Bohemian Massif, Czech part: palaeomagnetic directions for rocks of the Early Permian (*1-7*), the Late Carboniferous (*8-13*) and of the Late Visean (*14*). *15* – palaeomagnetic direction derived on augite microgranodiorite at Nezdice near Kašperské Hory of presumably Early Permian age. *Early Permian*: *1, 2* – Blanice furrow, northern and southern parts, Autunian, red sediments; *3, 4* – Boskovice furrow, southern and central parts, Autunian, red sediments; *5* – Krkonoše Piedmont Basin, Late and Middle „Rotliegendes", red sediments; *6* – Krkonoše Piedmont Basin, Early „Rotliegendes", red sediments; *7* – Krkonoše Piedmont Basin, Autunian, oil-shales. *Carboniferous: 8* – Plzeň Basin, Wesphalian C – Stephanian, red sediments; *9* – Kladno-Rakovník Basin, Westphalian C – Stephanian, red sediments; *10* – Blanice furrow, northern part, Stephanian, red sediments; *11* – Boskovice furrow, southern part, Stephanian, red sediments; *12* – Krkonoše Piedmont Basin, Stephanian, red sediments; *13* – Inner Sudetic Basin, Westpalian B – Stephanian, red sediments, tuffs; *14* – Moravian-Silesian region, Late Visean, prevailingly roof shales

Table 5. Bohemian Massif: Early Permian basic palaeomagnetic data

Region	Reference No., see Fig.1	Age, lithology	Geographic co-ordinates		Mean palaeomagnetic directions		α_{95}(°)	k	n	Palaeomagnetic pole positions		Ovals of confidence		Reference
			φ(°)N	λ(°)E	D(°)	I(°)				φ_p (°)N	λ_p (°)E	dm(°)	dp (°)	
Blanice furrow, northern part	1	Autunian, red beds	50.07	14.87	207.71	-11.56	3.56	38.49	43	40.04	157.70	3.61	1.84	M.Krs, 1968
Blanice furrow, southern part	2	Autunian red beds	49.38	14.78	204.06	-9.14	1.99	154.07	34	40.80	162.31	2.01	1.01	M.Krs, 1968
Boskovice furrow, southern part	3	Autunian, red beds	49.15	16.35	201.17	-5.77	3.13	53.28	40	40.34	168.11	3.14	1.58	M.Krs, 1968
Boskovice furrow, central part	4	Autunian, red beds	49.48	16.62	207.26	-12.91	3.54	37.10	45	41.33	159.32	3.61	1.84	M.Krs, 1968
Krkonoše Piedmont Basin	5	Late and Middle "Rotliegendes", red beds	50.53	15.65	199.91	-10.62	3.70	13.52	116	41.85	168.58	3.75	1.90	M.Krs, 1968
Krkonoše Piedmont Basin	6	Early "Rotliegendes", red beds	50.57	15.53	200.15	-2.41	2.77	30.29	89	37.76	169.70	2.77	1.39	M.Krs, 1968
Krkonoše Piedmont Basin	7	Autunian, oil shales	50.624	15.599	Calculation was carried out using virtual pole positions (N=5)					40.12	167.22	α_{95} = 5.3°		M.Krs et al, 1992 a
Nezdice near Kašperské Hory	15	Most probably Early Permian	49.106	13.749	Calculation was carried out using virtual pole positions (N=3)					42.2	157.9	α_{95} = 15.1°		M. Krs, S.Vrána, 1993

n-number of strata; N-number of sites

Table 6. Bohemian Massif: Carboniferous basic palaeomagnetic data

Region	Reference No., see Fig.1	Age, lithology	Geographic co-ordinates		Mean palaeomagnetic directions		α_{95}(°)	k	n, N	Palaeomagnetic pole positions		Ovals of confidence		Reference
			φ(°)N	λ(°)E	D(°)	I(°)				φ_p (°)N	λ_p (°)E	dm(°)	dp (°)	
Plzeň Basin	8	Westphalian C--Stephanian, red beds	49.82	13.33	214.65	2.05	5.09	12.95	n=65	31.13	151.72	5.09	2.55	M.Krs, 1968
Kladno--Rakovník Basin	9	Westphalian C--Stephanian, red beds	50.17	14.00	211.72	-5.41	2.59	42.02	n=73	35.49	153.83	2.60	1.30	M.Krs, 1968
Blanice furrow, northern part	10	Stephanian, red beds	50.03	14.82	210.25	-14.05	3.06	90.73	n=25	40.22	153.92	3.13	1.60	M.Krs, 1968
Boskovice furrow, southern part	11	Stephanian, red beds	49.15	16.35	200.92	-4.73	3.94	33.97	n=40	39.92	168.63	3.95	1.98	M.Krs, 1968
Krkonoše Piedmont Basin	12	Stephanian, red beds	50.50	15.38	195.10	-13.66	3.42	31.22	n=57	44.65	174.07	3.49	1.78	M.Krs, 1968
Inner-Sudetic Basin	13	Westphalian B--Stephanian, red beds, tuffs	50.58	16.08	196.19	2.20	4.54	12.01	n=88	36.50	175.79	4.54	2.27	M.Krs, 1968
Moravian--Silesian region	14	Late Visean, prevailingly roof shales	49.84	17.98	205.4	-1.3	6.5	—	N=17	36.24	165.85	6.50	3.25	M.Krs et al. 1993

n-number of strata; N-number of sites

Table 7. Bohemian Massif (Barrandian, Moravian Zone): Devonian palaeomagnetic data

Region	Reference No.	Age, lithology	Geographic co-ordinates		Mean palaeomagnetic directions		α_{95} (°)	k	n,N	Palaeomagnetic pole positions		Ovals of confidence		Reference
			φ (°)N	λ (°)E	D(°)	I(°)				φ_p (°)	λ_p (°)	dm (°)	dp (°)	
Moravian Zone, Křtiny, Quarry	16	Famennian, limestone	49.143	16.737	133.9	-19.1	5.8	25.9	n=25	35.17 S	77.03 E	6.05	3.15	Unpublished data
Moravian Zone, Josefov	17	Givetian, limestone	49.142	16.691	111.4	-24.4	6.0	11.7	n=52	23.58 S	98.89 E	6.43	3.44	Unpublished data
Moravian Zone, Celechovice	18	Eifelian, limestone	49.532	17.087	104.8	-31.1	4.0	39.2	n=34	22.24 S	107.17 E	4.47	2.50	Unpublished data
Prague Basin	19	Early Devonian, mainly Pragian, limestone	50.005	14.299	203.6	-32.1	4.73	19.5	n=49	52.30 S	24.36 W	5.33	3.00	I.Chlupáč et al., 1990
					202.2	-31.5	11.1	37.4	N=6	52.50 S	22.11 W	12.45	6.98	

n- number of strata; N-number of sites

de it possible to clean the tested rocks efficiently. For instance, in the case of the Hynčice locality (the north-eastern part of the Inner-Sudetic Basin), the following coordinates for the Autunian sediments were derived: φ_p = 40.92°N, λ_p = 165.96° E, dm = 16.54°, dp = 8.37° and the result is in good accord with the findings presented in Table 5; see Krs – Chvojka – Valín (1988). The laboratory thermal-cleaning methods implemented were reaching temperatures up to the unblocking temperature for haematite (less than 680 °C).

Another important criterion for verification of reliability of palaeomagnetic data is investigation of rocks of different origin. For example, in Fig. 19, results of Thellier – Thellier's (1959) method applied to calculation of palaeogeomagnetic field intensity are presented for a sample of ingimbrite of the Autunian age from the Hynčice locality. As it can clearly be seen in the figure, the single-component magnetization is of primary (thermoremanent) origin and it was not remagnetized by any thermal fields (below the unblocking temperature of haematite) in its geological history (Krs 1969). Any kind of remagnetization by thermal fields with temperatures over 680 °C can be ruled out on the basis of other criteria (geological and petrological).

Rocks with micro-organic matter frequently contain ferrimagnetic minerals greigite and smythite of bacterial origin (Krs et al. 1990, 1992b). In accordance with their thermal history, such rocks may contain other minerals – thermal alteration products (pyrrhotite, α-Fe_2O_3; γ-Fe_2O_3; η-Fe_2O_3 and magnetite depending on redox conditions). These rocks are represented by a whole range of petrographic types (oil-, bituminous, black, coal-bearing, roof shales, etc.). For our palaeomagnetic investigations, it was decided to collect oil-shales of the Autunian age from the Krkonoše-Piedmont Basin (Krs et al. 1992a). Samples were taken from the Rudnice horizon located in the lower section of the Vrchlabí Formation. Remanence directions of natural samples and of thermally treated samples (200, 330 °C) and mean site directions are presented in Fig. 20. Each sample was subjected to remanence analysis and laboratory thermal demagnetization, an example of the analysis is presented for the sample No 5784 A1 in Fig. 21. A characteristic magnetization component is detectable within the temperatures ranging from 200 to 420 °C, its XY and XZ components are oriented towards the origin of coordinates even in temperatures higher than 420 °C. Palaeomagnetic data derived on the Autunian oil-shales are in good agreement with analogous data derived on surrounding „red beds", see Table 5.

In the area of Nezdice, in the vicinity of Kašperské Hory, southern Bohemia, an investigation was carried out on samples of a massive unweathered augite microgranodiorite (Krs – Vrána 1993). The samples were collected at three sites, site means of remanence directions of thermally treated samples are presented in Fig. 22. Magnetization and palaeomagnetization components are, principally, carried by pyrrhotite. In temperatures exceeding the unblocking temperature for pyrrhotite, a small component parallel to the direction of remanent magnetic polarization of pyrrhotite was found. This component corresponds to the magnetization of an Fe-oxide rich in Ti. The palaeomagnetic pole position derived is in good correlation with pole positions derived on the Variscan Formations from the Bohemian Massif; most closely it corresponds to the Early Permian pole positions. All the samples were tested with progressive thermal demagneti-

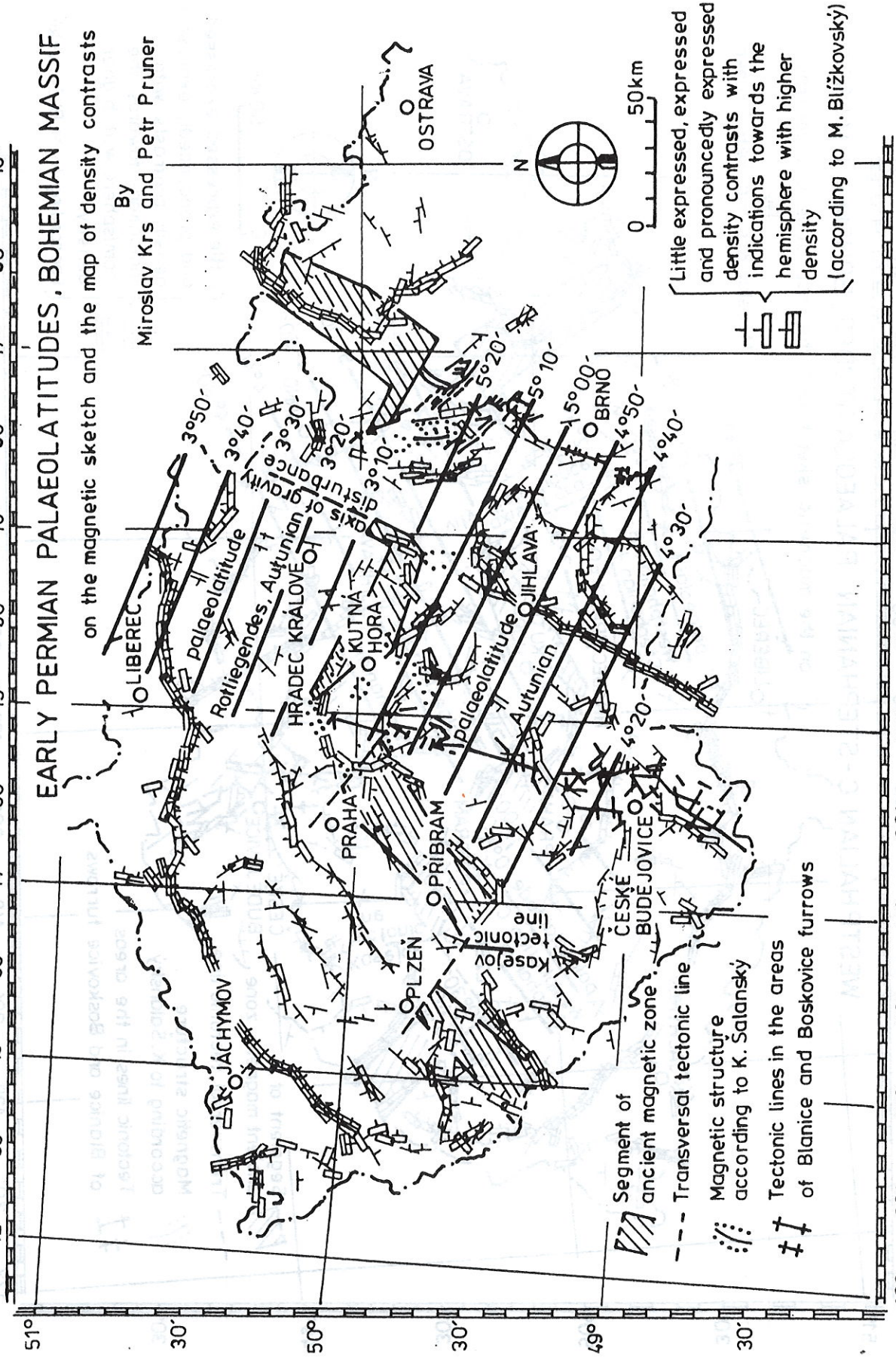

Fig. 17. Bohemian Massif: palaeogeographical latitudes derived on Early Permian rocks, Autunian, a wider area of the Blanice and Boskovice furrows; „Rotliegendes", Autunian, Krkonoše Piedmont and Inner Sudetic Basins

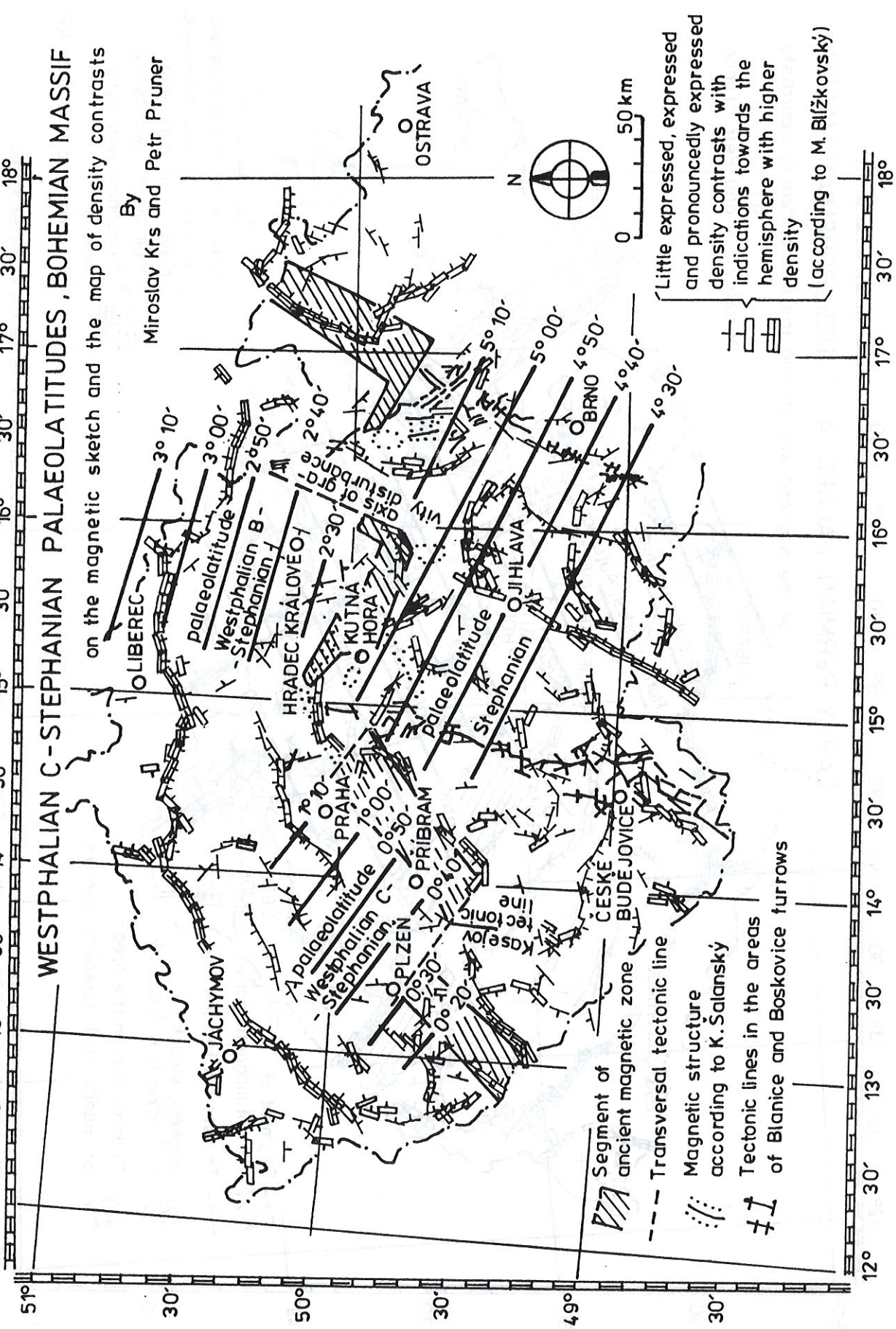

Fig. 18. Bohemian Massif: palaeogeographical latitudes derived on Late Carboniferous rocks of three blocks. Westphalian C to Stephanian, a wider area of the Plzeň and Kladno-Rakovník Basins; Stephanian, a wider area of the Blanice and Boskovice furrows; Westphalian B to Stephanian, Krkonoše Piedmont and Inner Sudetic Basins

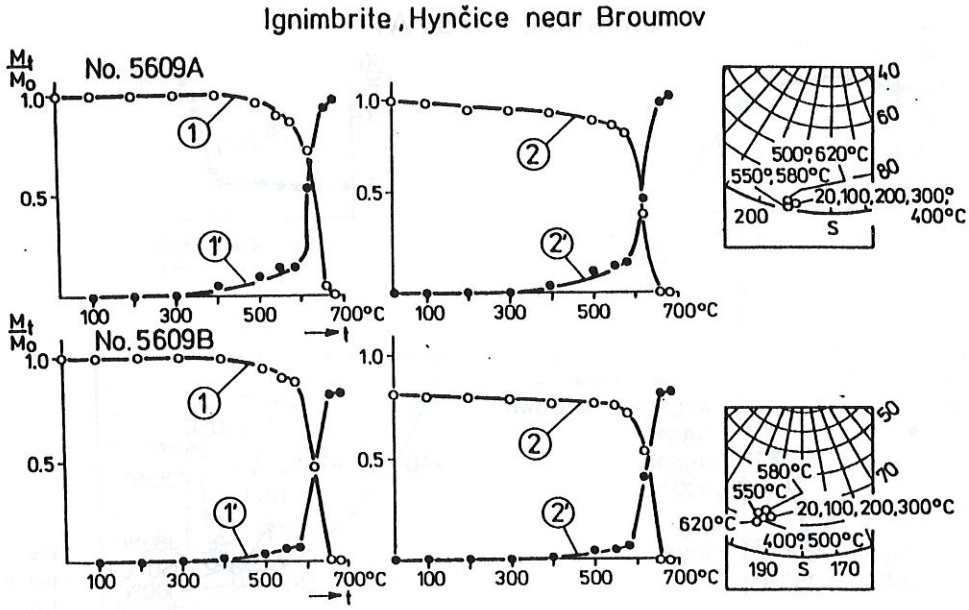

Fig. 19. Double-heating method applied to Autunian ignimbrite sample, Hynčice near Broumov. M_t – remanent magnetic moment of the sample thermaly demagnetized at temperature t; M_0 – natural remanent magnetic moment; 1-1': the first cycle of laboratory demagnetization and magnetization; 2-2': the second cycle of laboratory thermal treatment of the same sample (Krs 1969)

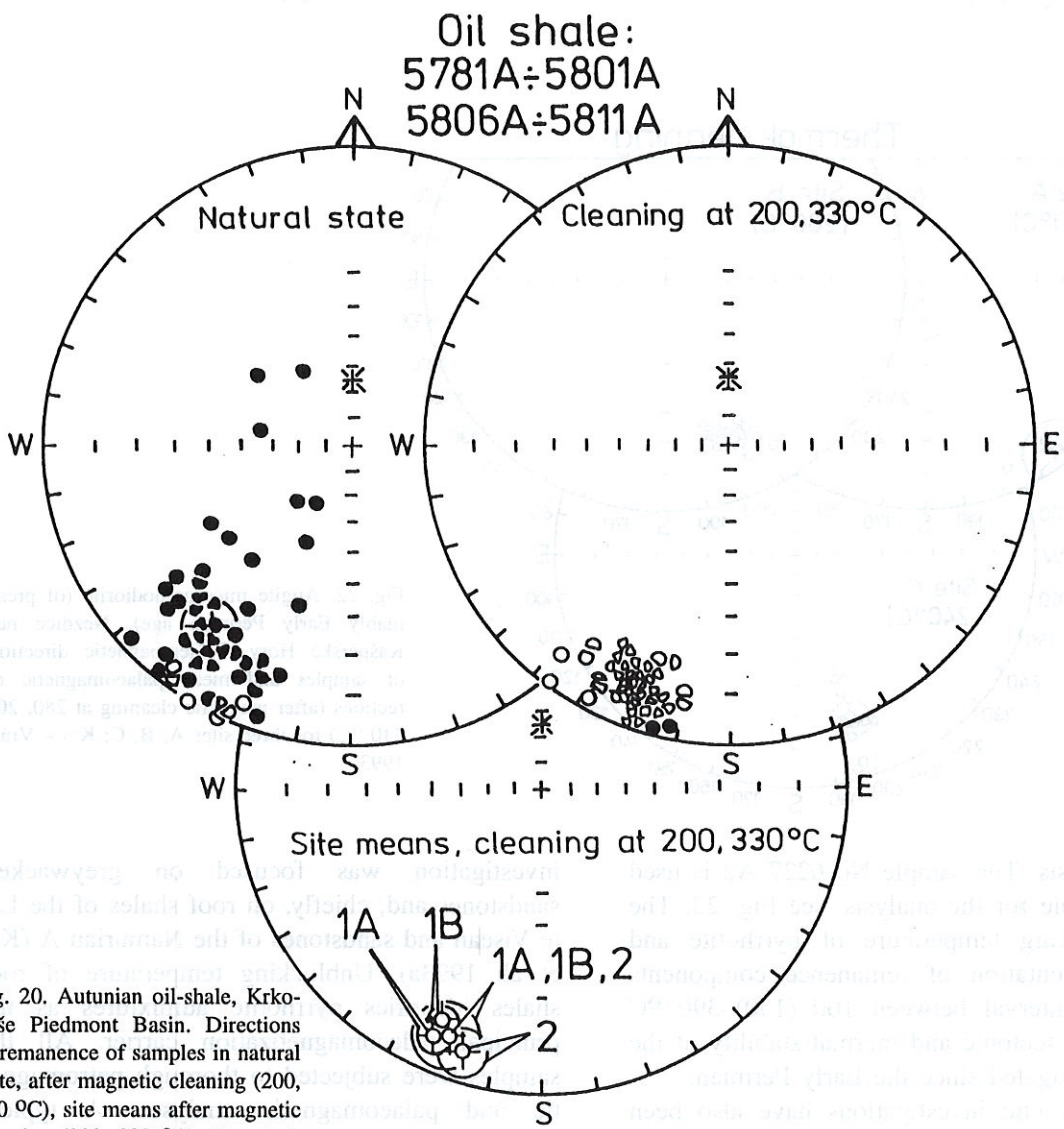

Fig. 20. Autunian oil-shale, Krkonoše Piedmont Basin. Directions of remanence of samples in natural state, after magnetic cleaning (200, 330 °C), site means after magnetic cleaning (200, 330 °C); Krs et al. 1992a

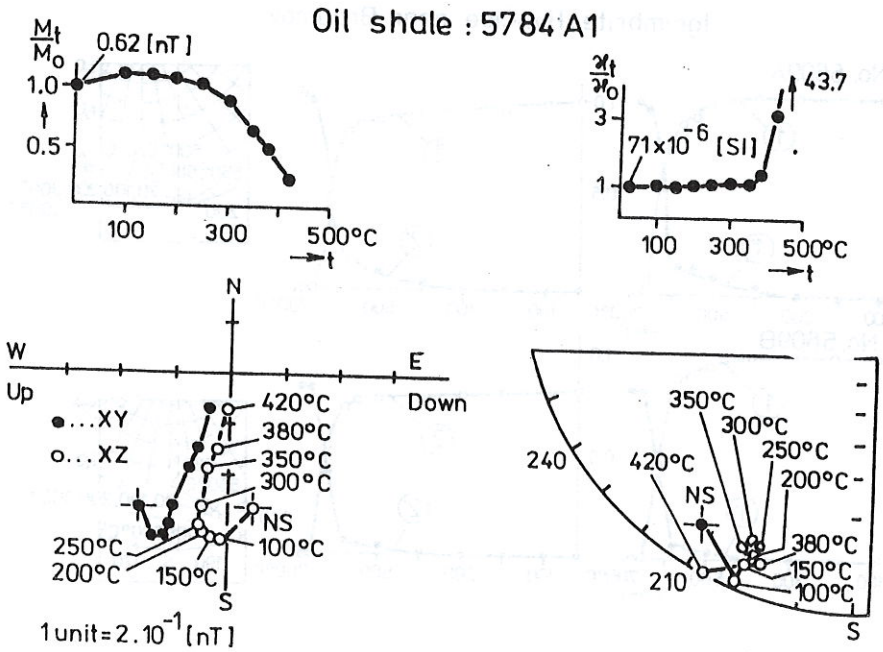

Fig. 21. Thermal demagnetization of Autunian oil-shale, Vrchlabí, road cutting; Krs et al. 1992a

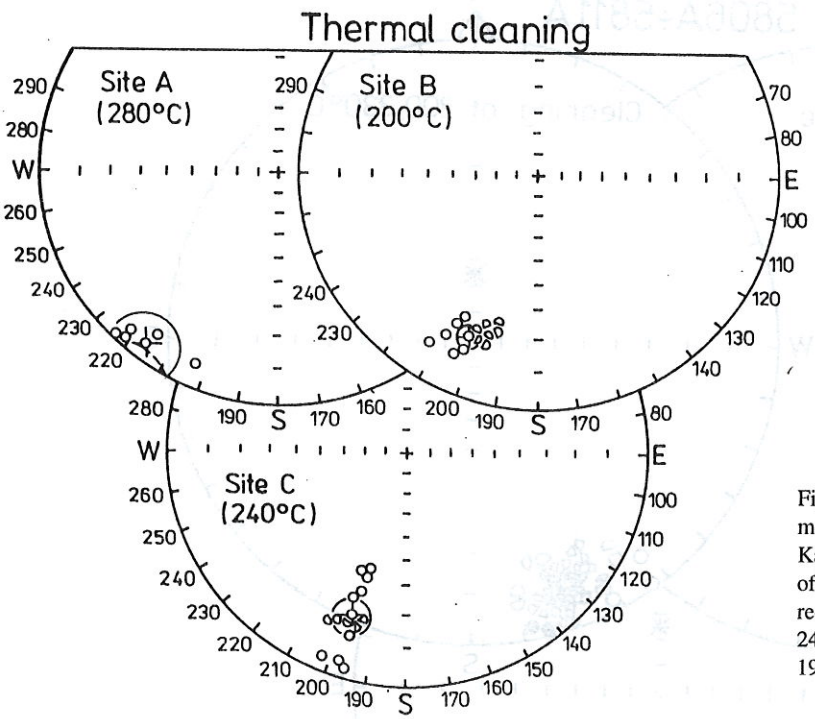

Fig. 22. Augite microgranodiorite (of presumably Early Permian age), Nezdice near Kašperské Hory. Palaeomagnetic directions of samples and mean palaeomagnetic directions (after magnetic cleaning at 280, 200, 240 °C) for three sites A, B, C; Krs – Vrána 1993.

zation analysis. The sample No 6227 A2 is used as an example for the analysis, see Fig. 23. The low unblocking temperature of pyrrhotite and identical orientation of remanence components within the interval between 100 (150)–390 °C indicates the tectonic and thermal stability of the region investigated since the Early Permian.

Palaeomagnetic investigations have also been carried out in the Moravian-Silesian Zone including the Upper-Silesian Black-coal Basin. The investigation was focused on greywackes, sandstones and, chiefly, on roof shales of the Late Visean and sandstones of the Namurian A (Krs et al. 1993a). Unblocking temperature of roof shales identifies pyrrhotite admixtures as the principal palaeomagnetization carrier. All the samples were subjected to thorough petromagnetic and palaeomagnetic analyses. A typical example, the analysis of the sample of a roof shale from Lhotka – Nové Těchanovice locality is

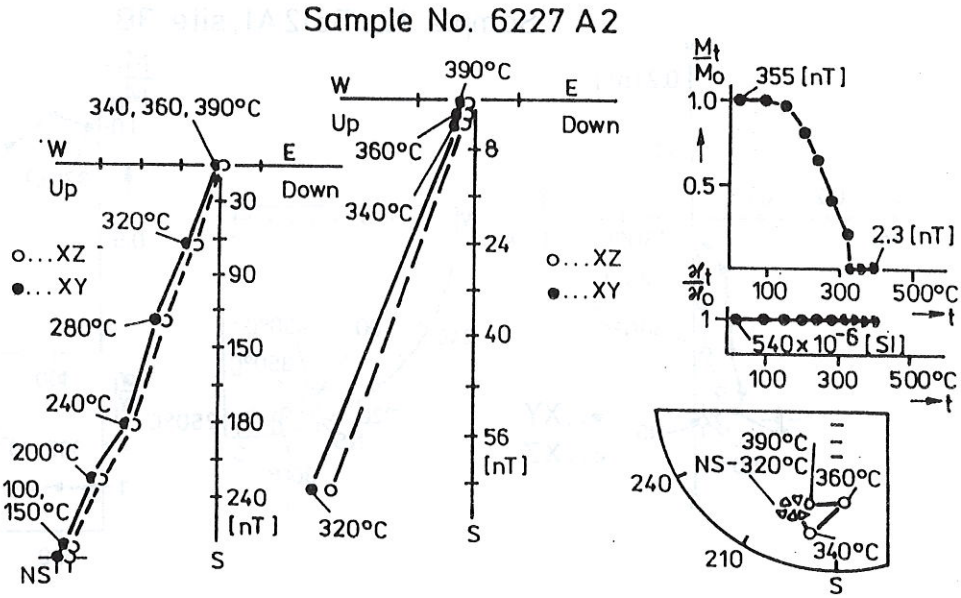

Fig. 23. Augite microgranodiorite, Nezdice near Kašperské Hory. Results of progressive thermal demagnetization by means of the MAVACS apparatus; Krs – Vrána 1993

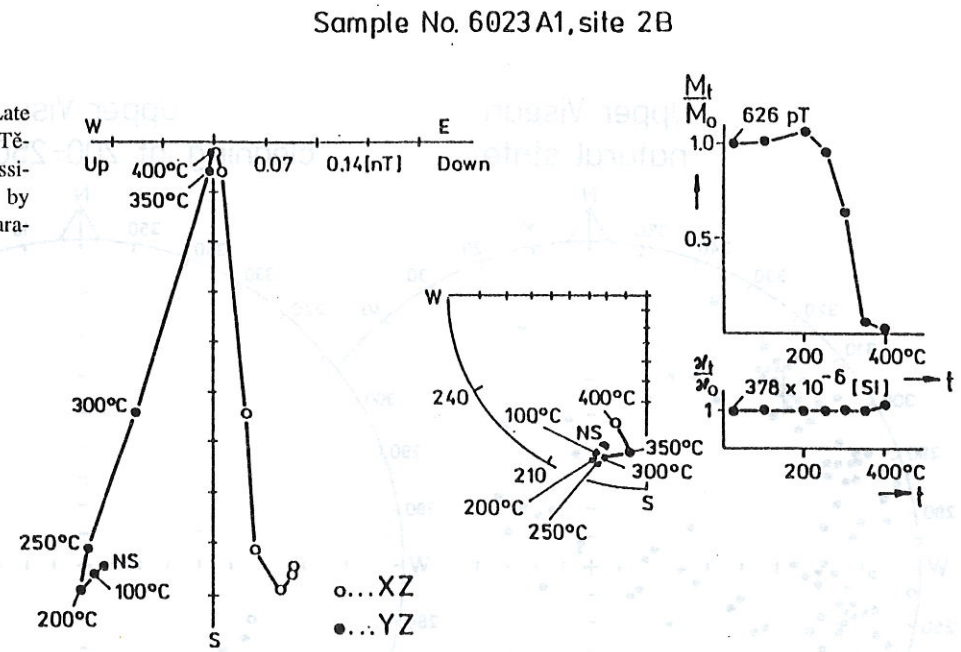

Fig. 24. Roof shale of the Late Visean age, Lhotka – Nové Těchanovice. Results of progressive thermal demagnetization by means of the MAVACS apparatus, Krs et al. 1993a

presented in Fig. 24. The sample was collected from the underground workings of a gallery 50 m under the surface, from the Moravice Formation. Even though the unblocking temperature identifies pyrrhotite as the main magnetization and palaeomagnetization carrier, remanence direction is identical to characteristic remanence direction starting from 200 °C up to 400 °C. The results of thermal demagnetization of the greywacke sample from Vondruška's Quarry near the Budišovice settlement (the Late Visean, the lower section of the Kyjovice Formation) are presented in Fig. 25. In this as well as in other cases, the samples of sandstones and greywackes show remanence directions identical to the characteristic remanence direction up to temperatures of 430 °C. Fig. 26 shows a stereographic projection of directions of natural remanent magnetic polarization (J_n) on the left-hand side and the directions of remanence of thermally cleaned samples on the right-hand side. Fig. 27 shows the remanence direction means for respective sites; the localities are denoted by numbers and the sites by letters (Krs et al. 1993a). In spite of the fact that the Moravian-Silesian Zone, including the Upper-Silesian Black-coal Basin, is located in the vicinity of an important lithospheric boundary (the boundary between the North-European Platform

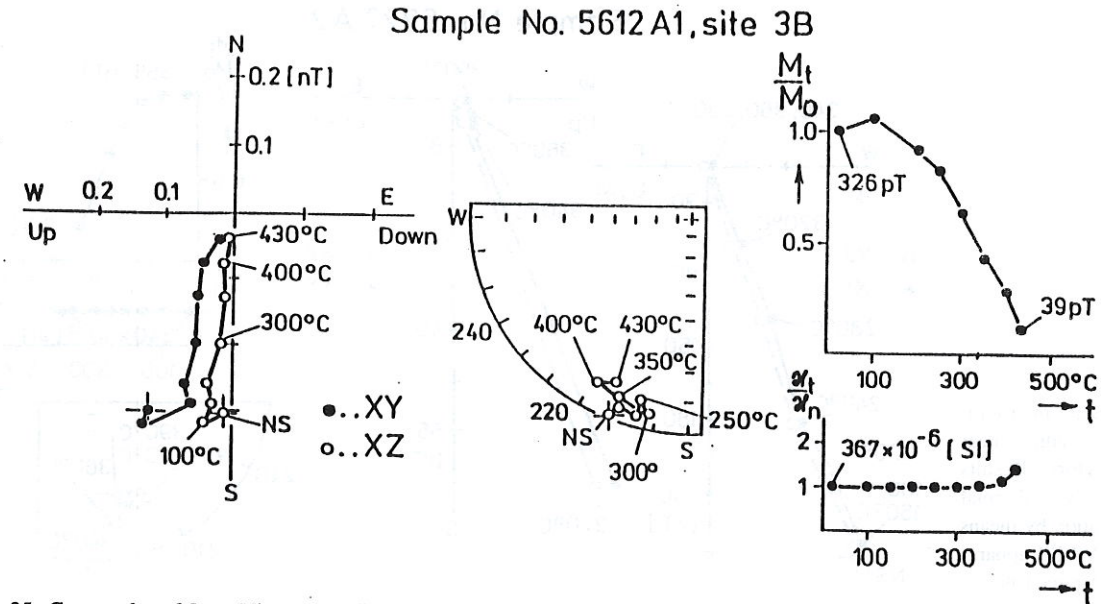

Fig. 25. Greywacke of Late Visean age (lower part of the Kyjovice strata), Vondruška's quarry near Budišovice. Results of progressive thermal demagnetization by means of the MAVACS apparatus, Krs et al. 1993a

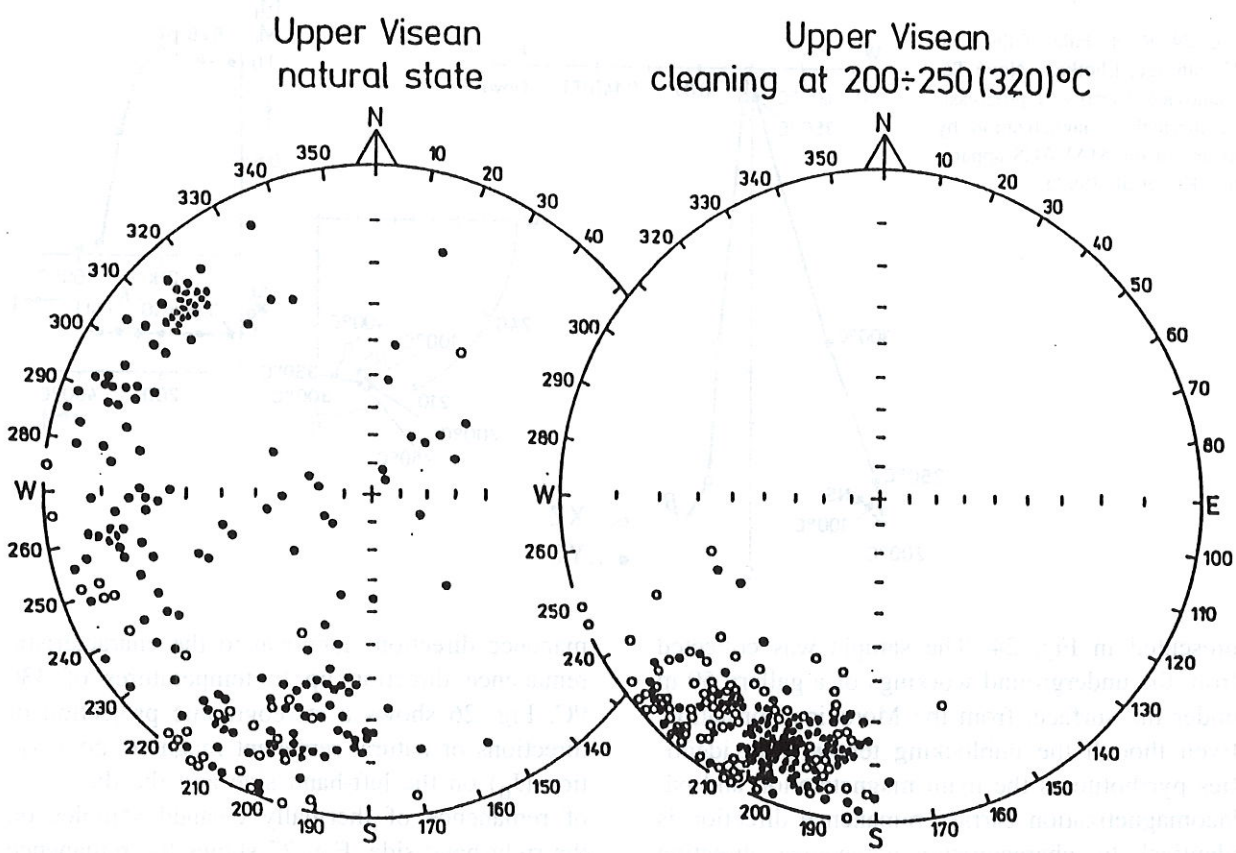

Fig. 26. Roof shales (prevailingly) of Late Visean age, Moravian-Silesian region. Left-hand side: directions of natural remanent magnetic polarization. Right-hand side: directions of remanent magnetic polarization after thermal cleaning at temperature of 200-250 (320) °C, Krs et al. 1993a

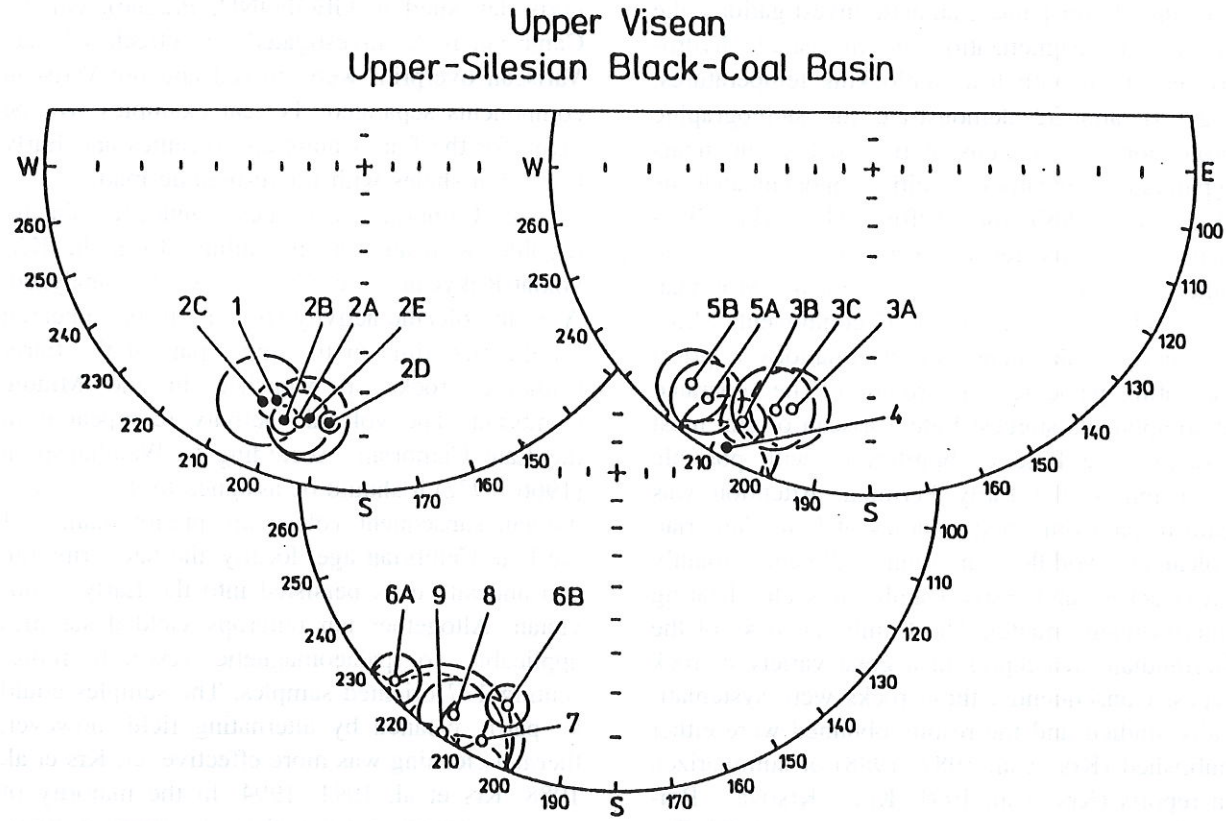

Fig. 27. Roof shales (prevailingly) of Late Visean age, Moravian – Silesian region. Mean palaeomagnetic directions for respective sites (sites means); Krs et al. 1993a

and the Alpine-Carpathian collision zone), the proximity of this boundary does not appear in palaeomagnetic directions, no effects of Alpine tectonics were recognized. Major divergence in palaeomagnetic declinations appears between different sites of the same outcrop (see, for instance, 6A and 6B mean directions in Fig. 27). However, the dominant part of palaeomagnetic directions was derived from rocks with relatively low unblocking temperatures. The fold test could not be applied. For this reason, it will be indispensable to carry out palaeomagnetic investigations on Early and Middle Carboniferous rocks to search for possible remagnetization during the Late Carboniferous or Early Permian.

Examples of Late Variscan overprint may be demonstrated on Devonian limestone samples collected from four of five localities so far studied in the Moravian Zone, the eastern part of the Bohemian Massif: locality Čelechovice na Hané, Late Eifelian to Early Givetian; locality Josefov – Habrůvka, Givetian; locality Křtiny Marble Quarry, Late Famennian; locality Mokrá, Late Frasnian to Early Famennian and locality Lažánky, Givetian. Fine grained magnetite, most probably biogenic magnetite, was found as the principal carrier of palaeomagnetization in limestone samples on four of five localities investigated. The rocks belong to moderately magnetic or even extremely low magnetic materials. Three components of remanence, A-component of viscous origin, B-component of Late Variscan origin and C-component of pre-Variscan or Early Variscan origin were found in moderately magnetic samples of limestones from the localities Čelechovice, Josefov – Habrůvka and Křtiny Marble Quarry. The B-components are very pronounced, they were proved at four localities, and their moduli represent up to 95% of the moduli of total remanent magnetization. The B-components were derived by the process of progressive thermal demagnetization using the MAVACS apparatus at temperature intervals from 150 or 200 °C up to 350 or 400 °C and the C-components were derived at temperature intervals from 400 or 425 °C up to 500 or 530 °C. Typical examples are shown in Fig. 28 for Čelechovice, in Fig. 29 for Josefov – Habrůvka and in Fig. 30 for Křtiny Marble Quarry. The samples from Mokrá showed B-components only, the C-components were not separable due to extremely low values of remanence. The limestone samples from Lažánky are

not suitable for palaeomagnetic investigations, the carriers of magnetization are metastable hydroxides of Fe with low unblocking temperatures. Figs 31 and 32 demonstrate the stereographic projection of directions of B- and C-components separated by means of multi-component analysis (Kirschvink 1980) for Josefov – Habrůvka, Givetian. Analogous results were obtained for the other localities so far studied from the Moravian Zone, cf. Krs et al. 1994. C-components show anomalous palaeomagnetic declinations a priori indicating palaeotectonic rotation. The separated B-components suggest Late Variscan origin, most probably the Late Carboniferous, with possible extension to the Early Permian. Attention was paid to palaeomagnetic studies of Late Cambrian volcanics, Middle Cambrian sediments, mainly greywackes, and Early Cambrian shales bearing micro-organic matter. The Cambrian rocks of the Barrandian area represent a great variety of rock types. Consequently, these rocks were systematically studied and the results obtained were either published (Krs et al. 1987, 1988) or summarized in reports (Krs et al. 1991; Krs – Krsová – Pruner 1993; Krs – Pruner – Krsová 1993, 1994. Reports deposited in GEOFOND, Prague). On the Cambrian rocks investigated, the effects of Late Variscan overprint were proved and pre-Variscan components separated. Typical examples will be given for the Late Cambrian volcanics and Early Cambrian shales with micro-organic matter:

Late Cambrian volcanics (andesite, dacite, rhyolite, with andesite prevailing) from the Křivoklát-Rokycany complex were analyzed. A weak volcanic activity (rhyolite tuffs) appeared for the first time in the upper part of the Early Cambrian rocks, it vanished in the Middle Cambrian. The volcanic activity re-appeared in the Late Cambrian. According to Waldhausrová (1966, 1972) it should be assigned to the post-Cadomian subsequent volcanism, predominantly of the Late Cambrian age; locally, the latest rhyolite and andesite tuffs persisted into the Early Ordovician. Altogether ten outcrops yielded samples applicable to palaeomagnetic research representing 137 oriented samples. The samples could be partly cleaned by alternating field, however, thermal cleaning was more effective, cf. Krs et al. 1988; Krs et al. 1991, 1994. In the majority of samples, the magnetite is the palaeomagnetization

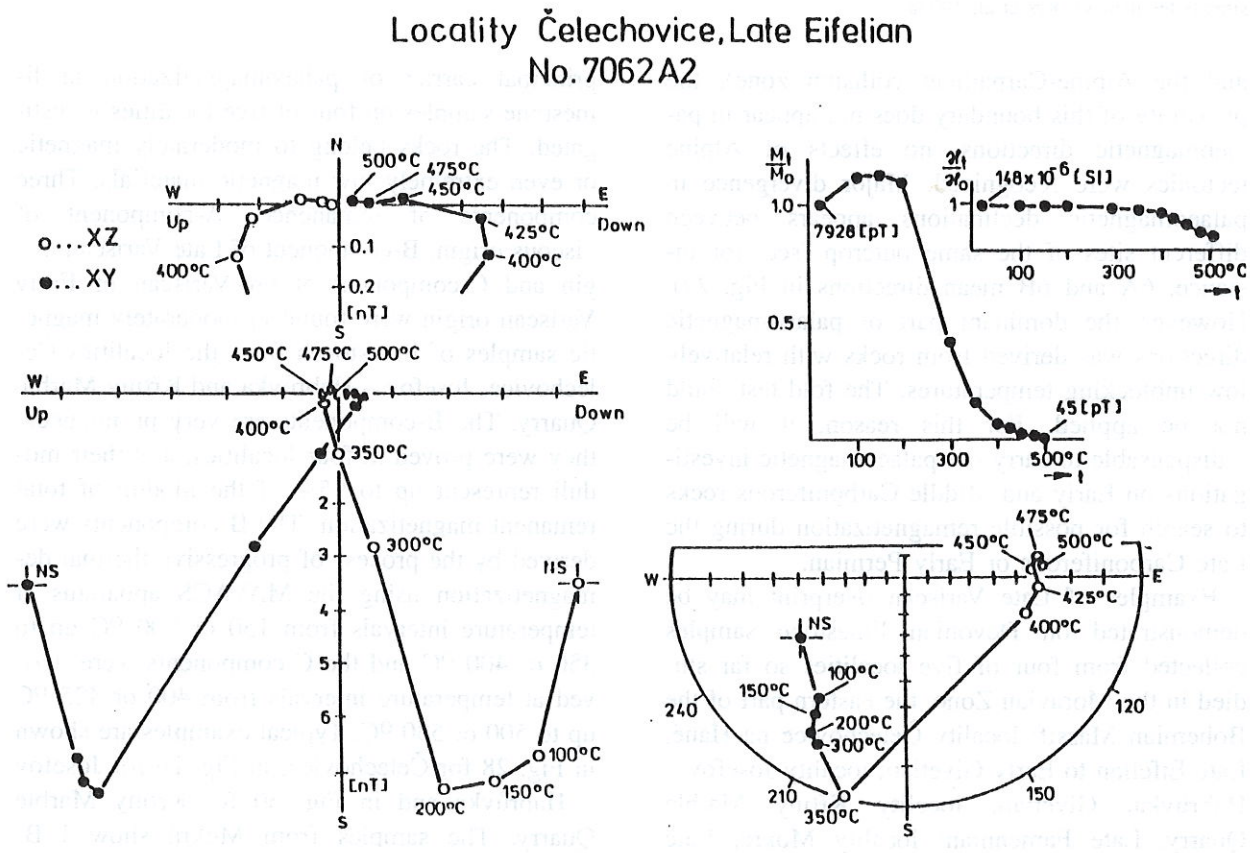

Fig. 28. Limestone of the Late Eifelian age, Čelechovice na Hané, Bohemian Massif, Moravian Zone. Results of progressive thermal demagnetization by means of the MAVACS apparatus

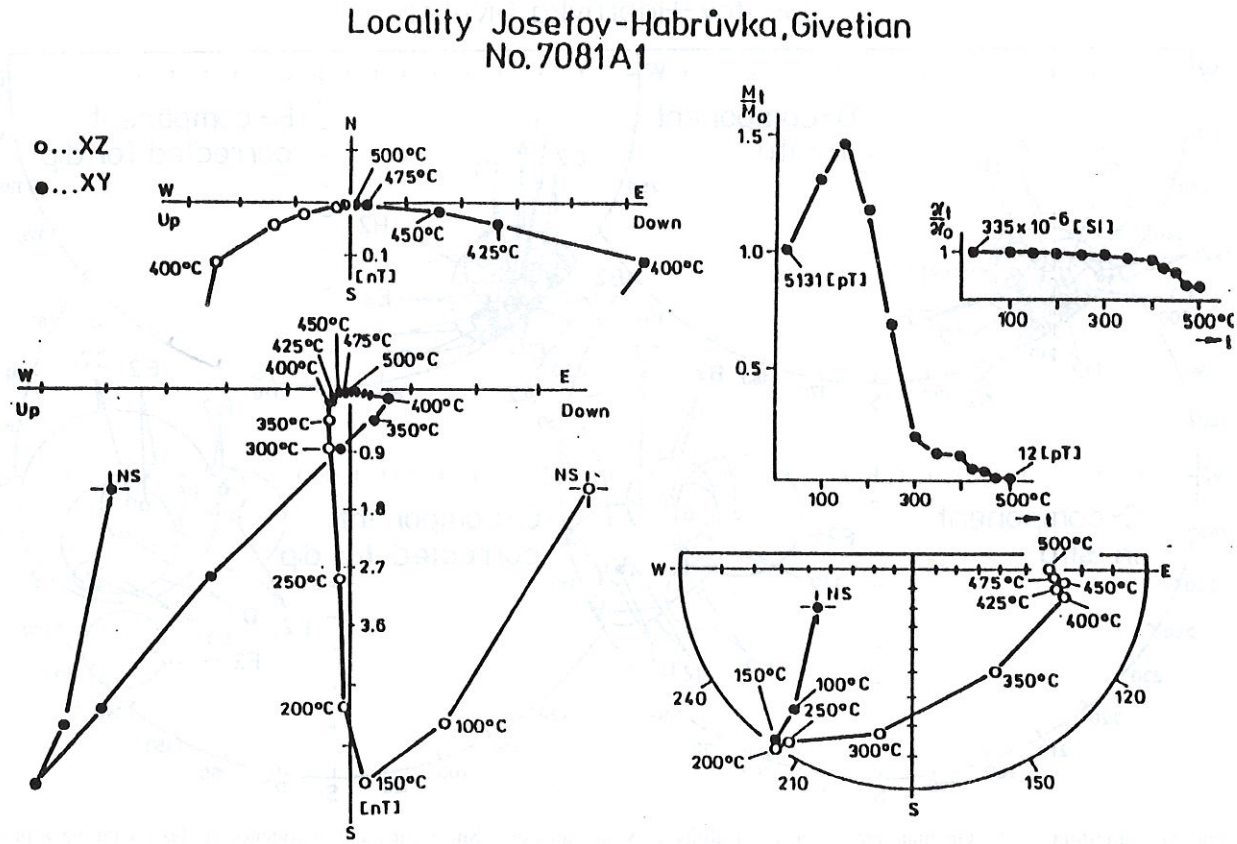

Fig. 29. Limestone of the Givetian age, Josefov – Habrůvka, Bohemian Massif, Moravian Zone. Results of progressive thermal demagnetization by means of the MAVACS apparatus

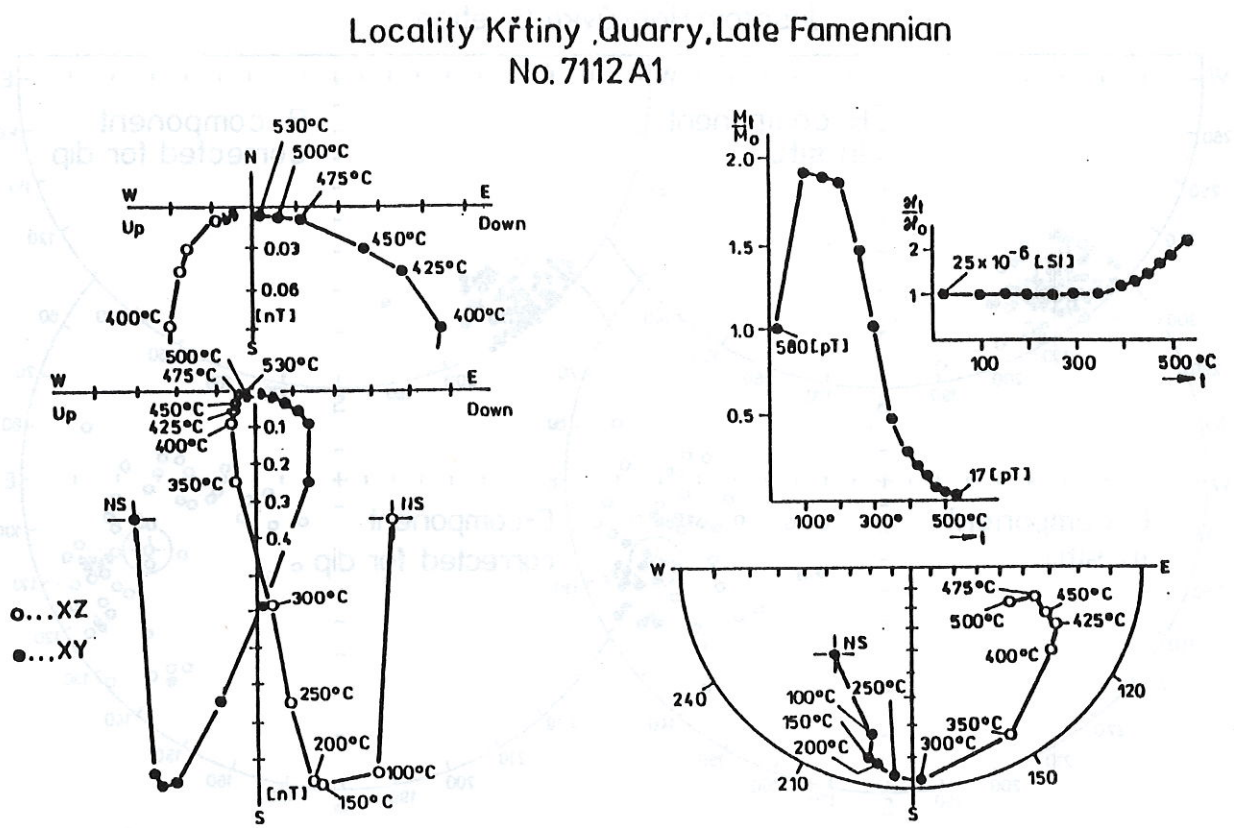

Fig. 30. Limestone of the Late Famennian age, Křtiny Marble Quarry, Bohemian Massif, Moravian Zone. Results of progressive thermal demagnetization by means of the MAVACS apparatus

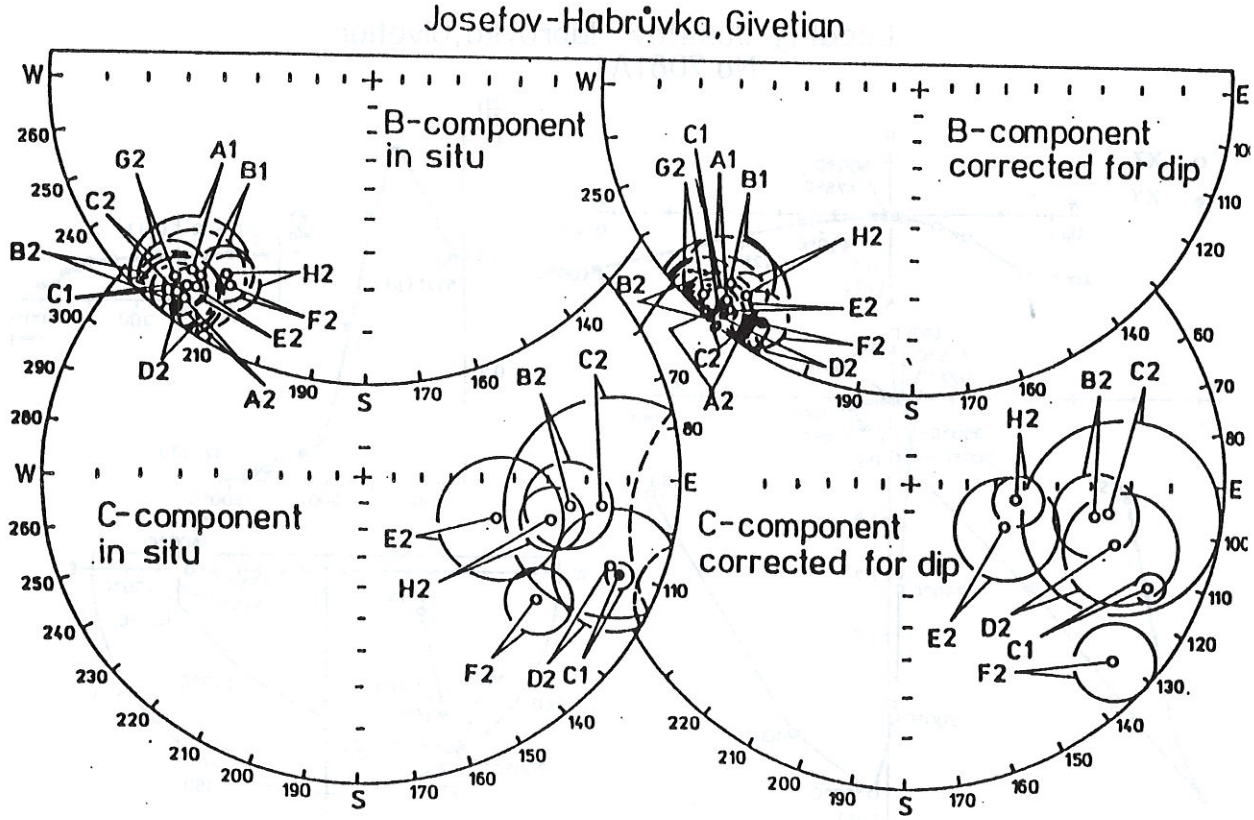

Fig. 31. Limestone of the Givetian age, Josefov – Habrůvka, Moravian Zone. Site means and confidence circles (at the 95% probability level) of directions of B- and C-components of remanence separated by the multi-component analysis. Left-hand side of the Fig.: directions not corrected for dip of rocks (in situ); right-hand side of the Fig.: directions corrected for dip of rocks

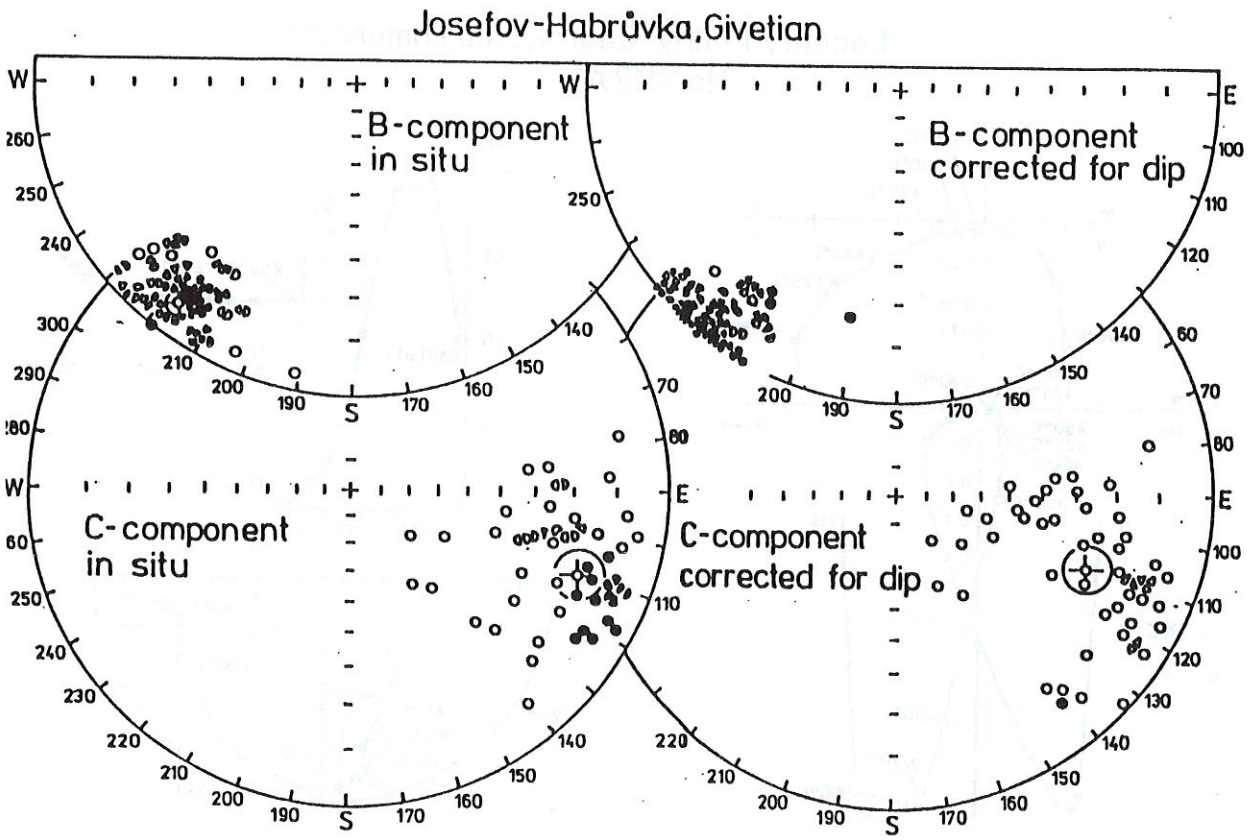

Fig. 32. Limestone of the Givetian age, Josefov – Habrůvka, Moravian Zone. Directions of B- and C-components of remanence of samples collected from strata, mean directions (strata means) and confidence circles, see caption to Fig. 31

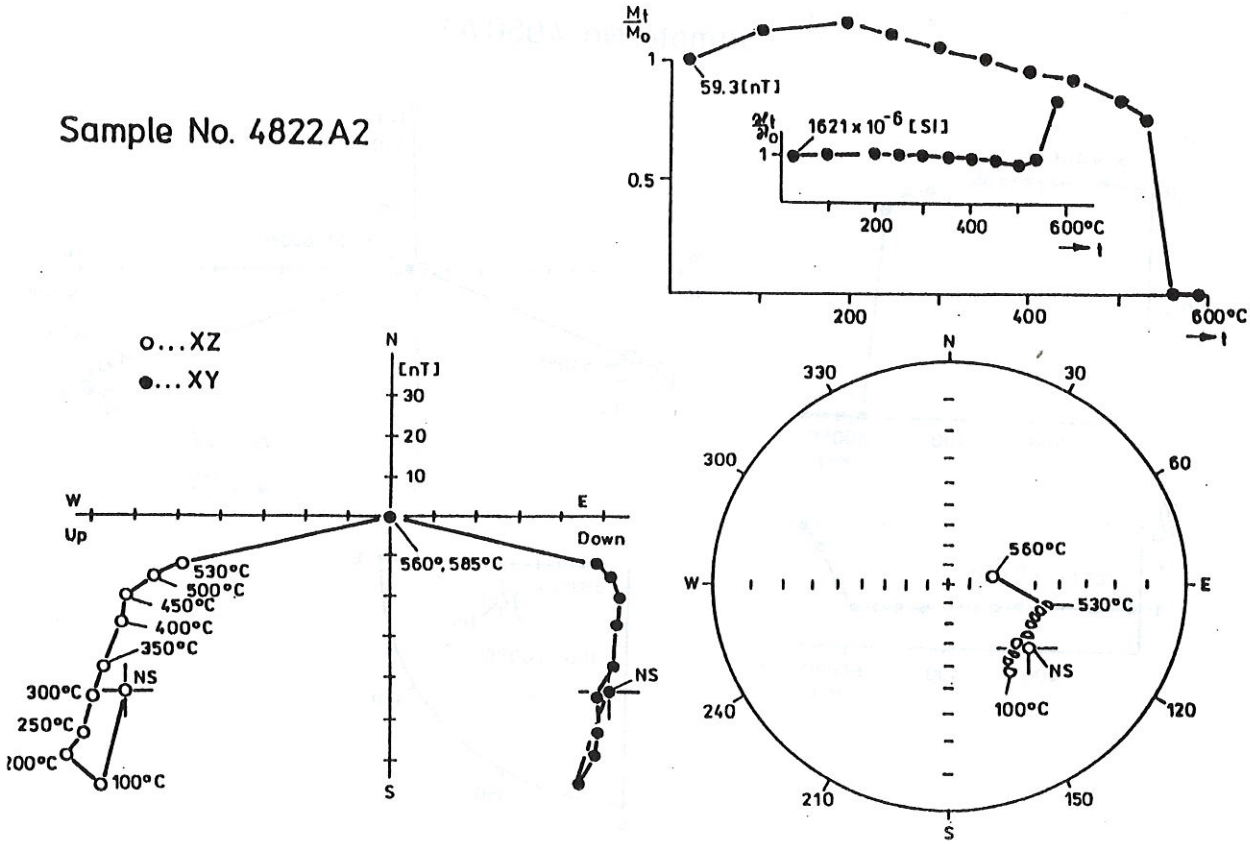

Fig. 33. Andesite of the Late Cambrian age, SSW part of Roztoky, site 4 of Late Cambrian volcanics, Barrandian. Results of progressive thermal demagnetization by means of the MAVACS apparatus

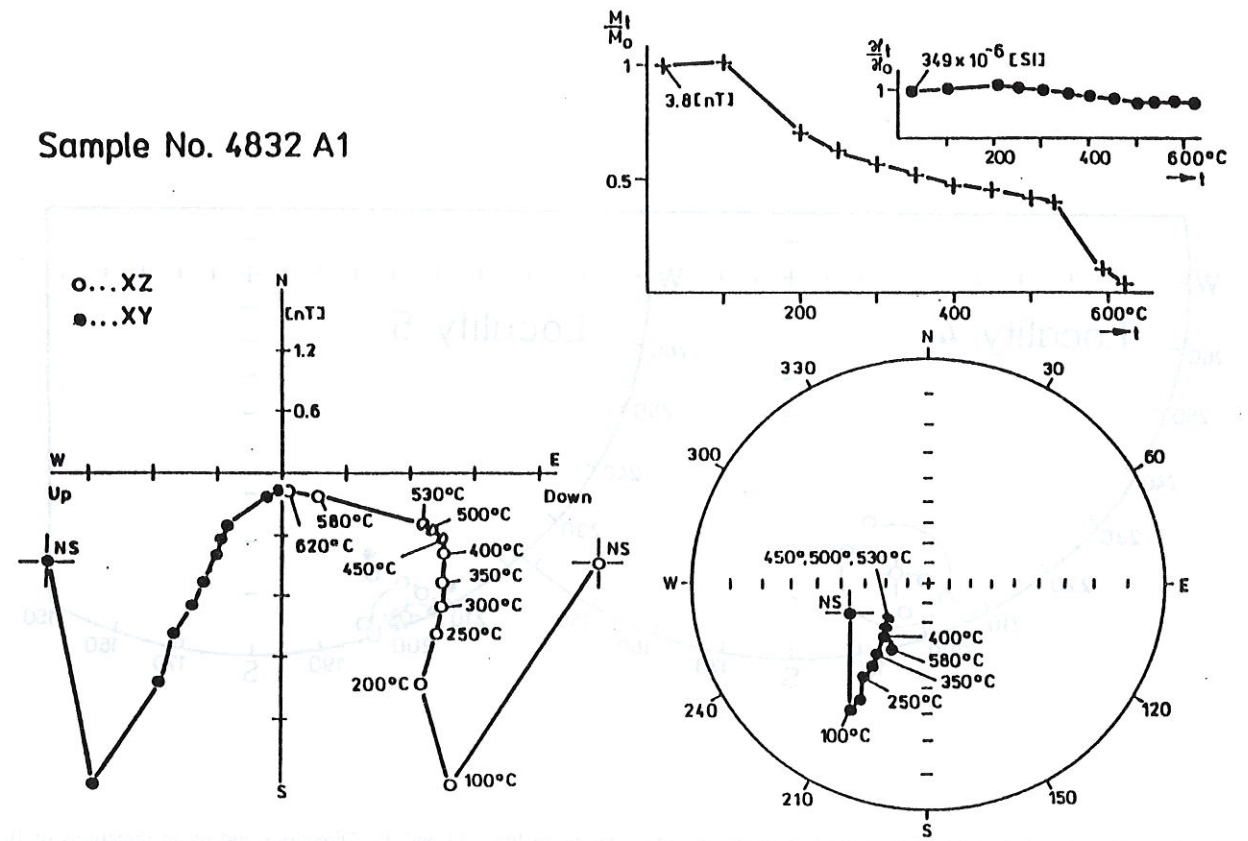

Fig. 34. Rhyolite of the Late Cambrian age, approx. 4 km SE of Skryje, site 5 of Late Cambrian volcanics, Barrandian. Results of progressive thermal demagnetization by means of the MAVACS apparatus

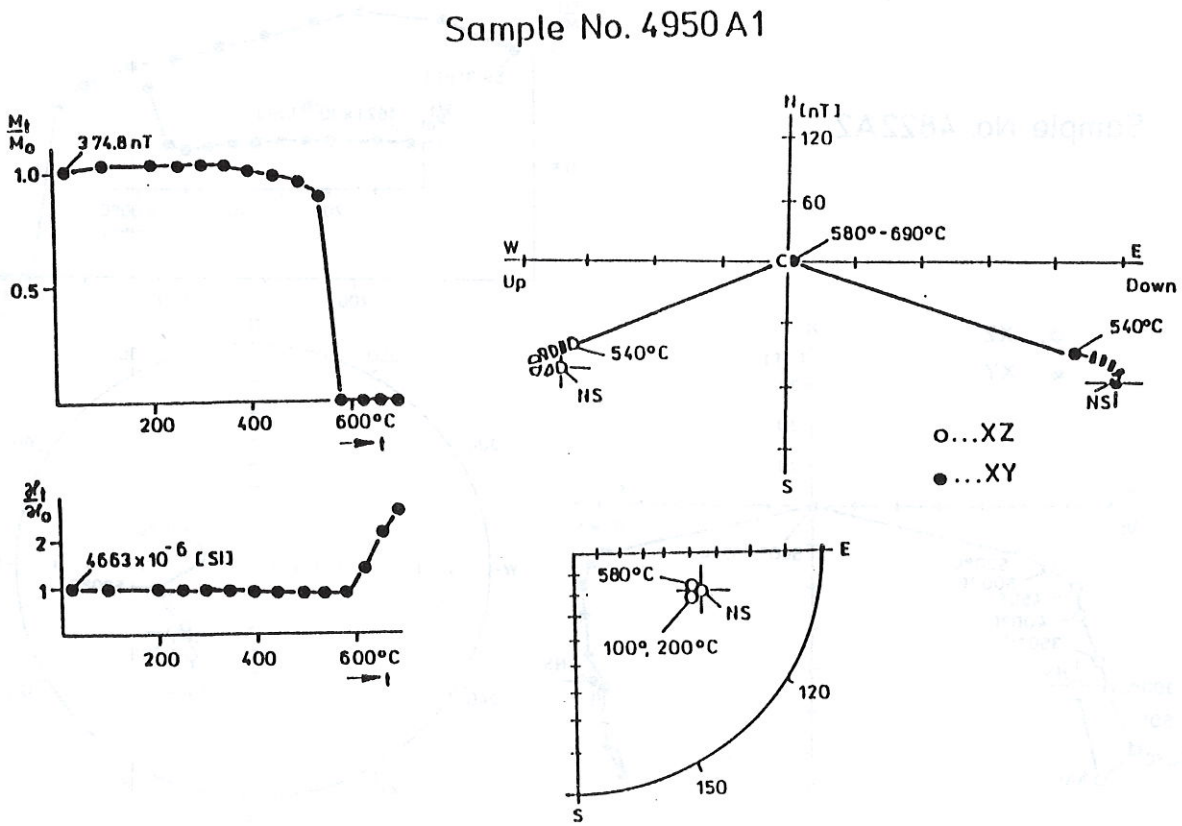

Fig. 35. Andesite of the Late Cambrian age, SSW part of Roztoky, site 8 of Late Cambrian volcanics, Barrandian. Results of progressive thermal demagnetization by means of the MAVACS apparatus

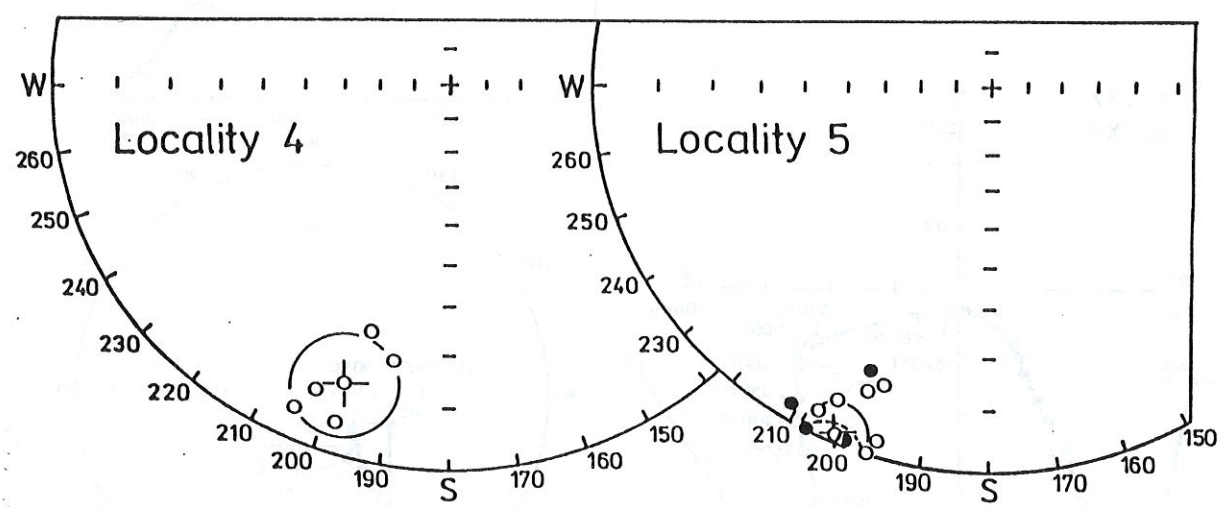

Fig. 36. Andesite and rhyolite of the Late Cambrian age, see captions to Figs. 33 and 34. Directions and mean directions of B-components (Late Variscan components) of remanence separated by the multi-component analysis

carrier, in three outcrops a small portion of haematite appeared, and one outcrop of andesite with haematite was found. A high unblocking temperature of ferrimagnetic minerals was one of basic prerequisites for derivation of palaeomagnetic directions. However, in many samples, clear Late Variscan components of remanence were separated by multi-component analysis (Kirschvink 1980). Typical examples are shown in Figs 33 and 34. On the contrary, few samples showed results indicating high magnetic hardness. Due to the narrow spectrum of high unblocking temperatures, such samples did not record Late Variscan overprint, for a typical example see Fig. 35. Directions of separated Late Variscan components are shown in Fig. 36 for andesite at Roztoky (locality 4) and rhyolite at Skryje (locality 5). This demonstrates that samples used for derivation of Late Cambrian palaeomagnetic directions also contain overprint components of the Late Variscan origin.

Sedimentary rocks containing fossil micro-organic matter are usually suitable for palaeomagnetic research. However, their palaeomagnetization carriers being products of alteration (of original metastable sulphides) may be represented by α-Fe_2O_3, γ-Fe_2O_3, η-Fe_2O_3, or magnetite depending on redox conditions (cf. Krs et al. 1990; Krs et al. 1992b). Shales bearing micro-organic matter were found (by Dr. V. Havlíček) at the locality „Kočka", Brdy Mts. They are part of the Paseky Shale corresponding to the „Hořice – Holšiny" formation, in the middle part of the Early Cambrian rocks of the Barrandian (Krs – Krsová – Pruner 1993). The samples were demagnetized either by means of the alternating field using the Schonstedt GSD-1 apparatus, or by means of thermal demagnetization using the MAVACS system, or by combined procedures. Typical examples are shown in Figs. 37 and 38. Three components (A, B, C) were separated by application of multi-component analysis of remanence. The samples showed only small A-components of viscous origin. All samples, without exception, contain a well pronounced B-component. This component (if considered not corrected for dip of rocks, related to rocks in situ position) shows very shallow inclination values a priori

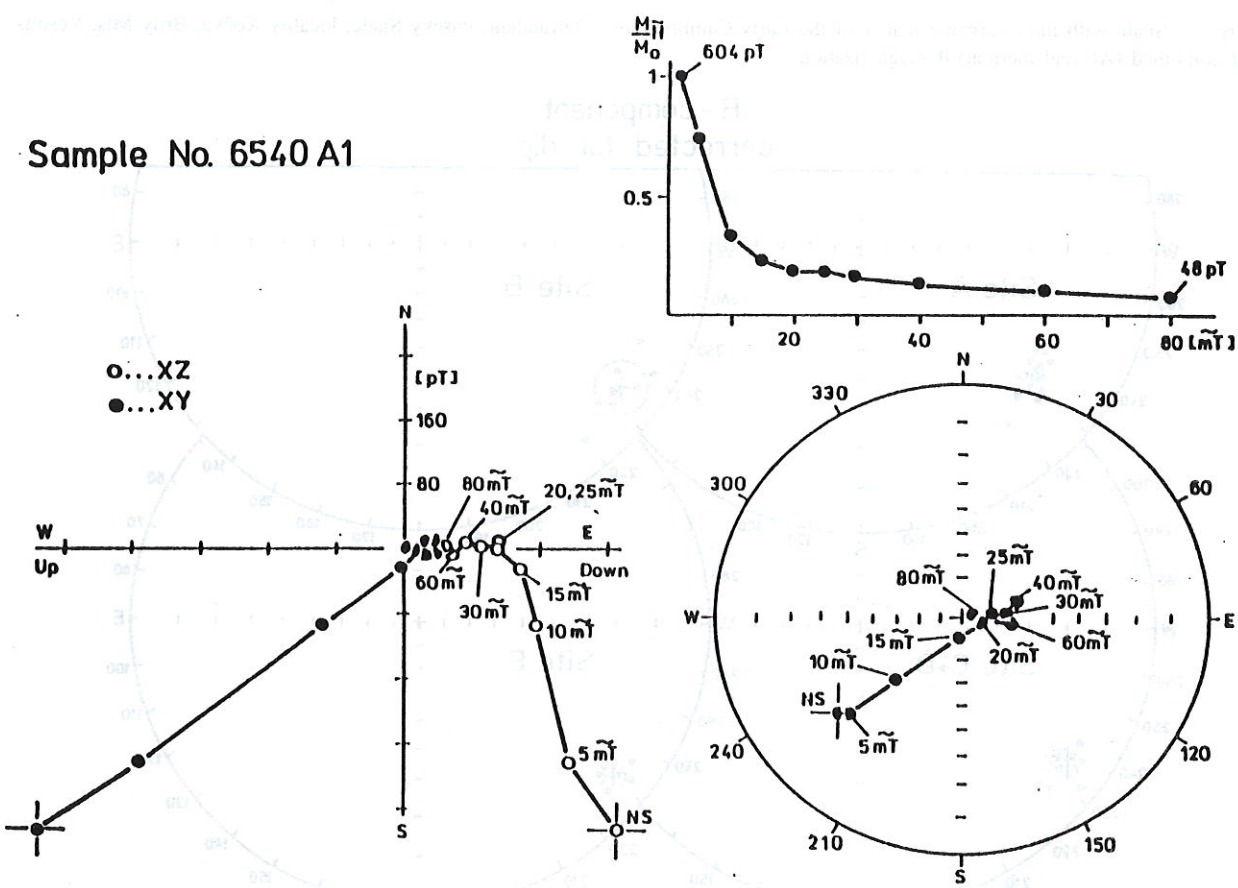

Fig. 37. Shale with micro-organic matter of the Early Cambrian age, Barrandian, Paseky Shale, locality Kočka, Brdy Mts. Results of alternating field (AF) demagnetization by means of the Schonstedt GSD-1 apparatus

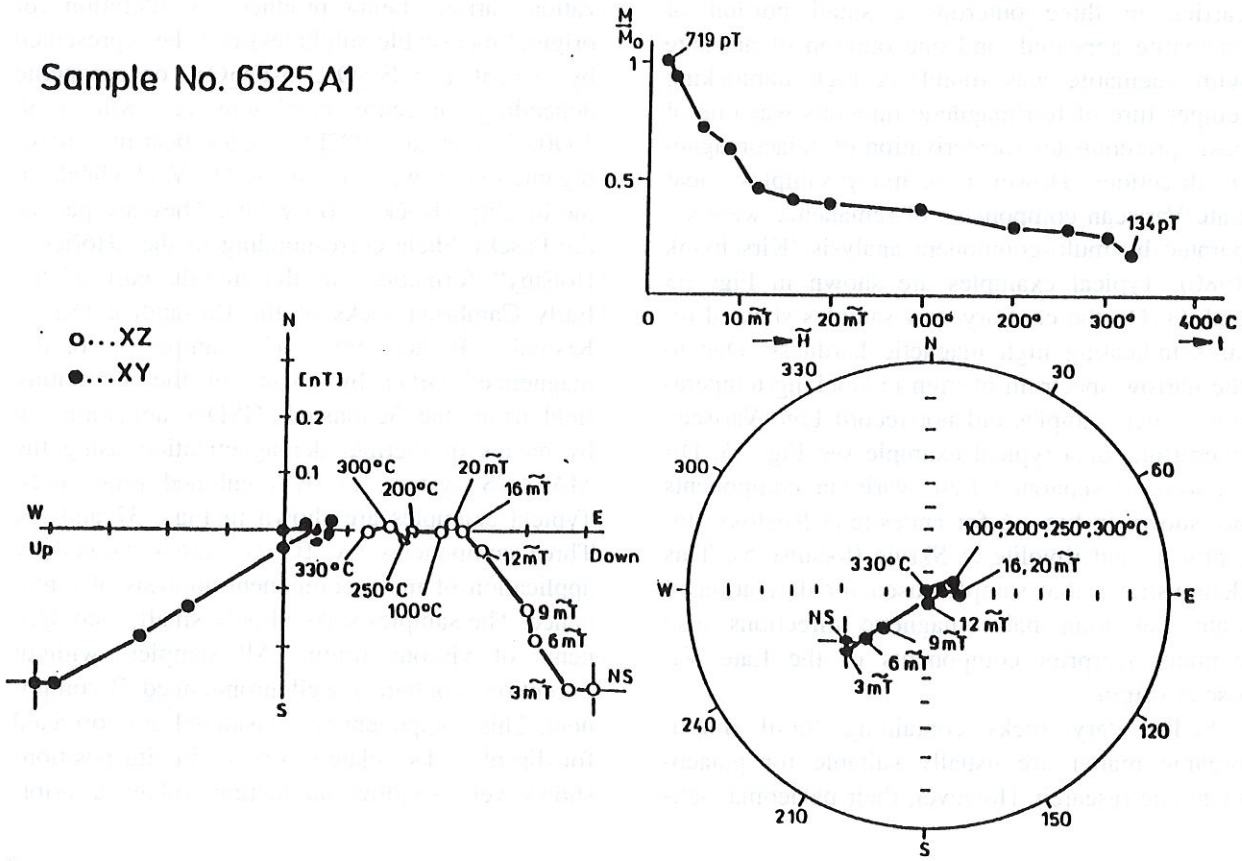

Fig. 38. Shale with micro-organic matter of the Early Cambrian age, Barrandian, Paseky Shale, locality Kočka, Brdy Mts. Results of combined (AF and thermal) demagnetization

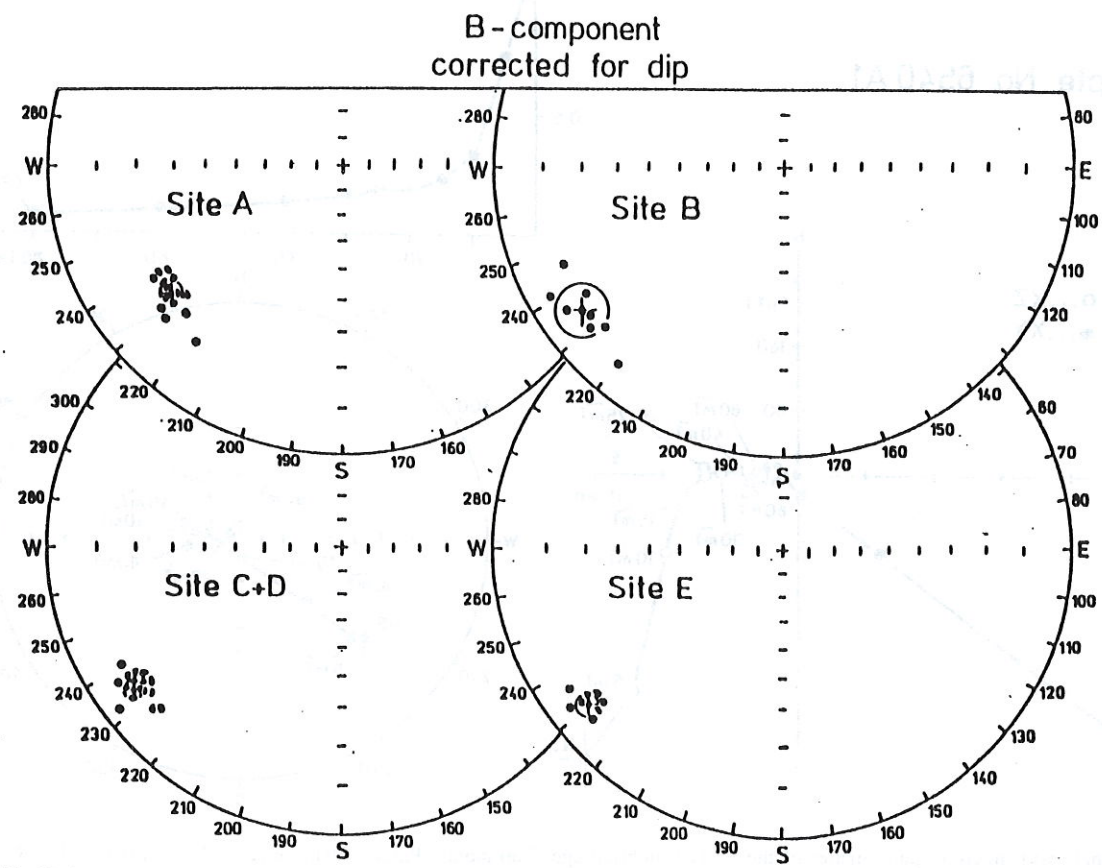

Fig. 39. Shale with micro-organic matter of the Early Cambrian age, Barrandian, Paseky Shale, locality Kočka, Brdy Mts. Directions of B-component of remanence corrected for dip of rocks

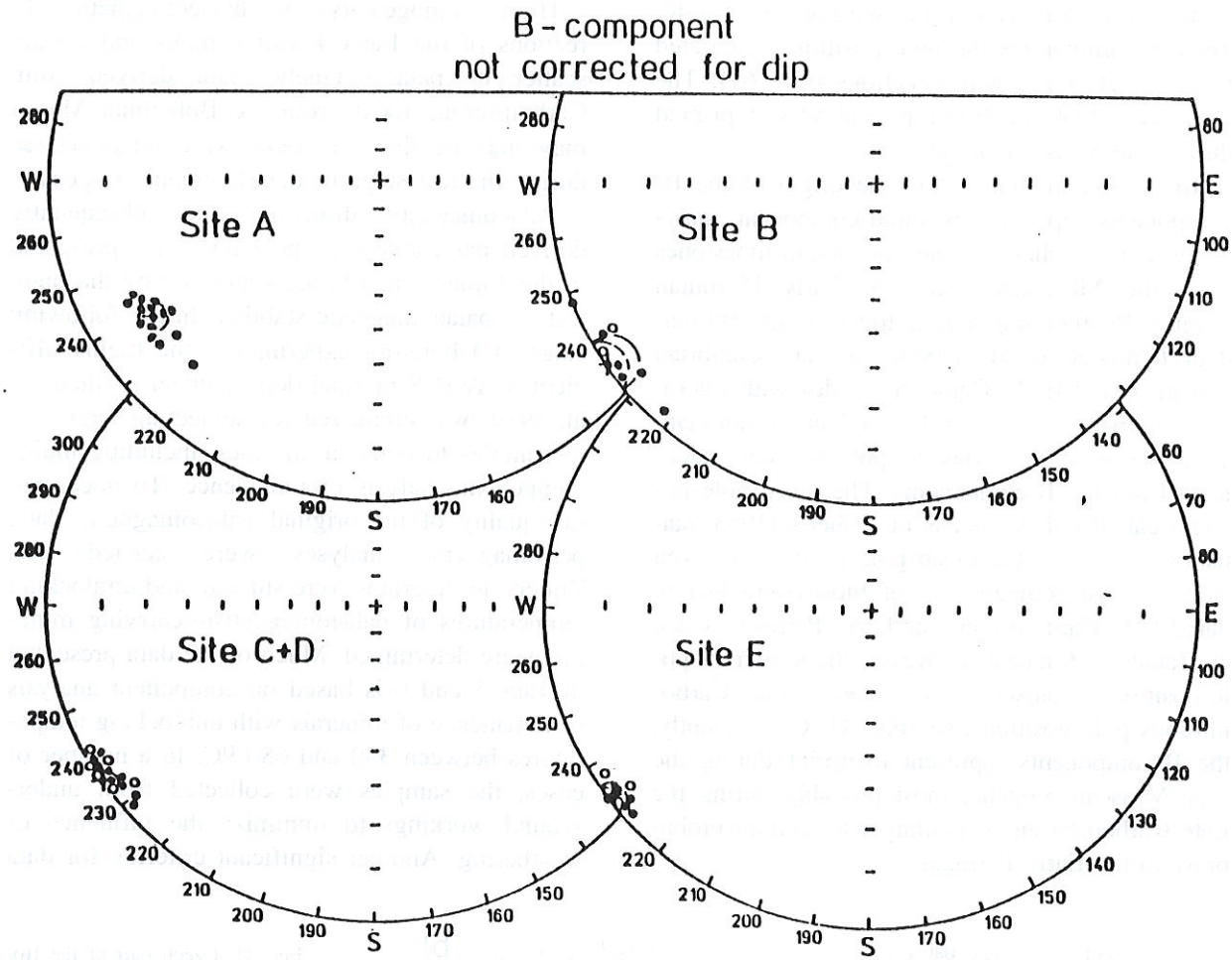

Fig. 40. Shale with micro-organic matter of the Early Cambrian age, Barrandian, Paseky Shale, locality Kočka, Brdy Mts. Directions of B-component of remanence not corrected for dip of rocks (in situ)

Table 8. Bohemian Massif: Late Variscan overprint components, corresponding pole positions

Region, locality	Reference No., see Fig.41	Age, lithology of overprinted rock formation	Geographic co-ordinates		Mean directions of overprint components		α_{95}(°)	k	n,N	Corresponding pole positions		Ovals of confidence		Reference
			φ(°)N	λ(°)E	D(°)	I(°)				φ_p (°)S	λ_p (°)W	dm(°)	dp (°)	
Moravian Zone, Křtiny	32	Late Famennian, limestone	49.143	16.737	198.3	-9.9	2.9	83.3	n=30	43.20	8.67	2.93	1.48	M. Krs et al., 1994
Moravian Zone, Josefov--Habrůvka	33	Givetian, carbonates	49.142	16.691	217.7	-7.4	2.0	69.5	n=70	34.44	31.03	2.01	1.01	M. Krs et al., 1994
Moravian Zone, Čelechovice	34	L. Eifelian--E. Givetian, limestone	49.532	17.087	221.9	8.7	2.6	45.8	n=66	25.06	30.23	2.62	1.32	M. Krs et al., 1994
Barrandian, S. of Srbsko, Suchomasty	35	Early Devonian, limestone	49.919	14.107	197.2	-12.8	3.2	429.1	N=6	44.23	10.10	3.26	1.66	I. Chlupáč et al., 1987
Barrandian, Křivoklát--Rokycany complex	36	Late Cambrian, andesite, rhyolite	49.982	13.816	201.6	-5.2	4.8	63.5	n=15	39.20	14.51	4.81	2.41	cf. M. Krs et al., 1991
Barrandian, Příbram syncline, locality "Kočka"	37	Early Cambrian, oil-shale	49.617	13.786	235.5	6.2	2.5	53.1	n=61	18.97	46.69	2.51	1.26	cf. M. Krs, P. Pruner, M. Krsová, 1993, 1994

n-number of strata; ,N-number of sites

Mean values: φ_p = 35.0°S; λ_p = 24.9°W; α_{95} = 13.5°; k = 25.5

indicating its Variscan origin, see Figs. 39 and 40. Table 8 summarizes the pole positions calculated from the B-component directions (n = 61). The data show that the B-component was imprinted during the Variscan orogeny.

To discuss in more detail the origin of the B-components separated by multi-component analysis on Late Eifelian to Late Famennian limestones from the Moravian Zone, on Early Devonian (mainly Pragian stage) limestones of the Barrandian (Chlupáč et al. 1987), on Late Cambrian volcanics and Early Cambrian shales with micro-organic matter from the Barrandian, a summary Table 8 was set up reviewing pole positions calculated from the B-components. The mean pole position calculated by means of Fisher's (1953) statistics is close to the mean pole positions derived from the palaeomagnetism of biostratigraphically dated Late Carboniferous or Early Permian rocks, cf. Tables 5, 6 and 8. However, the scatter of pole positions is closer to the scatter of Late Carboniferous pole positions, see Fig. 41. Consequently, the B-components represent overprint during the Late Variscan orogeny, most probably during the Late Carboniferous, extending with certain probability to the Early Permian.

High homogeneity of palaeomagnetic directions of the Early Permian rocks and certain scatter of palaeomagnetic data derived from Carboniferous rocks from the Bohemian Massif may indicate that the rocks were remagnetized during the late stage of the Hercynian orogeny.

Palaeomagnetic directions and subsequently derived palaeomagnetic pole positions, presented in the Tables 5 and 6, are supported by thorough tests of palaeomagnetic stability. In the following stage of laboratory experiments, the highly efficient MAVACS thermal demagnetizer (Příhoda et al. 1989) was employed for subjecting large sets of samples to detailed analyses, including multi-component analysis of remanence. To document the quality of the original palaeomagnetic data, petromagnetic analyses were carried out, Zijderveld diagrams were studied, and unblocking temperatures of palaeomagnetism-carrying minerals were determined. Much of the data presented in Tabs 5 and 6 is based on component analysis of remanence of minerals with unblocking temperatures between 390 and 680 °C. In a number of cases, the samples were collected from underground workings to minimize the influence of weathering. Another significant criterion for data

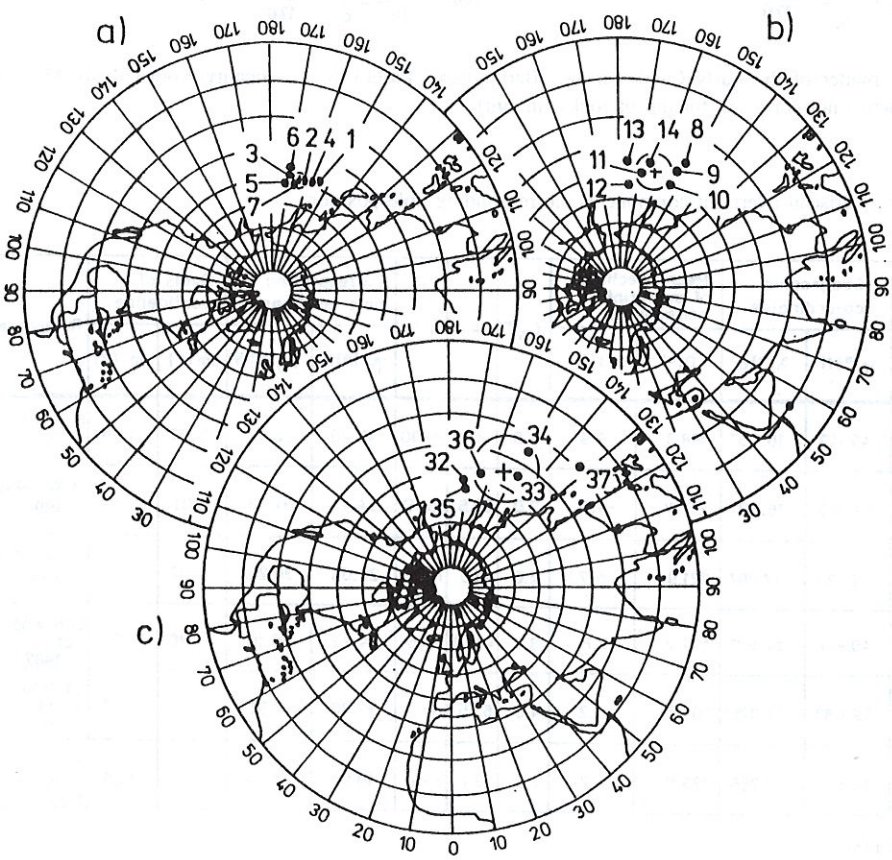

Fig. 41. Czech part of the Bohemian Massif: a comparison of Early Permian and Carboniferous pole positions derived on biostratigraphically dated rocks with pole positions calculated from mean directions of Late Variscan overprint components of remanence derived by multi-component analysis on pre-Variscan rock formations. a) *1* to *7* – Early Permian pole positions, see Table 5. b) *8* to *14* – Carboniferous pole positions, see Table 6. c) Pole positions calculated from mean directions of Late Variscan overprint components of remanence of the following rock formations: *32* – Late Famennian limestone, Moravian Zone; *33* – Givetian carbonates, Moravian Zone; *34* – Late Eifelian to Early Givetian limestone, Moravian Zone; *35* – Early Devonian (Pragian stage) limestone, Barrandian; *36* – Late Cambrian andesite, rhyolite, Barrandian; *37* – Early Cambrian shale with micro-organic matter, Příbram syncline, Barrandian, see Table 8

reliability is the petrographic diversity of the palaeomagnetically studied rocks, such as „red beds", tuffs and tuffites, ignimbrite, claystones and sandstones, oil-shales, micro-granodiorite, roof shales and greywackes.

5. Model interpretations of palaeotectonic rotations

Middle and Early Carboniferous rocks from the West-European Hercynides show signs of major palaeotectonic horizontal rotations (Edel 1987). Similar findings on palaeomeridian azimuths indicating clockwise palaeotectonic rotations were found recently for Middle to Late Devonian rocks from the Moravian Zone (Krs et al. 1994). To clarify this question we will discuss a model that explains the specific distribution of pole positions in the collision zone.

Major palaeotectonic rotations are documented by numerous examples from the Alpine tectonic belt. From the Neogene to the Permian periods, statistical mean values of palaeomagnetic data from the following regions have been set up: the Northern Apennines, Southern Alps, North-Eastern Alps, Eastern Alps, Istria, the Transdanubian region, the Outer Western Carpathians (flysch), the Outer Eastern Carpathians, Western Alps, the Inner Western Carpathians including the Little Carpathians (Krs – Krsová – Pruner 1992, in press). A region with identical or similar palaeotectonic evolution may be defined by a respective set of palaeomagnetic pole positions, but only within the limits of statistically defined inaccuracies of derivation. Due to the amount of data available, a specific distribution of pole positions could be recognized. Within the scatter and distribution of palaeomagnetic pole positions, from the Neogene to the Permian periods, the palaeotectonic rotation notably prevails in certain regions (zones, nappes). In Fig. 42, examples of Permian pole distributions are presented for the following regions: Eastern Alps (EAL), Northern Apennines (NAP), Southern Alps (SAL), North-Western Slovenia (NWS), the Villány region (VIL), the Inner Western Carpathians (IWC). The positions of respective poles reflect both translation of the lithospheric plate, to which the region (zone, nappe) in question shows palaeogeographic affinity (motion due to continental drift or rotation of plate with a distant pole of rotation) and palaeotecto-

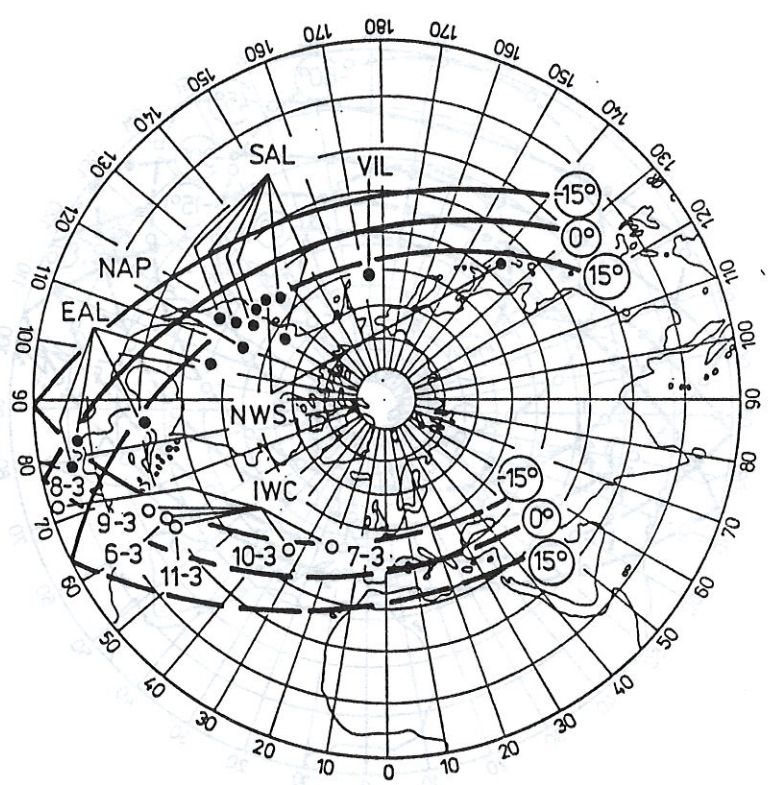

Fig. 42. Alpine-Carpathian-Pannonian Zone: distribution of pole positions derived on Permian rocks from different regions (nappes, nappe systems), VIL – region of Villány; SAL – Southern Alps; NAP – Northern Appennines; EAL – Eastern Alps; NWS – North-Western region of Slovenia; IWC – Inner Western Carpathians, cf. Krs, Krsová, Pruner in press. Theoretically derived paths for pole positions due to palaeotectonic rotations are demonstrated by *solid full lines* (on upper hemisphere) and *dashed lines* (on lower hemisphere) for rocks with different palaeoinclination values of -15°, 0°, 15°

nic rotations (motion due to local to regional rotations or rotations with a close pole of rotation). In other words, palaeogeographic affinity is based on palaeogeographic latitudes. A theoretical model was proposed to simulate the above-mentioned movements (Krs – Pruner – Potfaj 1992). For the region with the geographic coordinates φ = 50°N and λ = 13°E, palaeomagnetic pole positions were calculated for rocks with the corresponding values of palaeomagnetic inclination I_p and with the respective values of palaeomagnetic declinations D_p. The individual paths were calculated for D_p from 0° to 360° at the steps of dD_p = 20°. In this way, theoretical paths were constructed that match with certain approximation the paths of experimentally derived pole positions. Path 1: I_p = 0°, φ_m = 0°; path 2: I_p = -15°, φ_m = -7.6°; path 3: I_p = -30°, φ_m = -16.1°; path 4: I_p = -45°, φ_m = -26.6°; path 5: I_p = -60°, φ_m = -40.9°; path 6: I_p = -75°, φ_m = -61.4°, see Fig. 43. The model presented is supported by a number of case histories from the Alpine tectonic belt and explains the specific pole distribution in the collision zone. In the territories of the West-European Hercynides, anomalous palaeomagnetic declinations were found for Middle Carboniferous rocks and notably anomalous declinations were detected in the case of Early Carboniferous rocks (Edel 1987). Those declinations imply clockwise palaeotectonic rotations, see Figs. 5 and 6, and the data in Table 3. The mean palaeomagnetic pole positions presented in Fig. 44 cover rocks of the following periods: the Permian (P), the Late Carboniferous (C_3), the Middle Carboniferous (C_2), and the Early Carboniferous (C_1). Since changes in palaeogeographic latitudes are relatively small in comparison with changes in pole positions caused by palaeotectonic rotations, a theoretical path of poles for the Permian pole position (P) was calculated with dD_p = 20°. Pole positions C_3, C_2, and C_1 represent experimentally derived mean pole positions localized within that path. Pole position C_2 shows a clockwise rotation about 40° higher than pole position C_3, and C_1 is higher than C_3 by about 110°. The mentioned changes in palaeomagnetic declinations correlate to changes in palaeotectonic rotations.

The comparison of the presented model with experimentally derived data and with their statistically calculated mean values prove that rocks in the West-European Hercynides underwent palaeotectonic rotations comparable to rotations so far documented for the Alpine tectonic belt.

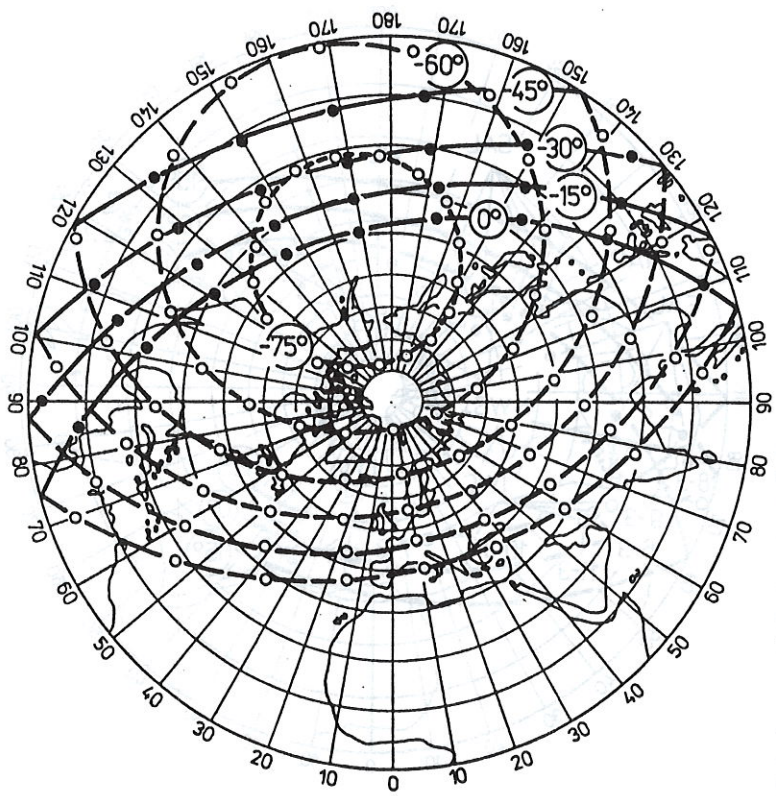

Fig. 43. A theoretical model showing distribution of pole positions due to pronounced palaeotectonic rotations for rocks with palaeoinclination values of 0°, -15°, -30°, -45°, -60°, -75°. Theoretical paths are demonstrated by *solid full lines* on upper hemisphere and *dashed lines* on lower hemisphere. The individual paths were calculated for palaeomagnetic declinations D_p at the steps of dD_p = 20° from 0° to 360°

6. Principal results

Palaeomagnetic data were accumulated over approximately the last 30 years and, then, statistically evaluated to allow formulation of a number of results concerning palaeogeography and palaeotectonic deformations of rocks from the Hercynian orogenic belt. The territories under consideration are located north of the Alpine tectonic belt and west of the Ural Mts. up to Great Britain:

i) The Permian period is characterized by a homogeneous grouping of palaeomagnetic pole positions in the territories to the north of the Alpine tectonic belt covering the East-European Platform, Fennoscandia, Central and West-European Hercynian belt. Accordingly, palaeogeographic latitudes and palaeomeridians are of similarly homogeneous orientation. In the Early Permian, the European lithospheric plate consolidated without major palaeotectonic rotations of its segments during later geological history. From the Early Permian to recent times, a major movement of the whole lithospheric plate has been occurring as a consequence of the continental drift from its palaeogeographic subequatorial position to its present location.

ii) In the western part of the Bohemian Massif and in the West-European Hercynides, rocks of the Late Carboniferous show palaeotectonic rotation deformations. In the West-European Hercynides, the palaeotectonic rotations are notably high, they are considerably higher for the Early Carboniferous and predominantly of clockwise sense. If the Early Permian palaeogeographic coordinate net of the European plate is taken as a reference net, then the rotations reach about 50° for the Middle Carboniferous and 120° for the Early Carboniferous rocks. Similar clockwise palaeotectonic rotations have recently been derived for the Middle to Late Devonian limestone formations from the Moravian Zone, the eastern part of the Bohemian Massif. Palaeomagnetic declinations reach 105° for the Late Eifelian-Early Givetian (locality Čelechovice), 111° for the Givetian (locality Josefov – Habrůvka) and 134° for the Late Famennian (locality Křtiny Marble Quarry), see Fig. 45.

iii) Palaeotectonic rotations of the above mentioned magnitudes are quite common in the Alpine tectonic belt and they, undoubtedly, represent a characteristic feature of tectonic collision zones, as was shown on a model simulating translation and rotation movements.

iv) Palaeomagnetic data derived so far, however, indicate certain differences between the Alpine and Hercynian orogeny belts as well. In the Alpine tectonic belt, variable deformations were found in rocks of the same age in particular nappes or systems of nappes, while, in the Hercy-

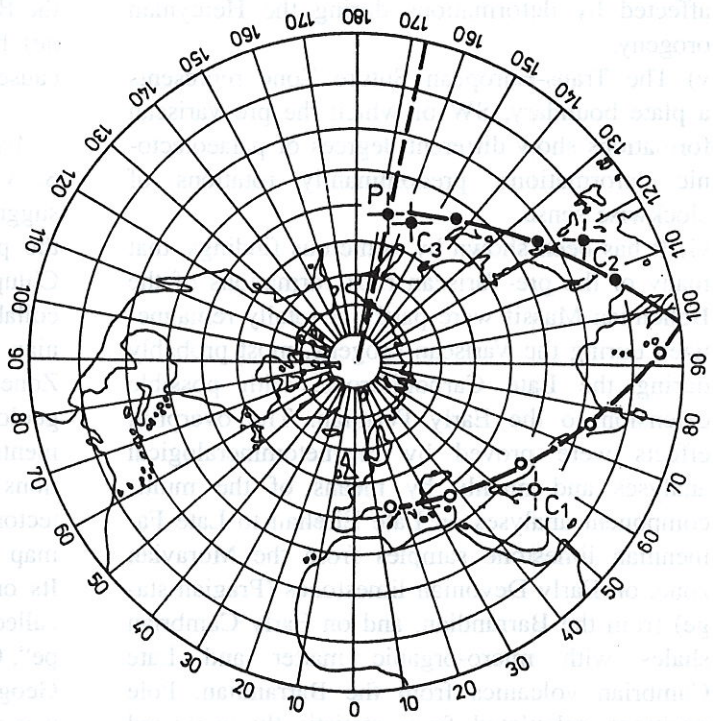

Fig. 44. Mean pole positions derived statistically for the West-European Hercynides. P – Permian; C_3 – Late Carboniferous; C_2 – Middle Carboniferous; C_1 – Early Carboniferous. *Solid full (dashed) line* indicates a theoretical path for the pole position P if subjected to pronounced palaeotectonic rotations. This theoretical path is close to pole positions derived experimentally on rocks of different genesis for the Late, Middle and Early Carboniferous

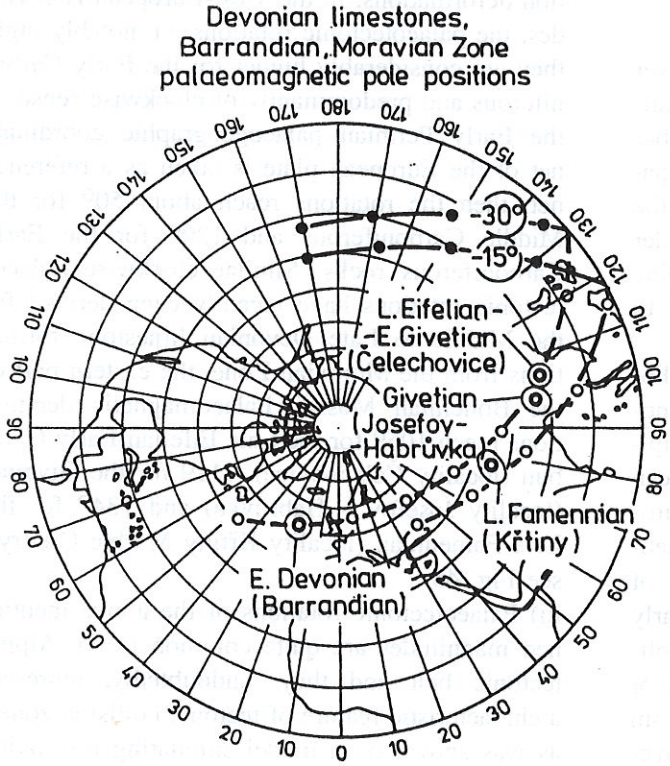

Fig. 45. Palaeomagnetic pole positions derived on the Devonian rocks (prevailingly limestones) from the localities Čelechovice na Hané (Late Eifelian-Early Givetian), Josefov – Habrůvka (Givetian) and Křtiny Marble Quarry (Late Famennian). Theoretical distribution of pole positions due to palaeotectonic rotations was calculated for rocks with palaeomagnetic inclination values of $I_p = -15^o$, $I_p = -30^o$. Projection of pole positions (paths) onto the upper hemisphere is demonstrated by *full circles* (*full solid lines*) and onto the lower hemisphere by *empty circles* (*dashed solid lines*). Ovals of confidence circumscribed around the mean pole positions derived experimentally on the Devonian rocks were calculated at the 95% probability level

nian orogeny belt, the magnitude of palaeotectonic deformations grows with rock age from the Late to Early Carboniferous or Middle Devonian. To solve the suggested problem, further palaeomagnetic investigations need to be carried out on precisely stratigraphically classified rocks and affected by deformations during the Hercynian orogeny.

v) The Trans-European Suture Zone represents a plate boundary, SW of which the pre-Variscan formations show different degrees of palaeotectonic deformations, predominantly rotations of clockwise sense.

vi) It has been shown by numerous findings, that many of the pre-Variscan rock formations of the Bohemian Massif were partly or totally remagnetized during the Variscan orogeny, most probably during the Late Carboniferous, with possible extension to the Early Permian. The overprint effects were proved by magnetomineralogical analyses and mainly by means of the multicomponent analyses on Late Eifelian to Late Famennian limestone samples from the Moravian zone, on Early Devonian limestones (Pragian stage) from the Barrandian, and on Early Cambrian shales with micro-organic matter and Late Cambrian volcanics from the Barrandian. Pole positions calculated from statistically evaluated overprint components fall well into the Late Carboniferous pole positions derived on biostratigraphically dated rocks from the Bohemian Massif.

vii) Palaeogeographic and palaeotectonic reconstructions of Pre-Variscan formations (e.g. of the Barrandian regarded as peri-Gondwanic terrane) have to respect palaeotectonic deformations caused by the Variscan orogeny.

Acknowledgements. We would like to thank Dr. S. Vrána and the anonymous referee for their suggestions for improving the original version of the paper. We also are indebted to Professor I. Chlupáč and Dr. J. Hladil for their advice and collaboration during collecting samples of Devonian rocks from the Barrandian and the Moravian Zone. The authors wish to thank several other geologists for their collaboration, their names are mentioned as co-authors in respective publications and reports. – A simplified and 1:2 reduced tectonic map of Europe was utilized as a basic map for demonstration of palaeomagnetic data. Its original scale was 1 : 2,500,000; the map is called „Carte tectonique internationale de l'Europe", Comm. Cartes Tect. Intern. et Sec. Sci. Géol. Géogr., Acad. Sci., Moscow 1962. Dr. Z. Roth was very helpful in its revision.

Appendix

References to pole positions statistically evaluated in Tabs 1 to 4.

Russian Platform, Ural Mts. – Middle Triassic
52.2; 55.0; Southern Ural, Yushaty + Bukobai suites, N, 06002; 52.5; 55.0; Southern Ural, Donguz suite, N, 06003; 57.0; 62.0; Central Ural, basalt, tuff, tuffite, N+R, 06005; 58.0; 62.0; Central Ural, basalt, tuff, tuffite, N+R, 06006; 48.0; 38.0; Donbass area, Serebryansk suite, N+R, 06008; (Khramov 1984).

Russian Platform, Ural Mts. – Early Triassic
60.6; 49.0; Duza River, loose sediment (loam), AC+TC, R, 06073; 60.0; 50.0; Viatka River, red beds, TC, N, 06044; 48.0; 47.0; Bogdin + Tananyk suites, sediments, TC, N, 06009; 53.0; 52.0; Obshtchi Syrt, red beds, TC, N+R, 06046; 52.3; 54.8; Southern Ural, red beds, N+R, 06016; 57.0; 45.0; Vetluga River, red beds, AC+TC, N+R, 06076; 58.0; 46.0; Vetluga River, red beds, AC+TC, N+R, 06075; 61.5; 46.5; North Dvina River, sediments, R, 06011; 60.3; 48.3; Duza River, red beds, AC+TC, N+R, 06074; 59.0; 51.0; Viatka River, red beds, AC, N+R, 06045; 52.5; 51.0; Zavolhye, Romashkin+Buzuluk+Tananyk suite, N+R, 06013; 48.5; 52.0; Prikaspik area, red beds, N, 06014; (Khramov 1984).

England, Ireland, France, Germany – Triassic
53.0; -2.0; England, Keuper, marls, N+R, 6; 50.7; -3.2; England, Keuper, marls mixed, AC, R, 7; 48.5; 7.0; France, Vosge, sandsone, red beds, combined, N+R, 3; Germany, Bunter, sandstone mixed, N, 4; (Irving – Tanczyk – Hastie 1976b). England, Saint Bee Sandstone; Ireland, Kingscourt, red beds, quality index Q = 4; France, Keuper, red beds, quality index Q = 3; France, Upper Buntsandstein, quality index Q = 6; East Germany, Bunter and Musschelkalk, quality index Q = 6; (Van der Voo 1990).

Fennoscandia – Triassic
59.7; 10.4; Oslo, igneous rocks, TC, R, 008-001; 61.0; 11.0; Brumunddal Lavas, AC+TC, R, 008-002; 61.0; 11.0; Brumunddal Lavas, AC+TC, N, 008-003; 61.0; 11.0; Brumunddal Lavas, AC+TC, N+R, 008-004; (Pesonen et al. 1991). Brumunddal Lavas, quality index Q = 4; (Van der Voo 1990).

Russian Platform, Ural Mts., Early – Middle Permian
45.3; 52.0; Mangyshlak, sandstone, TC, N+R, 06077; 51.7; 59.5; Southern Ural, granite of Adamov Massif, N, 06066; 56.0; 44.0; Volga River, red beds, TC, N, 07062; 57.0; 44.0; Vetluga River, red beds, N, 07031; 60.6; 44.2; Sukhona River, red beds, TC, N+R, 07059; 60.8; 45.2; Sukhona River, red beds, TC, N+R, 07058; 60.8; 46.5; Yug and S. Dvina River, sediments, TC, N+R, 07057; 58.0; 48.0; Viatka River, red beds, TC, R, 07023; 55.0; 49.0; Volga River, red beds, AC+TC, N+R, 07061; 59.0; 50.8; Viatka River, red beds, AC+TC, N+R, 07060; 53.5; 52.0; Zavolzhye, red beds, N+R, 07035; 52.9; 52.2; Obshtchi Syrt, red beds, AC, N+R, 07036; 52.5; 55.0; Southern Ural, red beds, AC, N+R, 07006; 56.0; 49.0; Volga River, red beds, AC+TC, R, 07063; 55.0; 49.0; Volga River, red beds, AC+TC, N+R, 07064; 56.0; 51.0; Viatka River, red beds, TC, R, 07024; 48.5; 52.0; Western Kazakhstan, red beds, N, 07007; 44.0; 53.0; Mangyshlak, Eastern Karatay, sediments, N+R, 07047; 41.0; 55.0; Turkmenia, Amanbulac suite, N+R, 07009; 54.2; 52.6; Zavolzhye, red beds, R, 07037; 56.6; 54.0; Kama River, red beds, AC+TC, R, 07079; 52.5; 55.0; Southern Ural, red beds, R, 07013; 55.5; 50.0; Kama River, red beds, R, 07026; 54.9; 53.0; Prikame area, red beds, AC+TC, R, 07080; 56.0; 51.0; Viatka River, red beds, TC, R, 07025; 56.0; 51.7; Kama River, red beds, TC, R, 07067; 57.4; 55.5; Kama River, red beds, R, 07081; 54.6; 52.6; Prikame area, sediments, AC+TC, R, 07069; 55.7; 52.7; Nort-Eastern Tataria, sediments, TC, R, 07071; 58.2; 56.5; Prikame area, sediments, R, 07070; 59.0; 57.0; Prikame area, sediments, R, 07039; 49.0; 38.0; Donbas, red sediments, R, 07011; 49.0; 36.3; Donbas, red beds, R, 07019; (Khramov 1984).

Bohemian Massif – Early Permian
49.5; 16.6; sandstone, R, 69; 50.0; 15.3; Turkank, veins, AC, R, 129; 50.0; 13.5; Westen Bohemia, haematite veins, AC, N+R, 134; 50.9; 13.4; Freiberg, mineralized veins, R, 158; 50.1; 12.8; Horní Slavkov, greisen, R, 159; (Irving – Tanczyk – Hastie 1976a). 50.1; 14.9; Blanice graben, North, red beds, R, 3; 49.4; 14.8; Blanice graben, South, red beds, R, 5; 49.2; 16.4; Boskovice graben, South, red beds, TC, R, 12; 49.5; 16.6; Boskovice graben, Centre, red beds, TC, R, 13; 50.5; 15.5; Sub-Krkonoše Piedmont Basin, Rotliegendes Up+Mid, red beds, TC, R, 7; 50.6; 15.5; Sub-Krkonoše Piedmont Basin, Rotliegendes Lower, red beds, TC, R, 7; (Krs 1968). 50.6; 15.5; Sub-Krkonoše Piedmont Basin, oil-shales, TC, R; (Krs et al. 1992a).

England, Scotland – Permian
51.0; -4.0; England, County Devon, Exeter traps, R, 14; 51.0; -4.0; England, County Devon, Exeter traps, AC, R, 88; 51.0; -4.0; England, County Devon, Exeter traps, AC+TC, R, 87; 51.0; -4.0; England, County Devon, Exeter traps, AC+TC, R, 316; 55.4; -4.5; Scotland, Ayrshire, Mauchline lavas, R, 16; 55.4; -4.5; Scotland, Ayrshire, Mauchline red beds, R, 17; (Irving – Tanczyk – Hastie 1976a).

Fennoscandia – Permian
55.9; 13.5; Sweden, Skane, melaphyre dykes, AC, R, 295; 59.7; 10.4; Norway, Oslo, igneous complex, AC+TC, R, 13; (Irving-Tanczyk-Hastie 1976 a). 58.5; 8.8; Norway, Arendal, diabase, AC+TC, R, 007-003; 58.5; 8.8; Norway, Arendal, diabase, AC+TC, R, 007-004; 58.5; 8.8; Norway, Arendal, diabase, AC+TC, R, 007-005; 58.5; 8.8; Norway, Arendal, diabase, AC+TC, R, 007-006; 58.5; 8.8; Norway, Arendal, diabase, AC+TC, R, 007-007; 58.6; 11.3; Norway, Bohuslän, dykes, AC, R, 007-011; 58.6; 11.3; Norway, Bohuslän, dykes, AC, R, 007-012; 58.6; 11.3; Norway, Bohuslän, dykes, AC, R, 007-013; 58.6; 11.3; Norway, Bohuslän, dykes, AC, R, 007-016; 58.0; 7.8; Norway, Ny-Hellesund, sills, AC+TC, R, 007-019; 59.7; 10.4; Norway, Oslo, igneous complex, AC+TC, R, 007-008; 55.5; 13.5; Sweden, Scania, melaphyre, AC+TC, R, 007-001; 61.7; 12.9; Sweden, Särna body, AC+TC, R, 006-002; 61.7; 12.9; Sweden, Särna body, AC+TC, R, 006-003; 58.6; 12.5; W-Västergötland sill, AC+TC, R, 007-017; 60.5; 4.7; Sunhordaland, dykes, AC+TC, R, 007-002; (Pesonen et al. 1991). Norway, Arendal, diabase, 7-07; Sweden, Ytteroy dykes, quality index Q=4, 7-19; Norway, Oslo – graben, lavas, quality index Q=5, 6-11; Norway, Oslo, igneous rocks, quality index Q=5, 6-01; (Torsvik et al. 1992).

West-European Hercynides – Permian
47.0; 4.0; Morvan, volcanics, quality index C-B; (Edel 1987). 43.5; 6.8; France, Esterel, rhyolite, R, 2; 43.5; 6.8; France, Esterel, igneous + sedimentary rocks, AC+TC, R, 5; 48.0; 6.0; France, Vosge, porphyry, R, 7; 53.9; 5.7; France, Nideck-Do-

non volcanics, TC, R, 54; 53.9; 5.7; France, Vosge, Nideck volcanics, AC, R, 274; 50.3; 6.0; Belgium, Malmedy, conglomerates, R, 137; 48.5; 7.5; Germany, Rotliegendes sediments and lavas, R, 9; 50.0; 8.0; Germany, Nahe igneous rocks, AC, R, 11; 48.3; 7.7; Germany, Black Forest rocks, AC+TC, R, 216; 47.7; 7.6; Germany, Schopfheim, red beds, TC, R, 217; (Irving – Tanczyk – Hastie 1976a).

Russian Platform, Ural Mts. – Late Carboniferous
48.0; 38.0; Donbas, Medistn suite, red beds, R, 07021; 48.7; 38.2; Donbas, Medistn suite, red beds, R, 07020; 48.4; 38.2; Donbas, Araucarite + Avilov suites, red beds, R, 08002; 48.0; 41.0; Donbas, Isaev suite, slate + limestone, R, 08003; 54.2; 59.4; Southern Ural, granite + diorite, N+R, 08055; 51.5; 59.0; Southern Ural, Ashebutak comlex, granosyenite, N+R, 08056; 53.0; 59.0; Southern Ural, Magnitogorsk complex, grano-diorite, granite, gabbro-diorite, N+R, 08057; 54.0; 59.5; Southern Ural, Magnitogorsk complex, granite, N+R, 08032; 54.0; 60.0; Southern Ural, Achunov complex, granite, diorite, N+R, 08033; 55.5; 38.5; Moscow Basin, Gzhelian stage, red beds, AC, R, 08001 (Khramov 1984).

Russian Platform – Middle Carboniferous
48.0; 37.0; Donbas, claystone, siltstone, R, 08035; 48.0; 38.0; Donbas, limestone, siltstone, sandstone, R, 08051; 48.0; 38.0; Donbas, limestone, siltstone, sandstone, N+R, 08052; 56.5; 34.5; Rchev River, red beds, R, 08005; 55.0; 38.5; Ozeri River, red beds, R, 08008; 55.0; 36.0; Vereya River, red beds, R, 08006; 55.0; 37.5; Serpukhov River, red beds, R, 08007; 55.0; 42.0; Shapk River, red beds, R, 08009 (Khramov 1984).

Russian Platform, Ural Mts. – Early Carboniferous to Late Devonian
51.0; 57.0; Southern Ural, Zilair suite, sediments, N+R, 08019; 51.5; 57.0; Southern Ural, Zilair suite, sediments, AC, N, 08020; 53.0; 58.5; Southern Ural, Zilair suite, sediments, AC, N, 08021; 53.0; 59.0; Southern Ural, Kumak complex, gabbro-diorite, porpfyry, AC+TC, R, 08058; 53.0; 59.0; Southern Ural, sandstone, claystone, porphyry, tuff, N, 08016; 53.0; 57.0; Southern Ural, limestone, N+R, 08072; 52.0; 59.0; Southern Ural, basalt, diabase, porphyry, R, 08042; 53.8; 59.3; Southern Ural, Verchneural complex, plagio-granite, N, 08063; 54.9; 59.4; Southern Ural, Nuramin Massif, harzburgite, R, 08064; 53.3; 59.0; Southern Ural, Berozov suite, intrusive complex, TC, N+R, 08074; 50.3; 58.3; Southern Ural, sediments, TC, R, 08070; 52.5; 59.5; Southern Ural, sediments, tuff, tuffite, R, 08043; 51.2; 59.1; Southern Ural, Kurmansaisk complex, gabbro-diorite, diorite, grano-diorite, N+R, 08065; 59.4; 34.0; Tichvin, Boksitogorsk, red beds, N+R, 08014; 59.0; 33.5; Liubytino, Nebolotchi, Tulski horizon, red beds, N+R, 08015; 58.5; 34.0; Moscow Basin, sediments, R, 08061; 61.0; 37.0; Vytegra, red beds, R, 08013 (Khramov 1984).

West-European Hercynides – Early Permian to Late Carboniferous
48.0; -0.8; south Laval Basin, acid volcanics, TC, R, 1; 50.0; 4.8; Ardenne, intrusions, sediment, TC, R, 2; 50.0; 4.5; Brabant, dacites – sediments, TC, R, 2; 47.8; 7.0; South Vosges, volcanics, TC, R, 9+10+11; 48.4; 8.0; Central Black Forest, quartz porph., 296 Ma, TC, R, 13+14; 48.4; 8.0; Central Black Forest, quartz porph., 287 Ma, TC, R, 13+14; (Edel 1987). 48.4; 7.1; North Vosges, dykes, TC, R, 12; 47.1; 5.3; France, W. Germany, Stephanian combined, R, 4; (Irving – Tanczyk – Hastie 1976a).

West-European Hercynides – Middle Carboniferous
48.1; -0.5; north Laval Basin, acid volcanics, TC, R, 1; 50.0; 4.8; Ardenne, intrusions, sediment, TC, R, 2-3; 50.0; 4.8; Ardenne, intrusions, sediment, TC, N, 2-3; 46.4; 1.7; Aigurande plateau, amphibolites, TC, R, 4-5; 45.8; 1.2; Limousin, tonalites, TC, R, 6; 46.3; 2.0; Combrailles, diorites, TC, R, 4; 46.3; 2.0; Combrailles, diorites, TC, R, 4; 46.0; 2.9; Manzat, ignimbrite tuffs, TC, N, 4; 45.9; 4.2; Roannais, volcanics, TC, N, 4; 47.0; 4.0; Morvan, volcanics, TC, N, 15 ; 47.0; 4.0; Morvan, volcanics, TC, R, 15; 48.4; 7.1; North Vosges, rhyolite, TC, N, 12; 48.4; 7.1; North Vosges, idem+host rocks, TC, N, 12; (Edel 1987). 47.9; 7.8; South Black Forest, ignimbrite, TC, N, 13+14; (Irving – Tanczyk – Hastie 1976a).

West-European Hercynides – Early Carboniferous
45.8; 1.2; Limousin, metamorphic rocks, tonalites, TC, R, 6; 46.0; 2.9; Manzat, ignimbrite tuffs, TC, R, 4; 46.1; 3.5; Cussey, volcanics, TC, N, 16; 47.8; 7.0; South Vosges, volcanics, Cat. C_1, TC, R, 9+10; 47.8; 7.0; South Vosges, volcanics, Cat. C_2, TC, R, 9+10; 47.8; 7.0; South Vosges, volcanics, Cat. $C_{0,1,2}$, TC, R, 9+10; 47.8; 7.0; South Vosges, volcanics, Cat. C_1, TC, R, 9+10+11; 48.4; 7.1; North Vosges, diorites, Cat C_1, TC, R, 12; 48.4; 7.1; North Vosges, diorites, Cat C_2, TC, R, 12; 48.4; 7.1; North Vosges, diorites, Cat $C_{1,2}$, TC, R, 12; 48.4; 7.1; North Vosges, diorites, Cat C_3, TC, N, 12; (Edel 1987).

Bohemia, Poland – Late Carboniferous
50.5; 16.5; Poland, Silesian region, porphyries, AC, R, 94; (Irving – Tanczyk – Hastie 1976a). 49.8; 13.3; Plzeň Basin, red beds, TC, R, 1; 50.2; 14.0; Kladno-Rakovník Basin, red beds, TC, R, 2; 50.0; 14.8; Blanice graben, North, red beds, TC, R, 4; 50.5; 15.4; Sub-Krkonoše Piedmont Basin, red beds, TC, R, 6; 50.6; 16.1; Inner-Sudetic Basin, red beds, tuff, TC, R, 8; 49.2; 16.4; Boskovice graben, South, red beds, TC, R, 11; (Krs 1968). 49.8; 18.0; Moravian-Silesian region, roof shale, TC, N+R; (Krs et al. 1993a).

England, Scotland – Carboniferous
53.4; -6.2; Ireland, Dublin, limestone, AC, R, 312; 52.9; -8.0; Central-Southern Ireland, limestone, AC, R, 313; 52.9; -8.0; Ireland, limestone, AC, R, 315; 52.9; -8.0; Ireland, limestone, TC, R, 314; 52.7; -7.6; Ireland, limestone, shale, AC+TC, R, 305; 54.0; -3.0; England, limestone, N+R, 14; 53.0; -2.0; England, Keele, red beds, R, 18; 52.5; -2.0; England, Midlands, sills baked seds, R, 32; 54.0; -3.0; England, combined 1, N, 38; 54.0; -3.0; England, combined 2, N, 39; 55.0; -2.0; Northern England, Great Whin, sill, AC, R, 118; 55.0; -1.7; Northern England, Great Whin, sill, AC+TC, R, 139; 54.5; -1.8; Northern England, Wackerfield, dykes, AC, R, 310; 54.8; -2.1; Northern England, Pendleside, limestone, TC, R, 351; 54.8; -2.3; England, Craven, Bolladoceras beds, TC, R, 352; 54.8; -2.4; England, Craven, Sathill Reef-Knolls, TC, N+R, 353; 54.8; -2.3; England, Lancashire, Chatburn, limestone, TC, R, 354; 54.8; -2.2; England, Visean of Craven, combined, TC, N+R, 355; 51.0; -4.0; England, Culm Devonshire, sediments + dolerites, R, 165; 56.0; -3.0; Scotland, Kinghorn lavas 1, N, 11; 56.0; -3.0; Scotland, Kinghorn lavas 2, TC, N+R, 175; (Irving – Tanczyk – Hastie 1976a).

Fennoscandia – Carboniferous
58.0; 7.8; Southern Norway, Ny-Hellesund, diabase, AC+TC, R, 104; 58.5; 8.6; Southern Norway, Arendal, diabase dykes, AC+TC, R, 311; 58.2; 14.0; Southern Sweden, Mt-Billinger, sill, AC, R, 126; 58.5; 12.5; Southern Sweden, Mt-Hunneberg,

sill, AC, R, 127; 55.5; 13.5; Southern Sweden, Skane, dolerite dykes, AC, R, 128; 57.0; 14.0; Southern Sweden, intrusives combined, AC, R, 131; 55.9; 13.5; Sweden, Skane, quartz-dolerite dykes, AC, R, 324; (Irving-Tanczyk-Hastie 1976 a). 59.7; 10.4; Norway, Oslo, igneous rocks, TC, R, 006-001; 63.3; 8.5; Norway, Stabben, volcanics, AC+TC, R, 006-009; 58.0; 7.8; Norway, Ny-Hellesund, dykes, AC+TC, R, 007-009; 61.7; 12.9; Sweden, Särna body, 287 Ma, AC+TC, R, 006-002; 61.7; 12.9; Sweden, Särna body, 287 Ma, AC+TC, R, 006-003; 61.7; 12.9; Sweden, Särna body, 287 Ma, AC+TC, R, 006-004; 58.6; 13.5; Sweden, E-Vastergotland sill, AC+TC, R, 006-005; 55.5; 13.5; Sweden, Scania, dolerite, AC+TC, R, 006-006; 55.5; 13.5; Sweden, Scania, dolerite, AC+TC, R, 006-007; (Pesonen et al. 1991). Scania, Karelian, dolerite, 290 Ma, R, quality index Q=5, 6-06; Billefjorden Group, 350 Ma, R, quality index Q=5, 5-24; (Torsvik et al. 1992).

Russian Platform – NW of Moscow, Late Devonian
59.0; 33.0; sediment, TC, N+R, 09002; 59.0; 34.0; sediment, R, 09001; 58.0; 32.0; sediment, AC, N+R, 09005; 57.0; 31.0; sandstone, TC, N+R, 09004; 60.0; 33.0; sediment, TC, R, 09003; (Khramov 1984).

Ural Mts., Middle – Late Devonian
53.5; 56.5; southern Urals, Domanikov beds, limestone, AC, R, 09017; 54.0; 59.0; southern Urals, Zilair suite, sediment, N+R, 09006; 53.0; 58.5; southern Urals, Koltuban + Zilair suites, AC+TC, R, 09067; 57.0; 57.0; central Urals, bauxites + hydrohematites, TC, R, 09007; 50.0; 58.3; southern Urals, sandstone, limestone, R, 09058; 51.6; 58.7; southern Urals, sandstone, R, 09038; 52.1; 58.5; southern Urals, sediment and tuff rocks, AC+TC, R, 09068; 54.5; 59.5; southern Urals, tuff and tuff-breccia, AC+TC, R, 09009; 60.0; 60.0; northern Urals, red bauxities, AC, R, 09021; 55.5; 60.0; southern Urals, granite, AC+TC, 09030; 54.5; 59.5; southern Urals, diabase, tuff, AC+TC, R, 09013; (Khramov 1984).

Russian Platform, northern region, Middle – Late Devonian
67.0; 48.0; northern Timan, sediment, AC+TC, R, 09022; 67.0; 48.0; northern Timan, sediment, AC+TC, 09039; 67.0; 48.0; northern Timan, sediment, AC+TC, 09027; (Khramov 1984). 67.0; 48.0; Volonga River, redbeds, AC+TC, R, 132; (Irving – Tanczyk – Hastie 1976a).

Russian Platform – Dniester area, Early Devonian
49.0; 25.3; Dniester River, sediment, AC+TC, N+R, 09016; (Khramov 1984). 49.0; 25.0; Dniester area, sediment, R, 15; 49.0; 25.0; Dniester area, sediment, R, 104; 49.0; 25.0; Dniester area, Zhedian stage, R, 105; 49.0; 25.5; Dniester area, Zhedian stage, R, 106; 49.0; 25.5; Dniester area, Zhedian stage, R, 107; 49.0; 25.5; Dniester area, Zhedian stage, R, 108; (Irving -Tanczyk – Hastie 1976a).

Fennoscandia – Devonian
62.0; 12.0; Norway, Röragen, sandstone, AC+TC, R, 005-001; 61.6; 5.4; Norway, Hästeinen, sandstone, AC+TC, 005-002; 63.1; 11.6; Norway, Fongen-Hyllingen, gabbro, AC+TC, R, 005-004; 61.4; 5.6; Norway, Kramshesten, Old Red Sandst., AC+TC, R, 005-005 ; 61.4; 5.6; Norway, Kramshesten, Old Red Sandst., AC+TC, 005-007; 61.8; 5.3; Norway, Hornelen, sandstone, AC+TC, 005-009; 60.7; 5.6; Norway, Asköy pluton, AC+TC, 005-011; (Pesonen et al. 1991). Sweden, Saerv Nappe, dolerities, quality index Q=?; (Van der Voo 1990). Hitra, sandstone; Smola, redbeds; (Torsvik et al. 1990).

Britain, north of the Great Glen Fault – Devonian
57.2; -4.5; Scotland, Foyers, plutonic complex, AC, N+R, 148; 58.5; -1.5; Scotland Orkney + Shetland ors lavas, AC+TC, N+R, 180; (Irving – Tanczyk – Hastie 1976a). Scotland, Shetland, Esha Ness, quality index Q=6; (Van der Voo 1990). Hoy lavas; Shetland lavas; Eday Sandstone; Kishorn – Moine, metasedim.; Sarclet L Old Red Sandstone; Borrolan Syenite, Loch Ailsh, dykes; Moine, metasediments, (Ratagen); Moine, metasediments, (IB, Intermediate blocking); Moine, metasediments, (HB, High blocking); (Torsvik et al. 1990).

Britain, south of the Great Glen Fault, north of the Iapetus Suture – Devonian
55.5; -2.4; North England, Cheviot Hi., lavas, AC, N+R, 168; 55.5; -2.5; Scotland, Upper Old Red Sandstone, R, 6; 55.6; -4.0; Scotland, Lower Devonian, lavas 3, AC, N+R, 62; 55.7; -3.5; Scotland, Lower Devonian, lavas 4, AC, N+R, 61; 56.5; -3.0; Scotland, Strathmore, lavas, AC, N+R, 171; 56.5; -3.0; Hidland valey, Lower Devonian, AC+TC, N+R, 172; (Irving – Tanczyk – Hastie 1976a). Cheviot; Garabal Hill – Glen Fyne; Lorne Plateau, lavas; Old Red Sandstone, lavas and sediments; Strathmore, lavas; Lower Old Red Sandstone; Comrie complex; (Torsvik et al. 1990). Foyes Old Red Sandstone, quality index Q=3; Lower Caihness Red Beds, quality index Q=4; (Van der Voo 1990).

Britain, south of the Iapetus Suture – Devonian
52.0; -3.0; Old Red Sandstone, R, 2; 52.0; -3.0; Old Red Sandstone, TC, 77; (Irving – Tanczyk – Hastie 1976a). Lavas Somerset a Gloucester; (Torsvik et al. 1990). Hendre and Blodwell Intrusives; (Van der Voo 1990).

West-European Hercynides, incl. Armorican Massif, Poland, Moravian Zone – Devonian
51.5; -4.5; Southwest England, basic dyke + sill, R, 76; 51.4; -2.5; South England, Portishead, red beds, TC, R, 173; 51.0; 6.0; West Germany, Eifel, sandstone, R, 1; 48.3; 7.7; West Germany, Scharfenstein, porphyry, AC, 142; (Irving-Tanczyk--Hastie 1976 a). 50.5; 20.3; Poland, Holy Cross Mountains, sandstone, TC, R; (Levandovski-Jelenska-Halvorsen 1987). 49.1; 16.7; Jersey, dolerite; Jersey, lamprophyr. dykes; (Torsvik et al. 1990). Moravian Zone, Křtiny, lime-mud-stone, TC, R, 16; 49.1; 16.7; Moravian Zone, Josefov – Habrůvka, packstone, floatstone, TC, R, 17; 49.5; 17.1; Moravian Zone, Čelechovice, limestone, TC, R; (Krs et al. 1994).

Submitted March 7, 1995 *Translated by the authors*

References

Birkenmajer, K. – Krs, M. – Nairn, A. E. M. (1968): A palaeomagnetic study of Upper Carboniferous rocks from the Inner Sudetic Basin and the Bohemian Massif. – Geol. Soc. Amer. Bull., 79, 589-608. New York.

Butler, R. F. (1992): Paleomagnetism: Magnetic Domains to Geologic Terranes. – Blackwell Sci. Publ. Boston.

Chamalaun, F. H. – Creer, K. M. (1963): A revised Devonian pole for Britain. – Nature, 198, 4878, 375. London.

– (1964): Thermal demagnetization studies on the Old Red Sandstone of the Anglo-Welsh Cuvette. – J. Geophys. Res., 69, 8, 1607-1616. Richmond.

Chlupáč, I. – Krs, M. (1967): Paläomagnetismus and Paläoklimatologie des Devons. – Geologie, 16, 8, 869-888. Berlin.

Chlupáč, I. – Krs, M. – Krsová, M. – Kouklíková, L. – Pruner, P. – Chvojka, R. (1987): Palaeomagnetism and palaeogeography of the Lower to Middle Devonian limestones in the Barrandian, Czechoslovakia. – Int. Rep., Geofyzika Co., Dept. in Prague, 1-22. Geofond Praha.

Edel, J. B. (1987): Paleopositions of the western Europe Hercynides during the Late Carboniferous deduced from paleomagnetic data: consequences for „stable Europe". – *In: D. V. Kent – M. Krs* (Eds.): Laurasian Paleomagnetism and Tectonics. – Tectonophysics, 139, 31-41. Amsterdam.

Fisher, R. (1953): Dispersion on a sphere. – Proc. Roy. Soc., A 217, 295-305. London.

Irving, E. – Tanczyk, E. – Hastie, J. (1976a): Catalogue of paleomagnetic directions and poles. – Third Issue, Geomagnetic Ser., 5, 1-99. Ottawa.

– (1976b): Catalogue of paleomagnetic directions and poles. – Fourth Issue, Geomagnetic. Ser., 6, 1-70. Ottawa.

Kent, J. T. – Briden, J. C. – Mardia, K. V. (1983): Linear and planar structure in ordered multivariate data as applied to progressive demagnetization of palaeomagnetic remanence. – Geophys. J. Roy. astron. Soc., 75, 593-621. London.

Khramov, A. N. (1984): Paleomagnetic directions and pole positions. – Data for the USSR, Summary catalogue, 1, 1-94. Moscow.

Kirschvink, J. L. (1980): The least-squares line and plane and the analysis of palaeomagnetic data. – Geophys. J. Roy. astron. Soc., 62, 699-718. London.

Krs, M. (1967): Research Note: On the palaeomagnetic stability of Red sediments. – Geophys. J. Roy. astron. Soc., 12, 313-317. London.

– (1968): Rheological aspects of palaeomagnetism? – Proc., XXXIII Int. Geol. Congr., 5, 87-96. Praha.

– (1969): Paleomagnetismus. – Knih. Ústř. Úst. geol., 40, 1-202. Praha.

– (1978): Palaeomagnetic evidence of tectonic deformation of blocks in the Bohemian Massif. – J. Geol. Sci., Geol., 31, 141-154. Praha.

– (1982): Implication of statistical evaluation of Phanerozoic palaeomagnetic data (Eurasia, Africa). – Rozpr. Čs. Akad. Věd, Ř. mat.-přír. Věd, 93, 3, 1-86. Praha.

Krs, M. – Chvojka, R. – Valín, F. (1988): A contribution to methodology of magnetostratigraphic studies of strongly remagnetized Lower Permian rocks, Bohemian Massif. – Z. geol. Wiss., 16, 10, 945-957. Berlin.

Krs, M. – Hladil, J. – Krsová, M. – Pruner, P. (1994): Paleomagnetické a paleogeografické výzkumy ve vazbě na vrt KTB-1, etapa 1994. – Int. Rep., Geol. Inst. Acad. Sci., 1-27. Praha.

Krs, M. – Krsová, M. – Kouklíková, L. – Pruner, P. – Valín, F. (1992a): On the applicability of oil shale to palaeomagnetic investigations. – Phys. Earth Planet. Inter., 70, 178-186. Amsterdam.

Krs, M. – Krsová, M. – Martinec, P. – Pruner, P. (1993a): Palaeomagnetism of the Carboniferous and variegated layers of the Moravian-Silesian region. – Geol. Zbor. Geol. carpath., 44, 5, 301-314. Bratislava.

Krs, M. – Krsová, M. – Pruner, P. (1992): Hlubinná stavba a geodynamický model Západních Karpat – paleomagnetické výzkumy 1991.- Int. Rep., Geofyzika Co., Dept. in Prague, 1-44. Geofond Praha.

– (1993): Palaeomagnetic and palaeogeographic investigations in relation to the super-deep drill KTB-1, 1992. – Int. Rep., Geol. Inst. Acad. Sci., 1-32. Geofond. Praha.

– (in press): Palaeomagnetism and palaeogeography of the Western Carpathians: summary of results from the Neogene to the Permian. Proceedings of the Symposium „Palaeomagnetism in the Mediterranean region", (*Eds.: A. Morris – D. H. Tarling*), Burlington House, Piccadilly. London.

Krs, M. – Krsová, M. – Pruner, P. – Chvojka, R. – Havlíček, V. (1987): Palaeomagnetism, palaeogeography and the multi-component analysis of Middle and Upper Cambrian rocks of the Barrandian in the Bohemian Massif. – *In: D. V. Kent – M. Krs* (Eds.), Laurasian Paleomagnetism and Tectonics. – Tectonophysics, 139, 1-20. Amsterdam.

Krs, M. – Krsová, M. – Pruner, P. – Chvojka, R. – Potfaj, M. (1993b): Palaeomagnetic investigations in the Biele Karpaty Mts. unit, Flysch Belt of the Western Carpathians. – Geol. Zbor. Geol. carpath., 45, 1, 35-43. Bratislava.

Krs, M. – Krsová, M. – Pruner, P. – Havlíček, V. (1988): Palaeomagnetism, magnetism and palaeogeography of the Middle and Upper Cambrian rocks of the Barrandian area in the Bohemian Massif. – Sbor. geol. Věd, užitá Geofyz., 22, 9-48. Praha.

Krs, M. – Krsová, M. – Pruner. P. – Zeman, A. – Novák, F. – Jansa J. (1990): A petromagnetic study of Miocene rocks bearing micro-organic material and the magnetic mineral greigite (Sokolov and Cheb basins, Czechoslovakia). – Phys. Earth Planet. Inter., 63, 98-112. Amsterdam.

Krs, M. – Novák, F. – Krsová, M. – Pruner, P. – Kouklíková, L. – Jansa J. (1992b): Magnetic properties and metastability of greigite-smythite mineralization in brown-coal basins of the Krušné Hory Piedmont, Bohemia. – Phys. Earth Planet. Inter., 70, 273-287. Amsterdam.

Krs, M. – Pruner, P. – Krsová, M. (1993): Paleomagnetické a paleogeografické výzkumy ve vazbě na vrt KTB-1, etapy 1991, 1992, 1993. – Int. Rep. Geol. Inst. Acad. Sci., 1-60. Geofond Praha.

– (1994): Paleomagnetismus a paleogeografie variských a pre-variských formací Českého masívu: stručný přehled. Shrnující zpráva úkolu Paleomagnetické a paleogeografické výzkumy ve vazbě na vrt KTB-1, etapy 1991-1994. – Int. Rep. Geol. Inst. Acad. Sci., 1-22. Geofond Praha.

Krs, M. – Pruner, P. – Krsová, M. – Kouklíková, L. (1991): Paleomagnetické a paleogeografické výzkumy ve vazbě na vrt KTB-1, etapa 1991. – Int. Rep., Geofyzika Co., Dept. in Prague, 1-38. Geofond Praha.

Krs, M. – Pruner, P. – Potfaj, M. (1992): Palaeotectonic development of Alpo-Carpatho-Pannonian and adjacent blocks in the light of statistically evaluated palaeomagnetic data. – New Trends in Geomagnetism, IIIrd Biannual Meeting on Rock Magnetism, Palaeomagnetism and Data Base Usage, Abstract Book. Symp. IAGA, Castle Smolenice. – Geol. Zbor. Geol. carpath., 43, 3, 185-187. Bratislava.

Krs, M. – Vrána, S. (1993): Palaeomagnetism and petromagnetism of augite microgranodiorite, Nezdice near Kašperské Hory, southern Bohemia. – J. Czech Geol. Soc., 38, 3-4, 201-207. Praha.

Lewandovski, M. – Jelenska, M. – Halvorsen, E. (1987): Paleomagnetism of the Lower Devonian sandstones from Holy Cross Mountains, Central Poland: Part 1. – *In: D. V. Kent – M. Krs (Eds.)*, Laurasian Paleomagnetism and Tectonics. – Tectonophysics, 139, 21-29. Amsterdam.

Pesonen, L. J. – Bylund, G. – Torsvik, T. H. – Elming, S. A. – Mertanen, S. (1991): Catalogue of palaeomagnetic directions and poles from Fennoscandia: Archaean to

Tertiary. – In: The European Geotraverse, Part 7, Edited by: *R. Freeman – M. Much – St. Mueller.* – Tectonophysics, 195, 2/4, 151-207. Amsterdam.

Příhoda, K. – Krs, M. – Pešina, B. – Bláha, J. (1989): MAVACS – a new system creating a non-magnetic environment for palaeomagnetic studies. – Spec. Issue Cuadernos de Geología Ibérica, 12, 223-250. Madrid.

Pruner, P. (1987): Palaeomagnetism and palaeogeography of Mongolia in the Cretaceous, Permian and Carboniferous – preliminary data. – *In: D. V. Kent – M. Krs* (Eds.), Laurasian Paleomagnetism and Tectonics. – Tectonophysics, 139, 155-167. Amsterdam.

– (1992): Palaeomagnetism and palaeogeography of Mongolia from the Carboniferous to the Cretaceous – final report. – Phys. Earth Planet. Inter., 70, 169-177. Amsterdam.

Soffel, H. Chr. (1991): Paläomagnetismus und Archäomagnetismus. – Berlin, Heidelberg.

Thellier, É. – Thellier, O. (1959): Sur l'intensité du champ magnétique terrestre dans le passé historique et géologique. – Ann. Géophys., 15, 285-376, Paris.

Torsvik, T. H. – Smethurst, M. A. – Briden, J. C. – Sturt, B. A. (1990): A review of Palaeozoic palaeomagnetic data from Europe and their palaeogeographical implications. – In: *W. S. Mc Kerrow – C. R. Scotese (Eds.)*: Palaeozoic Palaeogeography and Biogeography. – Geol. Soc. Mem., 12, 25-41.

Torsvik, T. H. – Smethurst, M. A. – Van der Voo, R. – Trench, A. – Abrahamsen, N. – Halvorsen, E. (1992): Baltica. A synopsis of Vendian-Permian palaeomagnetic data and their palaeotectonic implications. – Earth Sci. Rev., 33, 133-152. Amsterdam.

Van der Voo, R. (1990): Phanerozoic palaeomagnetic poles from Europe and North America and comparisons with continental reconstructions. – Rev. Geophys., 28, 2, 167-206, Amer. Geophys. Union. Washington.

– (1993): Paleomagnetism of the Atlantic, Tethys and Iapetus Oceans. Cambridge.

Waldhausrová, J. (1966): The volcanites of the Křivoklát-Rokycany zone. – In: Paleovolcanites of the Bohemian Massif. Proc. Přírodověd. Fak. Univ. Karl., 145-151. Praha.

– (1972): The chemistry of the Cambrian volcanics in the Barrandian area. – Krystalinikum, 8, 45-75. Praha.

Westphal, M. (1990): Paleomagnetic directions and pole positions. – Institut de Physique du Globe. Strasbourg.

Paleomagnetismus a paleogeografie variských formací Českého masívu, srovnání s ostatními regiony v Evropě

Hlavním cílem předložené práce bylo shrnout základní paleomagnetická data dosud odvozená na horninách variských formací v Českém masívu, provést paleogeografické rekonstrukce a srovnat výsledky s obdobnými interpretacemi z jiných evropských regionů v územích s. od alpínského tektonického pásma. Toto zpracování představuje zhodnocení výsledků paleomagnetického výzkumu variských formací nashromážděných za posledních cca třicet let. V práci jsou shrnuty jen základní výsledky, množství paleomagnetických údajů doložených zkouškami stability, magnetomineralogickými rozbory, Zijderveldovými diagramy a demagnetizačními grafy, studiem fázových změn minerálů – nositelů magnetizace a paleomagnetizace, výsledky multi-komponentní analýzy remanence apod. najde čtenář v odkazech na katalogy a publikace citované v práci.

Střední polohy paleomagnetických pólů a jejich rozptyly byly vypočteny s použitím Fisherovy (1953) statistiky, výsledky shrnují tabulky 1 až 4. Pro českou část Českého masívu jsou základní paleomagnetická data doložena pro časný perm, karbon a devon v tabulkách 5 až 7. Tabulka 8 shrnuje směry remanence pozdně variského přemagnetování (overprint), odvozené na dosud zkoumaných časně variských a prevariských formacích Českého masívu, a jim odpovídající polohy paleomagnetických pólů.

Ze středních poloh pólů byly vypočteny paleogeografické šířky a orientace paleomeridiánů pro příslušné regiony, části litosférických desek a pro evropskou desku v období od devonu do triasu (viz obr. 1 až 15). Legenda k paleomagnetickým údajům vyhodnoceným statisticky je uvedena v Appendixu nejstručnější formou: Pro každou zkoumanou geologickou formaci jsou napsány geografické souřadnice (geografická šířka, geografická délka dnešní globální sítě), případně název území, typ vyšetřovaných hornin, poznámky k použité laboratorní metodě demagnetování (tepelné demagnetování – TC, demagnetování střídavým polem – AC, kombinované demagnetování – TC + AC), zmínka o normální (N), inverzní (R) anebo kombinované polaritě (R+N) paleomagnetizace, referenční číslo k příslušnému katalogu anebo publikaci. Nebyla uvažována paleomagnetická data nevyhovující obecně přijatým kritériím, když pro střední paleomagnetické směry $\alpha_{95} > 15^{o}$ (Fisher 1953), kritérium spolehlivosti je B (Irving et al. 1976) anebo kvalita Q < 3 (Van der Voo 1990).

Na obr. 16 jsou přehledně uvedeny paleomagnetické směry a jejich rozptyly dosud odvozené na časně permských a karbonských formacích z české strany Českého masívu. Ze středních poloh paleomagnetických pólů byly vypočteny paleogeografické šířky (obr. 17 a 18), které korelují s obdobnými údaji z jiných regionů Evropy v území severně od alpínského tektonického pásma.

Vliv pozdně variského přemagnetování je možno dobře demonstrovat při odvozování paleomagnetismu pre-variských formací jak z moravské zóny, tak z Barrandienu. Na přemagnetování devonských vápenců z Barrandienu bylo upozorněno již v počátcích paleomagnetického výzkumu (Chlupáč – Krs 1967). V průběhu systematického paleomagnetického vyšetřování v pozdějších letech bylo tomuto problému věnováno nemálo úsilí, které nakonec vedlo k vývoji vysoce účinného tepelného demagnetizátoru zvaného MAVACS (Magnetic Vacuum Control System, cf. Příhoda et al.1989). Např. kambrické horniny Barrandienu představují širokou škálu horninových typů. Pro paleomagnetický výzkum se ukázaly obzvláště vhodné pozdně kambrické vulkanity, středně kambrické sedimenty (převážně droby) a časně kambrické břidlice obsahující mikro-organickou hmotu. Postupně získávané výsledky byly buď publikovány (Krs et al. 1987, 1988), anebo byly předkládány v samostatných zprávách (Krs et al. 1991; Krs – Krsová – Pruner 1993; Krs – Pruner – Krsová 1993, 1994). S použitím multi-komponentní analýzy remanence byly separovány složky variského přemagnetování (overprint).

Dosud bylo v moravské zóně studováno pět lokalit středně až pozdně devonských vápenců (ve spolupráci s Dr. J. Hladilem): Čelechovice na Hané, pozdní eifel-časný givet; Josefov – Habrůvka, givet; Křtinský mramorový lom, pozdní famen; Mokrá, pozdní

frasn-časný famen; Lažánky, givet. Nositelem magnetismu a paleomagnetismu u většiny zkoumaných vápenců je jemnozrnný magnetit, nejpravděpodobněji biogenní magnetit. U středně magnetických vápenců byly zjištěny tři složky remanence; A-složka je převážně viskózního původu; B-složka, dosahující až 95% hodnoty totální remanence, představuje pozdně variskou složku přemagnetování; C-složka je časně variská a je nositelem primárních paleomagnetických směrů. Z hlediska úvah o paleoteplotních a jiných fyzikálně-chemických polích potřebných k přemagnetování zkoumaných hornin jsou rozhodující blokující teploty minerálů – nositelů příslušných složek remanence. B-složky byly separovány v teplotních intervalech od 150 °C příp. 200 °C do 350 °C příp. 400 °C, C-složky byly odvozeny v teplotních intervalech od 400 °C příp. 425 °C do 500 °C příp. 530 °C a výše, viz obr. 28-32.

Značná pozornost byla věnována též problému pozdně variského přemagnetování kambrických hornin Barrandienu. Podíl B-složek remanence v totální remanentní magnetizaci je možno dobře demonstrovat na příkladech studia paleomagnetismu pozdně kambrických vulkanitů a časně kambrických břidlic s mikro-organickou hmotou. Pozdně kambrické vulkanity, andezit, dacit, rhyolit, přičemž andezit převládá, byly studovány z křivoklátsko-rokycanského komplexu (ve spolupráci s Dr. Vl. Havlíčkem). Z celkového odběru vzorků v několika etapách poskytlo deset výchozů horniny vhodné k paleomagnetickému rozboru. Vzorky byly očistitelné s použitím střídavého (elektromagnetického) pole, větší účinnosti se dosáhlo tepelným demagnetováním s použitím aparatury MAVACS. Ze všech zkoumaných vzorků 137 poskytlo dobře reprodukovatelné výsledky, doložené magnetomineralogickými studiemi a Zijderveldovými diagramy postupně demagnetované remanence. Magnetit je hlavním nositelem magnetizace a paleomagnetizace, pouze u jednoho výchozu andezitu tímto nositelem je hematit. Vyšší blokující teplota ferrimagnetických minerálů je jedním ze základních předpokladů pro odvození paleomagnetických směrů. Řada vzorků vykázala silný podíl pozdně variských složek remanence, dobře rozpoznatelný s použitím multi-komponentní analýzy (Kirschvink 1980). Typické příklady uvádějí obr. 33 a 34. Byl zjištěn i výchoz andezitu (jjz. od Roztok) mimořádně vysoké magnetické tvrdosti odolávající variskému přemagnetování, viz obr. 35. Příklady pozdně variských složek remanence odvozených multi-komponentní analýzou uvádí obr. 36 pro vzorky andezitu (Roztoky, lokalita 4) a rhyolitu (Skryje, lokalita 5). Vzorky hornin použité pro odvození pre-variských a post-kadomských paleomagnetických směrů vykazují tedy též směry remanence pozdně variského původu.

Břidlice s mikro-organickou hmotou časně kambrického stáří (pasecká břidlice, hořicko-holšinské souvrství) z lokality „Kočka", Brdy, poskytly rovněž tři složky remanence, A-složku převážně viskózního původu, B-složku pozdně variskou a C-složku nejpravděpodobněji primárně paleomagnetickou. Horniny obsahující mikro-organickou hmotu bývají vhodné k paleomagnetickému výzkumu, ovšem nositelem paleomagnetizace zřídka bývají původní metastabilní ferrimagnetické minerály greigit a smythit bakteriálního původu (Krs et al. 1990, 1992b). U starších hornin s mikro-organickou hmotou při různém stupni karbonifikace jsou nositeli paleomagnetizace produkty alterace původních sulfidů, jako α-Fe_2O_3 , γ-Fe_2O_3, η-Fe_2O_3 anebo jemnozrnný magnetit v závislosti na redox podmínkách. Všechny zkoumané vzorky z lokality „Kočka" vykázaly výrazný podíl B-složek pozdně variského původu, viz obr. 37-40.

Tabulka 8 shrnuje směry B-složek pozdně variského původu dosud odvozené na devonských horninách z moravské zóny, devonských a kambrických horninách z Barrandienu. Odpovídající polohy paleomagnetických pólů byly vypočteny z příslušných středních směrů B-složek. Střední poloha pólů vypočtená s použitím Fisherovy (1953) statistiky odpovídá středním polohám pozdně karbonských a časně permských pólů odvozeným z paleomagnetismu biostratigraficky datovaných hornin, viz. tabulky 5, 6 a 8. Rozptyl poloh pólů odvozených z B-složek časně variských a pre-variských formací odpovídá ovšem lépe rozptylu pozdně karbonských poloh pólů než rozptylu časně permských pólů, viz obr. 41. Z uvedeného vyplývá poznatek, že B-složky pozdně variského původu s nejvyšší pravděpodobností vznikly v pozdním karbonu s možným přesahem do spodního permu.

Permské horniny vykazují nápadně vysokou homogenitu paleomagnetických dat. Paleogeografické šířky střední Evropy jsou blízko ekvátoru, ale vesměs na severní polokouli. Obdobnou homogenitu vykazují i časně a středně triasové horniny. Změny v paleogeografických šířkách od spodního permu do středního triasu směrem do vyšších paleogeografických šířek na severní polokouli jsou vyvolány kontinentálním driftem celé severoevropské litosférické desky. Horniny postižené variským orogénem zaznamenaly různý stupeň paleotektonické rotace. Středoevropské pozdně karbonské formace vykazují vzájemně porovnatelné paleotektonické rotace nepřesahující 15-20°. Středně a časně karbonské horniny západoevropských hercynid jsou výrazně rotovány, cca 50° a 120° ve smyslu pohybu hodinových ručiček vůči permskému paleomeridiánu. Obdobné rotace byly zjištěny též pro horniny devonu z moravské zóny (Krs et al. 1994). Byl navržen model vysvětlující specifickou distribuci poloh pólů, podmíněnou paleotektonickou rotací pro horniny s odlišnými paleogeografickými šířkami. Podnět k navržení modelu poskytly experimentálně odvozené polohy paleomagnetických pólů z alpsko-karpatsko-panonské zóny a z detailních paleomagnetických výzkumů prováděných na území Západních Karpat pro horniny od permu do neogénu (Krs – Krsová – Pruner v tisku), viz obr. 42. Obdobný model pro variské a pre-variské formace (obr. 43) byl testován s experimentálně odvozenými polohami paleomagnetických pólů pro západoevropské variscidy (obr. 44) a pro devonské horniny moravské zóny Českého masívu (obr. 45). Vyniká nápadná podobnost mezi distribucí poloh pólů postižených paleotektonickou rotací jak v alpínském, tak v hercynském tektonickém pásmu, a to jak experimentálně, tak i teoreticky odvozených poloh pólů. V alpínském tektonickém (kolizním) pásmu převládají ovšem paleotektonické rotace převážně proti pohybu hodinových ručiček, zatímco ve variském pásmu převládají paleotektonické rotace převážně ve smyslu pohybu hodinových ručiček. Paleotektonické rotace podmíněné variským orogénem se promítají i do pre-variských a časně variských formací, dosud byly dobře doloženy např. pro pozdně kambrické vulkanity Barrandienu a pro vápence stáří pozdní eifel až pozdní famen z moravské zóny Českého masívu (cf. Krs – Pruner – Krsová 1994).